Fault Tolerant Control Schemes for Wireless Networked Control Systems with an Integrated Scheduler

Von Der Fakultät für Ingenieurwissenschaften der
Abteilung Elektrotechnik und Informationstechnik
der Universität Duisburg-Essen

zur Erlangung des akademischen Grades

Doktor der Ingenieurwissenschaften

genehmigte Dissertation

von

Dongmei Xu

aus

Jiangsu, V.R. China

1. Gutachter: Prof. Dr.-Ing. Steven X. Ding
2. Gutachter: Prof. Christophe Aubrun

Tag der mündlichen Prüfung: 24.10.2014

Acknowledgements

This thesis was finished while the author was with the Institute for Automatic Control and Complex Systems (AKS) in the Faculty of Engineering at the University of Duisburg-Essen, Germany. I would like to express my deepest appreciation to my mentor, Professor Dr.-Ing. Steven X. Ding. He offered me this opportunity to study in AKS four years ago. Without his patient guidance, perpetual encouragement and support, this work cannot be completed. I am also grateful to Professor Christophe Aubrun from Research Center for Automatic Control of Nancy, France, for his review and valuable critiques to my work.

Many thanks to my dear colleagues at AKS for creating an inspiring and friendly atmosphere, which made me feel less homesick and concentrate on my study. Special thanks to Prof. Dr. Bo Shen, who helped me to understand basic concepts of fault tolerant control theory during the beginning of my research, guided me to the way of doing researches and writing papers. It's my great honor to meet him at AKS. My sincere appreciation goes to Dr.-Ing. Birgit Köppen-Seliger, M. Sc. Linlin Li, M. Sc. Yong Zhang, M. Sc. Kai Zhang, M. Sc. Zhiwen Chen, M. Sc. Sihan Yu, M. Sc. Hao Luo, M. Sc. Shouchao Zhai for their reviews and suggestions to my dissertation. I have worked with my teammate Dr.-Ing. Ying Wang during the most time of my Ph.D life. I would like to acknowledge her great help and support and I truly cherish this experience. During the writing work, it's M. Sc. Linlin Li, who stands as the great support of my theoretic research. I sincerely thank her a lot. I would also like to thank the financial support of China Scholarship Council (CSC) gratefully during my study.

Finally, I would like to express my gratitude to my family, especially to my parents and husband Lei Zhou, for their consistent patience and support.

Duisburg, Oct. 2014
Dongmei Xu

Contents

List of Figures

List of Tables

Abbreviations and notations

Abbreviations

Abbreviation	Expansion
AF	additive fault
CL	control loop
CS	control station
CSMA/CA	carrier sense multiple access with collision avoidance
CTS	clear to send
DAS	distributed aggregation scheduling
DMAC	data MAC protocol
DMTS	delay measurement time synchronization
EEWS	energy efficient wakeup scheduling
FAR	false alarm rate
FD	fault diagnosis
FDI	fault detection and isolation
FE	fault estimation
FIFO	first input first output
FTC	fault tolerant control
FTSP	flooding time synchronization protocol
GCD	greatest common divisor
GMT	Greenwich mean time
GPS	global positioning system
HRTS	hierarchy reference time synchronization
LCM	least common multiple
LTI	linear time invariant
LTP	linear time periodic
LTV	linear time-varying
MAC	medium access control
MDS	minimum delay scheduling
MF	multiplicative fault
MIMO	multiple input multiple output

MSMC	multirate sampling and multiple control
NCS	networked control system
QoS	quality of service
RBS	reference broadcast synchronization
RTS	request to send
TDMA	time division multiple access
TPSN	timing-sync protocol for sensor networks
TRAMA	traffic-adaptive MAC protocol
WiNC	wireless networked control
W-NCS	wireless networked control system

Mathematical notations

Notation	Description
l_2	l_2-norm
H_∞	∞-norm
$\hat{\mathbf{x}}$	estimate of $\mathbf{x}$
$\tilde{\mathbf{x}}$	estimate error of $\mathbf{x}$
$\bar{\mathbf{x}}$	integrated model of $\mathbf{x}$
$\mathbf{A}'$	transpose of $\mathbf{A}$
$\mathbf{A}^{-1}$	inverse of $\mathbf{A}$
$\mathbf{A}^{\dagger}$	generalized inverse of $\mathbf{A}$
$I_m(\mathbf{A})$	image space of $\mathbf{A}$
$\mathbf{A} > 0$	$\mathbf{A}$ is a real symmetric and positive definite matrix
$\mathbf{A} < 0$	$\mathbf{A}$ is a real symmetric and negative definite matrix
Z^+	set of positive integers
$\Re^n$	set of n-dimensional real vectors
$\Re^{m\times n}$	set of real matrices with $m \times n$ dimensional
$\mathbf{I}_{m\times n}$	identity matrix with dimension $m \times n$
$\mathbf{O}_{m\times n}$	zero matrix with dimension $m \times n$
$\in$	belong to
$\mathrm{diag}\{v\}$	transfer vector v to be a diagonal matrix
rank	matrix rank
s^c	complement of set s
$\mathrm{sgn}(x)$	extract the sign of x
$\sqrt{x}$	root of number x
$\dot{x}$	derivative of x

Control theoretical notations

Notation	Description
N	number of subsystems in W-NCS
i	index of subsystems
$T_{c,i}$	cycle of i-th subsystem
$T_{c,min}$	greatest common divisor of $T_{c,i}$
T_p	period of W-NCS
T_{slot}	interval of one time slot
(k, j)	j-th time segment in k-th T_p
μ	number of segments in a T_p
$\mathbf{A}$, $\mathbf{B}$, $\mathbf{C}$	system matrices of the plant model
$\mathbf{E}_d$, $\mathbf{F}_d$	disturbance matrices of the plant model
$\mathbf{E}_f$, $\mathbf{F}_f$	additive fault matrices of the plant model
$\mathbf{A}_s$	system matrix of scheduler model
$\mathbf{B}_{sr}$, $\mathbf{B}_{su}$	residual and command input matrices of scheduler model
$\mathbf{C}_{sr}$, $\mathbf{D}_{sr}$	output matrices of scheduler model with the residual input
$\mathbf{C}_{su}$, $\mathbf{D}_{su}$	output matrices of scheduler model with the command input
$\mathbf{L}$	observer gain matrix
$\mathbf{K}$	controller gain matrix
$\mathbf{x}$	state variable vector of plant model
$\mathbf{u}$	theoretic input signal vector of plant model
$\mathbf{u}_s$	practical input signal vector of plant model
$\mathbf{y}$	output signal vector of plant model
$\mathbf{e}$	state estimation error signal vector
$\mathbf{r}$	theoretic residual signal vector of plant model
$\mathbf{r}_s$	practical residual vector as output of scheduler model
ψ_s	state variable vector of scheduler model
$\tilde{\mathbf{u}}$	command packet as input of scheduler model
$\tilde{\mathbf{u}}_s$	command packet as output of scheduler model
n	order of plant model
p_1	order of $\mathbf{u}_s$
p_2	order of $\mathbf{u}$
m_1	order of $\mathbf{r}$

m_2	order of $\mathbf{r}_s$

1 Introduction

This chapter briefly introduces the motivation and objectives of this thesis. The outline and contributions of the thesis are presented at the end of this chapter.

1.1 Motivation

This thesis deals with the development of fault tolerant control (FTC) schemes for wireless networked control systems (W-NCSs) with an integrated scheduler. The motivation of this thesis is gained from three points: (1) the promising perspective of W-NCSs in industrial field; (2) the influence of the scheduler to the control performance of W-NCSs; (3) the importance of FTC for W-NCSs. These points will be elaborated consecutively.

1.1.1 W-NCSs

With the development of modern large-scale automation systems, a major trend in modern industrial and commercial systems is to integrate computing, communication and control into different levels of machine/factory operations and information processes. Compared with conventional control systems with point-to-point connections, networked control systems (NCSs) have received a great deal of attention and are broadly adopted in modern industrial manufacturings and automatic processes. NCSs are control systems wherein the messages are transmitted through digital communication networks. The use of NCSs results in low cost, improved usage of resources, simplicity of maintenance and fault diagnosis, and above all, the flexibility of reconfiguring different components [1]. Until now, the applications of NCSs have been found in a broad range of areas such as manufacturing [2, 3], transportation [4], power systems [5, 6] and remote control [7]. During the past decades, lots of research activities have been dedicated to the research of NCSs and abundant fruits have been obtained, see the survey papers [8, 9] and the references therein. The major topics of NCSs are: 1) development of advanced communication technologies, e.g., network protocols and scheduling; 2) analysis of system control performance with respect to the technical features of the network, which are expressed in terms of Quality of Service (QoS) parameters, such as transmission delay, packet loss rate and so on; 3) FTC

in NCSs to compensate the effects of faults and ensure the system control performance; 4) Network Security in NCSs against network attacks, etc. It is widely recognized that the research of NCSs has a very challenging and promising prospect.

Along with a wide application of NCSs, the traditional wired NCSs have exposed their drawbacks, such as increment of cabling costs, inexpedience of installation and maintenance, etc. Due to the rapid progress of microelectronics, information and communication technology, wireless network is increasingly showing its advantages, for instance, lower cabling costs; convenient installation in hazardous environments; faster and simpler commissioning and reconfiguration [10, 11], etc. Nowadays, there is a trend within industrial networking to implement field-bus protocols using wireless technologies. These NCSs with wireless communication technologies are called wireless NCSs (W-NCSs), as shown in Fig.1.1. So far, the studies of W-NCSs mainly focus on the development of advanced communication technologies, such as power-saving hardwares, energy-efficient protocols and mobile operating systems. These researches are from the perspective of communication. However, to the best of the author's knowledge, the controller design and control performance analysis of W-NCSs, especially the decentralized W-NCSs, haven't been fully investigated, which constitutes one of the three motivations for our current investigation.

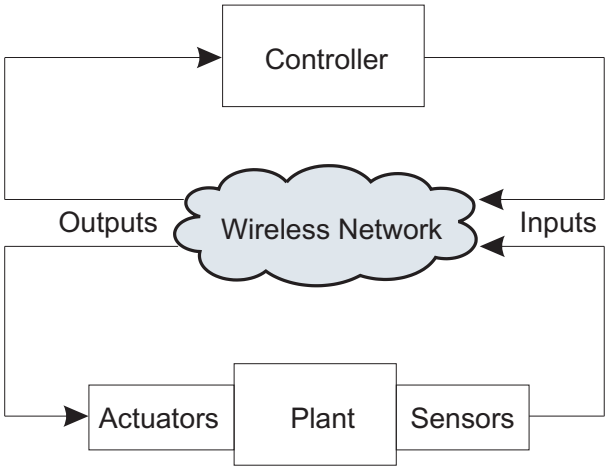

Figure 1.1: Structure of W-NCSs

1.1.2 Schedulers integrated in W-NCSs

In the literature, it is revealed that the control performances of W-NCSs not only depend on the developed control algorithms but also on the QoS parameters. The QoS parameters (for instance, time delay or packet loss) are usually supposed to be stochastic or bounded [12–16], and greatly rely on the parameters and schemes defined in the network

protocols at the medium access control (MAC) layer. These protocols includes time division multiple access (TDMA) [17, 18] and carrier sense multiple access with collision avoidance (CSMA/CA) [19, 20], etc. They determine the manner of multiple nodes accessing the network simultaneously. For instance, a node under CSMA/CA protocol sends the message only when the channel is checked and in an idle state. Otherwise, the node waits for a random period of time (namely back-off factor) and then checks the channel again. The back-off factor causes delay to the message transmission. Meanwhile, if the time deadline of the message is reached, the message will be discarded, which leads to packet loss. Therefore, the control performances of W-NCSs are affected primarily by network protocols. It is remarkable to notice that the research activities in the control community are mainly dedicated to the development of the advanced control and fault diagnosis (FD) schemes with the integrated QoS parameters, while the automatic industry fully concentrates on developing new generation of networks and MAC mechanisms [21]. In industrial application, the positions of devices will not change frequently, which provides the networks with static topologies. Moreover, it is required to satisfy the requirements for deterministic transmission behaviors via wireless networks, and ensure the high real-time ability and reliability of W-NCSs. Hence, TDMA (instead of CSMA/CA) mechanism is preferred in real-time wireless industrial process control systems.

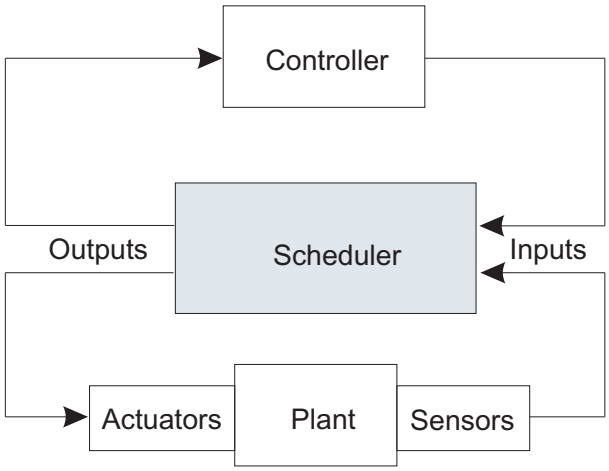

Figure 1.2: W-NCSs with an integrated scheduler

In W-NCSs, the MAC protocols, particularly TDMA, can be modeled in form of schedulers. Hence, scheduling of the message transmission orders plays a very important role in the control performance of W-NCSs, see Fig.1.2. Recently, the co-design problem of control and scheduling has attracted increasing attention. [22, 23] addressed this problem for stabilizing a linear time invariant (LTI) system, where only limited sensors and actuators can exchange information with a remote controller via a common communication

network. A predictive control and scheduling co-design approach was proposed in [24] to deal with the communication constraints for NCSs with network-induced delays, in which both static and dynamic scheduling algorithms were considered to schedule the transmissions of the signals. The necessary and sufficient conditions for quadratic stabilizability of linear NCSs by dynamic output feedback and communication protocols have been developed in [25]. Due to the static topologies of industrial networks, and also considering the demands for deterministic transmission behaviors, the W-NCSs usually work with a static scheduler. So far, relatively little attention has been paid to the performance analysis of decentralized W-NCSs with integrated schedulers. This gives rise to the second motivation of our research.

1.1.3 FTC for W-NCSs

During the system operation, faults or failures may occur in the actuators, the sensors, or the system components. To reduce performance degradation and enable the system to continue operating properly, there has been an enormous amount of research towards the design and implementation of FTC systems in recent decades. Fig.1.3 [26] illustrates our FTC architecture with an integration of a fault diagnosis (FD) module, a fault accommodation [27] mechanism in the supervision level, and a reconfigurable controller in the execution level. FTC methods are developed on the assumption of a successful FD [28]. The FD module contains a fault estimation (FE) submodule and estimates system state/output variables as well as fault information [29]. When a fault occurs, the controller is reconfigured with the estimated information to compensate the effects of the fault and ensure the system control performance [30–32].

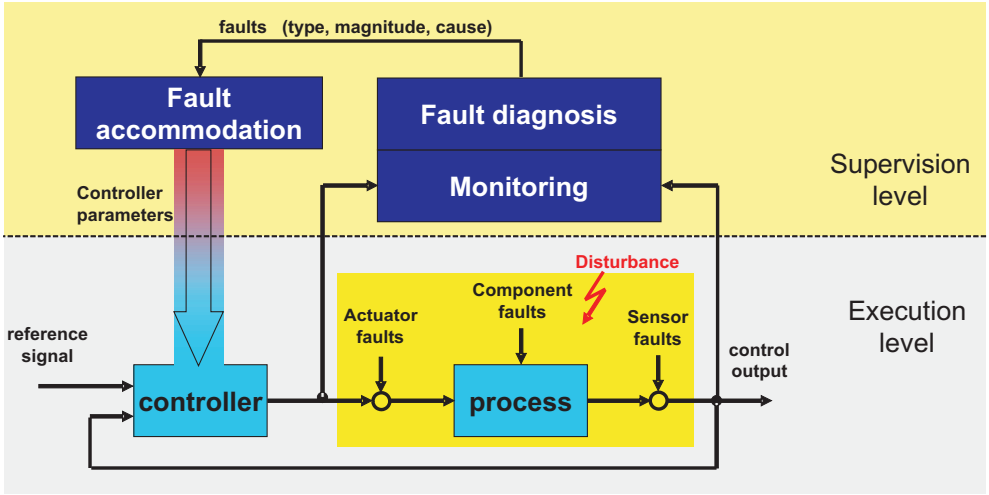

Figure 1.3: Active FTC architecture

Besides, based on their representation, the faults can be classified into two categories: additive faults (AFs) and multiplicative faults (MFs). The different effects of systems with these two kinds of faults are that: the occurrence of MFs will affect the system stability and is dependent of the system configuration, which is not the case with AFs. Since these two kinds of faults are very common in industrial processes, development of FTC strategies for systems with AFs and MFs has become an area of great interest in both academics and industry.

Recently, the study of advanced FTC strategies for NCSs has drawn increasing attention and some contributions have been published, see the survey papers [8, 26] and the references therein. The mainstream among these research activities is to investigate FTC strategies for NCSs with various faults, such as sensor/actuator faults [33, 34]. Moreover, in order to simulate a realistic network, several QoS parameters are considered in NCSs, for instance, transmission delay [35], packet loss [34, 36] and limited communication [37], etc. Besides, the nonlinear models [35, 37, 38] and uncertainties [36] increased the complexity to NCSs and also intensified the difficulty of achieving a satisfied FTC performance. However, most of these achievements have concentrated on the FTC problem of NCSs with AFs, few literature can be found on the problem with MFs. In addition, FTC strategies for decentralized large-scale industrial processes have also been investigated with the consideration of interconnection (or coupling) among subsystems in [39–44]. When we try to apply the existing FTC methods of NCSs to decentralized W-NCSs, some other problems also deserve more exploration. For instance,

(1) Multiple sampling rates: In the industrial process control systems, subsystems are set with multiple sampling rates according to the variation rates and the importance of the sampled data, which increases the complexity of the W-NCS model;

(2) Structure limitations: The limitation of information sharing among all subsystems leads to structure limitations on the W-NCS model, hence the solution for structure-limited model is strongly required;

(3) System states unmeasurable: In many systems, the controllers are designed to be related with the system states. However, not all the system states are measurable during the process. In the development of FTC schemes for such systems, the design of state observer and fault estimator is quite necessary.

Moreover, these proposed methods have only been demonstrated with numerical examples, which are not sufficient enough to illustrate their applicability in practice. By now, the design of FTC strategy for W-NCSs in industrial automatic control application is still an open issue, which becomes the third motivation of this work.

1.2 Objectives

Strongly motivated by the aforementioned studies, we are devoted to the development of FTC schemes for W-NCSs with an integrated scheduler. In the first part, the procedures of integrating a scheduler into W-NCSs are introduced. The integrated W-NCSs are modeled as discrete linear time periodic (LTP) systems. Based on this integrated discrete LTP systems, FTC strategies for W-NCSs with AFs and MFs are developed, respectively. More specifically, the goals of this thesis are stated as follows:

- Formulating the state-space representation of the W-NCS scheduler;
- Integrating the scheduler into W-NCSs with the consideration of the communication mechanism, and modeling W-NCSs into discrete LTP systems;
- Developing an FTC scheme for W-NCSs with sensor/actuator AFs;
- Exploring an FTC scheme for W-NCSs with actuator MFs;
- Demonstrating the validity of the proposed FTC approaches on the WiNC (wireless networked control) platform.

1.3 Outline and contributions

This thesis consists of eight chapters, as depicted in Fig.1.4. Chapter 1 describes the motivations and objectives of this thesis. Chapter 2 introduces the preliminaries of wireless network scheduling schemes and FTC technologies. Chapter 3 provides the procedures of modeling W-NCS schedulers. Chapter 4 presents the model of W-NCSs with an integrated scheduler. Chapter 5 and 6 propose the FTC strategies for W-NCSs with AFs and MFs, respectively. Chapter 7 demonstrates the experimental results of the proposed FTC strategies on WiNC platform. Last chapter concludes all the work and gives some future directions for this study. A brief summary of each chapter and the major contributions of this thesis are described as follows.

Chapter 1: Introduction
This chapter describes motivations, objectives, outline and contributions of this thesis.

Chapter 2: Overview of wireless network scheduling schemes and FTC technologies
In Chapter 2, the preliminaries of wireless network scheduling schemes and FTC technologies are reviewed. We briefly recall three key scheduling issues for industrial wireless

networks: wireless network protocols, time synchronization algorithms and wireless network scheduling algorithms. Then we focus on the FTC technologies. Two types of faults, i.e., AFs and MFs are considered. Aiming at different types of faults, the typical FE and FTC strategies are introduced.

Chapter 3: Modeling of W-NCS schedulers

This chapter presents the procedures of formulating the state-space representation of W-NCS schedulers. The information scheduler generated by the scheduling algorithms is transformed into a new matrix, called mathematical scheduler, which contains the key information in the information scheduler (such as the start and the end slots of each transmission task, delay or packet loss of all the transmission tasks). The mathematical scheduler is taken as a dynamic system and its state-space representation is formulated. It is found that the system matrices of the mathematicalal scheduler are influenced by the rates of sampling and control in each cycle, as well as the network topology. Therefore, three cases are considered in this thesis: (1) Once-sampling-once-control with single-hop network, (2) Once-sampling-once-control with multi-hop network and (3) Multi-sampling-multi-control with multi-hop network.

Chapter 4: Modeling of W-NCSs

Chapter 4 introduces the structure of fault tolerant W-NCSs, which consist of three functional layers: Execution layer, Coordination & Supervision layer, Management layer. The communication mechanism at each functional layer is analyzed firstly. Afterwards, each subsystem and the whole W-NCSs integrated with the scheduler are modeled as discrete LTP systems. Finally, the scheduler in the form of discrete LTP systems is also addressed.

Chapter 5: An FTC scheme for W-NCSs with AFs

In this chapter, we consider the integrated W-NCSs (in form of discrete LTP systems) with sensor/actuator AFs. The period of discrete LTP systems is divided into T time instants. Whether faults are considered at each time instant has significant influences on the development of FE and FTC schemes for LTP systems. The gains (for the state observer, fault estimator and the controller) have been achieved according to two cases: faults are considered (1) at all T time instants and (2) at partial time instants. Based on the state observer and fault estimator, a group of fault tolerant controllers are constructed for the AFs case, and seek to guarantee that the outputs of LTP systems satisfy a set of H_∞ performance indices. Due to the distribution of W-NCSs and the limitation of communication bandwidth, the structure-limited problem of the gains are unavoidable. Improved theorems are presented to achieve feasible solutions for these gains.

Chapter 6: An FTC scheme for W-NCSs with MFs
This chapter deals with the integrated W-NCSs with actuator MFs, where the faults are defined according to their physical meanings. A lifting technology is applied to the discrete LTP systems, firstly. Then an adaptive estimation method is used to the lifted system to construct an adaptive observer. A nominal controller is designed for the system with fault-free case. Finally, based on this nominal controller, an FTC strategy is developed with the information provided by the adaptive observer, and try to compensate the effects caused by faults and enable the LTP systems continue operating properly.

Chapter 7: Application to WiNC Platform
In this chapter, the proposed FTC schemes are implemented on the WiNC platform. According to the structure-limited gains, the FTC strategies are realized with shared and unshared information (i.e., residual signals and state estimates), respectively. The results indicate that the system achieves better FTC performances with shared information.

Chapter 8: Conclusion and future directions
This chapter provides a conclusion of the achievements in this thesis, and gives some future recommendations for possible extensions of this work.

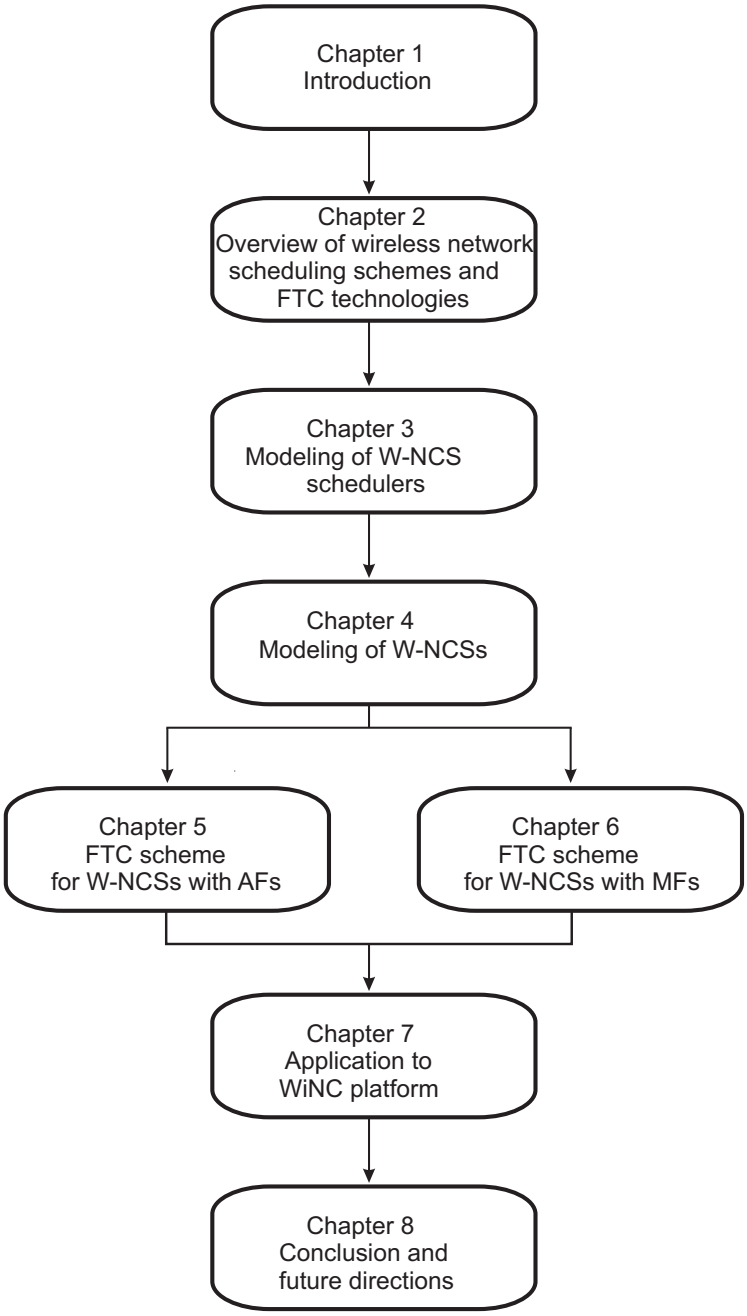

Figure 1.4: Organization of chapters

2 Overview of wireless network scheduling schemes and FTC technologies

This chapter reviews the essentials of wireless network scheduling schemes and FTC technologies. The preliminary knowledge of wireless network protocols, time synchronization algorithms and scheduling algorithms for TDMA protocol are presented firstly. Afterwards, we briefly introduce the relative FTC technologies, such as the principle of FTC strategies, the fault models and existing FE methods. Finally, the corresponding FTC schemes are discussed for different types of the faults.

2.1 Wireless network scheduling schemes

2.1.1 Wireless network protocols

The most essential demands of industrial wireless networks are to ensure deterministic data transmission behaviors and meet the real-time performances of automatic systems [21]. Therefore, collision management and avoidance are fundamental issues for choosing proper wireless network protocols [45]. There are two kinds of medium access methods which are typically used in wireless networks: TDMA and CSMA/CA.

TDMA: In a TDMA-based MAC protocol, a transmission channel is arranged to transmit certain information according to the assigned time slots. N devices are connected with one public channel. According to a certain order, each device is allocated in turn with a certain time slot to use the channel. When its slot comes, the device is linked to the channel and transmit the information. Meanwhile, the connections between other devices with the channel are all cut off. Until the allocated time slot arrives, the next device will be activated to the public channel [17];

CSMA/CA: CSMA/CA is a protocol for carrier transmissions in 802.11 [46] networks. In CSMA/CA, as soon as a node gets a packet that is to be sent, it checks whether the

channel is idle (no node is transmitting on the channel). If yes, the packet will be sent out. Otherwise, the node waits for a random period of time (namely back-off factor), and then checks the channel again. The back-off factor is counted down by a back-off counter. When it reaches zero and the channel is idle, the node transmits the packet. When it reaches zero and the channel is still occupied, the back-off factor will be set with a new one, and the node waits again [19, 20].

It is obvious that CSMA/CA is a contention-based protocol, which is not the case with TDMA. TDMA protocol is more power-efficient since nodes in the networks can enter inactive states until their allocated time slots come. It also eliminates communication collisions and bounds the delay time via wireless networks. Considering the realistic complexity and the overhead costs, and also considering the engineering demands for deterministic transmission behaviors, TDMA mechanism is widely adopted in industrial process control [21].

Before realizing TDMA protocol on a network, the knowledge of the network topology and time synchronization of nodes is required. In an industrial process, the positions of devices do not change frequently, so the network is treated with a static topology. For a given network topology, the realization of TDMA mechanism on wireless networks depends mainly on time synchronization of nodes.

2.1.2 Time synchronization algorithms

Time synchronization algorithm [47, 48] is to synchronize the clocks of the nodes in a network via radio communication. Nodes' clocks start when they are turned on, which may not be very accurate. Synchronization algorithms will synchronize the clocks to one or more reference nodes, which offers a relatively precise reference time. If real time is required, these nodes might be equipped with a global positioning system (GPS) module, which provides Greenwich mean time (GMT).

Time synchronization is very important if any application needs the nodes to execute a certain task at a certain time, or if some external events need to be logged together with the time when they happened. If synchronization is accurate enough, some applications might even use the time stamp of some events.

The most important performance metrics of synchronization algorithms are precision, energy efficiency, memory requirement and robustness [49, 50], etc. Until now, many activities have contributed to the research of time synchronization schemes, and lots of synchronization algorithms have been developed [51–54], for instance, reference broadcast synchronization (RBS) [55–57], timing-sync protocol for sensor networks (TPSN) [50, 58–60], hierarchy reference time synchronization (HRTS) [61–63], delay measurement time

synchronization (DMTS) [62, 64, 65], flooding time synchronization protocol (FTSP) [66–68], etc. Generally, all the developed algorithms can be classified into two main types: sender-receiver and receiver-receiver algorithms [49]. The most representatives for these two types are RBS and TPSN, respectively. For a detailed comparison of the existing synchronization algorithms, please refer to [49].

After the clocks are all synchronized to the reference nodes, the nodes can be further managed globally according to a prescribed transmission order, i.e., the scheduler.

2.1.3 Wireless network scheduling algorithms

In wireless networks, the problem of allocating transmission rights to the nodes over the network with the consideration of channel qualities is known as the scheduling problem. It arises in wireless environments because of three major reasons [69]: (1) spatial share of communication resources, (2) transmission conflict and interfere, (3) impairment of information transmissions, etc. Therefore, scheduling is very necessary in wireless environments for solving this problem.

TDMA is a schedule-based MAC protocol, which has attracted a wide range of attention in researches and applications [70]. TDMA provides collision-free transmissions among nodes since a set of time slots are preallocated. Thus, TDMA can adapt well to various network densities and offered loads. An efficient TDMA scheduler can save energy by allowing nodes to turn on the antenna only during their allocated time slots, without wasting energy by idle listening and overhearing. Furthermore, as TDMA does not require any message exchanges for building and disconnecting the communication links, e.g., request to send / clear to send (RTS/CTS), it limits overhead in communication. Finally it is noted that since wireless network in industry process is relatively stationary, the impact of dynamic environments on TDMA MAC schemes can be lessened. Thus, the deployment cost can be cushioned during the entire life-time of industrial networks [71].

The main criteria used to evaluate wireless scheduling algorithms for their application to wireless networks are efficiency, applicability, QoS support capability and fairness, etc [71, 72]. Until now, a wide range of scheduling algorithms for wireless TDMA protocol have been developed, for instance, energy efficient wakeup scheduling (EEWS) [73, 74], minimum delay scheduling (MDS) [75, 76], distributed aggregation scheduling (DAS) [77], traffic-adaptive MAC protocol (TRAMA) [78, 79], data MAC protocol (DMAC) [80], distributed coloring algorithm [81–83]. A comparison of the scheduling algorithms has been stated in [84]. It is remarkable in [84] that although there are various TDMA based MAC layer protocols proposed for wireless networks, there is no protocol accepted as a standard. One of the reasons for this is that the MAC protocol choice will, in general, be

application dependent, which means that there is no standard MAC protocol for wireless networks. Another reason is the lack of standardization at lower layers (physical layer) and the (physical) wireless hardware. Based on these achieved scheduling algorithms, in this thesis, we suppose the scheduler of W-NCSs has already been scheduled and is ready to be integrated into W-NCSs.

2.2 FTC technologies

2.2.1 Principle of FTC strategies

A process control or automation system concentrates on providing a quasi-optimal solution to obtain the best possible quality of the final product and consequently an increase in profits. The automatic control theory has been widely developed and applied to industrial processes. The object of the process control is to ensure the stability of the closed-loop systems and yield a predefined control performance in the case where all system components operate safely. However, the more the processes are automated, the more they are subject to the occurrence of faults. Consequently, a conventional feedback control method may give rise to an unsatisfactory control performance in the presence of malfunctions on sensors, actuators, or other components of the systems. This may even lead the systems to instability. In highly automated industrial systems where maintenance or repair cannot always be achieved immediately, it is efficient to design control methods of ensuring nominal control performance by taking the occurrence of faults into account. This control is referred to as FTC [28] which has become of paramount importance in the last few decades and much efforts have been made in this field, such as in nuclear and avionics industries [85, 86], chemical plants [87], Electrical machines [88, 89], etc.

The classification of FTC techniques is illustrated by the system control performances versus the severity of the failure [28], see Fig.2.1. For a priori known fault, a controller with fixed parameters could be set up with the objective of controlling the nominal system as well as the system affected by these known faults, which is known as passive methods. This strategy can be achieved by using the theories of robust control [90]. Since the controller must be insensitive to the occurrence of specific faults, these techniques are also known as reliable control techniques.

However, it is obvious that passive methods are very restrictive because of the lack of a priori knowledge of all the expected faults and their effects on the plant. Active approaches are preferable to identify the information of the faults and accommodate the controller so as to compensate the effects caused by faults to the system. These methods concern on adjusting the controllers on-line according to the identified fault magnitude and type, to

maintain the FTC performance of the system. If it remains possible to preserve the FTC performance of the faulty system close to the nominal one, it's in the reconfiguration stage, see Fig.2.1 [28]. In another word, active methods concentrate on reconfiguring the controllers. When it comes to more critical failures (such as a complete loss of an actuator), it's very difficult to maintain the nominal control performance anymore, the current FTC performance are reduced. In such cases, a restructuring strategy of modifying the system structure or the control objectives is used. Following this step, the system is led to a degraded operating mode. Moreover, for a certain type of failure, it is impossible to keep the system operating even in a degraded mode. In this case, the proper operation is to shut down the system safely. A general active FTC scheme is shown in Fig.2.2.

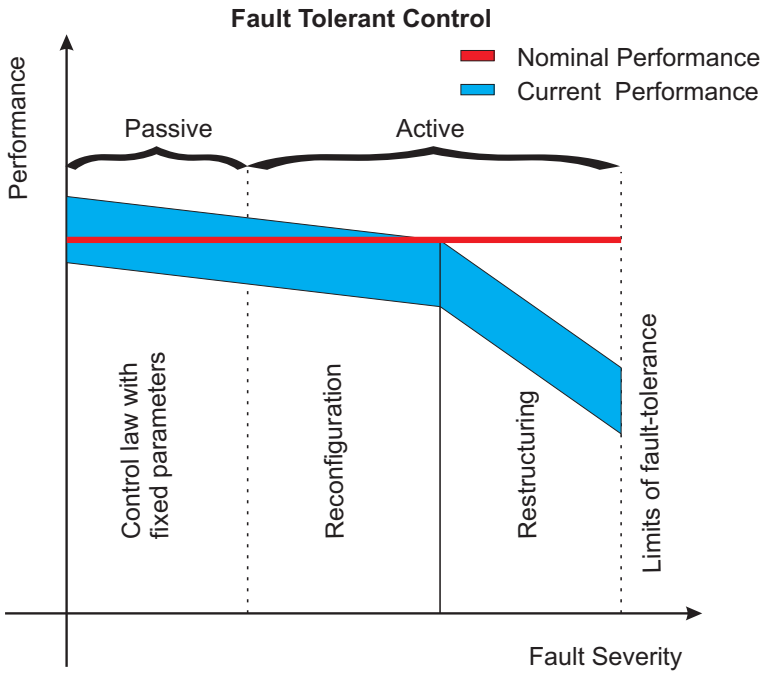

Figure 2.1: FTC strategies

In the literature, the design of FTC scheme is based on an assumption of successful FD strategies. Generally speaking, FD contains three steps: fault detection, fault isolation and fault estimation [91].

- Fault detection is to decide whether or not a fault has occurred. This step determines the time at which the system is subject to some fault;

- Fault isolation is to find in which component a fault has occurred. This step determines the location of the fault;

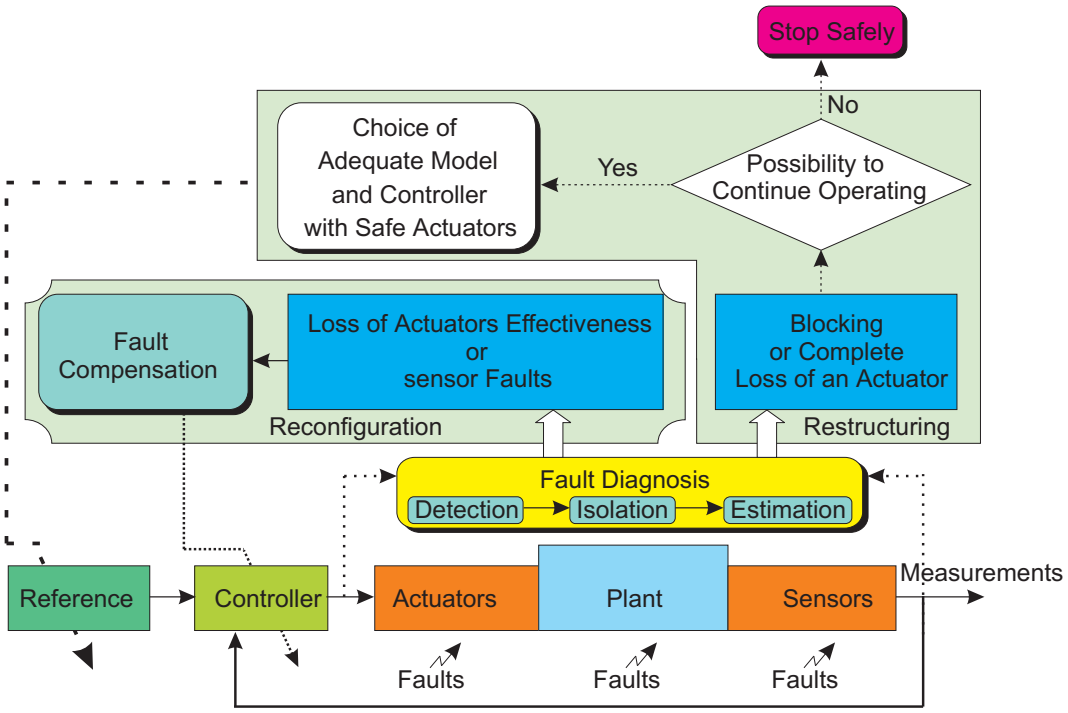

Figure 2.2: Active FTC scheme

- Fault estimation is to identify the fault and estimate its magnitude. This step determines the kind of fault and its severity.

The FD module, especially the FE submodule, offers the estimated information about faults. This information could be used as redundant information generated from the FD module and adopted for fault compensation in the reconfiguration step. In the restructuring step, the information from the FD module will be a significant reference to the decision making of the subsequent operations.

2.2.2 Fault models

In real application, where a digital process is used (micro-controller, programmable logic controller, computer, and data acquisition board, etc), the plant with fault-free case can be expressed in a discrete-time representation

$$\begin{aligned} \mathbf{x}(k+1) &= \mathbf{A}(k)\mathbf{x}(k) + \mathbf{B}(k)\mathbf{u}(k) \\ \mathbf{y}(k) &= \mathbf{C}(k)\mathbf{x}(k) \end{aligned} \tag{2.1}$$

where $\mathbf{x} \in \Re^n$ is the system state vector, $\mathbf{u} \in \Re^p$ is the control input vector, and $\mathbf{y} \in \Re^m$ is the measurement output vector. $\mathbf{A}(k)$, $\mathbf{B}(k)$ and $\mathbf{C}(k)$ are time-varying matrices with appropriate dimensions.

During the system operation, the occurrence of faults or failures is unavoidable and is an interruption of system's ability to perform the required functions under specified operating conditions. Generally, faults are classified into three categories [92]:

- Sensor faults: these faults have influence directly on the process measurement, e.g., sensor drift or offset;
- Actuator faults: these faults cause abnormal changes in the actuator inputs, e.g., actuator drifts;
- Component faults: these faults are used to indicate malfunctions within the system components.

Besides, according to the way of how they affecting the system dynamics, faults are divided into two classes: AFs and MFs.

Additve faults

For the actuator AFs, it can be expressed by

$$\mathbf{u}_f(k) = \mathbf{u}(k) + \mathbf{f}_a(k),$$

where $\mathbf{u}(k)$ and $\mathbf{u}_f(k)$ represent the normal and faulty actions, and $\mathbf{f}_a(k)$ is the actuator fault. In the presence of actuator AFs, the LTI system (2.1) can be addressed as

$$\mathbf{x}(k+1) = \mathbf{A}(k)\mathbf{x}(k) + \mathbf{B}(k)\mathbf{u}_f(k) = \mathbf{A}(k)\mathbf{x}(k) + \mathbf{B}(k)\mathbf{u}(k) + \mathbf{B}(k)\mathbf{f}_a(k). \tag{2.2}$$

The effect of AFs on sensors shows up with bias on the measurement output, i.e.,

$$\mathbf{y}(k) = \mathbf{C}(k)\mathbf{x}(k) + \mathbf{F}_s(k)\mathbf{f}_s(k), \tag{2.3}$$

where $\mathbf{F}_s(k)$ is the coefficient matrix and $\mathbf{f}_s(k)$ corresponds to the sensor faults.

Typical AFs met in practice are, for instance, an offset in sensors and actuators or a drift in sensors. The former can be described by a constant, while the latter by a ramp [92]. Since the controller is often designed to be related with the system state or the state estimate, it is very important to note that the occurrence of AFs will not affect the system stability and is independent of the system configuration.

Multiplicative faults

MFs are characterized by their (possible) direct influence on the system stability. Several kinds of MFs are described in [92]. In this thesis, we consider the following type of actuator MFs. The effect of this MFs is described as

$$\mathbf{u}_f(k) = \mathbf{f}_\theta(k)\mathbf{u}(k), \tag{2.4}$$

where $\mathbf{u}(k)$ and $\mathbf{u}_f(k)$ represent the normal and faulty actions, $\mathbf{f}_\theta(k)$ is the coefficient of actuator MFs, with $\mathbf{f}_\theta(k) = diag\{\cdots, \theta_i(k), \cdots\}$, $i = 1, \cdots, p$. The i-th actuator is faulty if $\theta_i(k) \neq 1$. The specific definition of the actuator fault is presented as follows

$$\begin{cases} \theta_i(k) = 1 & : \text{Fault-free case} \\ \theta_i(k) \in s^c & : \text{Loss of effectiveness} \\ \theta_i(k) = 0 & : \text{Out of order} \end{cases} \tag{2.5}$$

where $s = \{0, 1\}$, s^c denotes the complement of set s. In the presence of actuator MFs, the linearized system (2.1) can be addressed as

$$\begin{aligned} \mathbf{x}(k+1) &= \mathbf{A}(k)\mathbf{x}(k) + \mathbf{B}(k)\mathbf{u}_f(k) \\ &= \mathbf{A}(k)\mathbf{x}(k) + \mathbf{B}(k)\mathbf{f}_\theta(k)\mathbf{u}(k) \\ \mathbf{y}_f(k) &= \mathbf{C}(k)\mathbf{x}(k) \end{aligned} \tag{2.6}$$

Since in a close-loop system, the input is usually a function of the system state or the state estimate, obviously, $\mathbf{f}_\theta(k)$ plays an important role in the influence of the system stability.

2.2.3 FE schemes

As is well known, the design of FTC strategy is based on a successful FD technology, which comprises fault detection, fault isolation and FE. The object of FE is to identify the faults and estimate their magnitudes by using the available measurements. This step determines the types of faults and their severity. Compared with fault detection and fault isolation, the difficulties of developing FE methods would increase a lot, so FE is a more challenging issue. Furthermore, by using the obtained fault information, an active controller can be designed to compensate or mitigate the effect of the faults.

We consider the following state-space representation

$$\begin{aligned} \mathbf{x}(k+1) &= \mathbf{A}(k)\mathbf{x}(k) + \mathbf{B}(k)\mathbf{u}(k) + \mathbf{E}_d(k)\mathbf{d}(k) + \mathbf{E}_f(k)\mathbf{f}(k) \\ \mathbf{y}(k) &= \mathbf{C}(k)\mathbf{x}(k) + \mathbf{F}_d(k)\mathbf{d}(k) + \mathbf{F}_f(k)\mathbf{f}(k) \end{aligned} \tag{2.7}$$

where $\mathbf{x} \in \Re^n$, $\mathbf{u} \in \Re^p$ and $\mathbf{y} \in \Re^m$ are the system state vector, input vector and output vector, respectively. $\mathbf{d}(k) \in \Re^d$ denotes the disturbance. $\mathbf{f}(k) \in \Re^f$ is the fault vector to be estimated. $\mathbf{A}(k)$, $\mathbf{B}(k)$, $\mathbf{C}(k)$, $\mathbf{E}_d(k)$, $\mathbf{F}_d(k)$,$\mathbf{E}_f(k)$ and $\mathbf{F}_f(k)$ are time-varying matrices with appropriate dimensions.

To illustrate the state observer structure of (2.7), $\hat{\mathbf{x}}(k)$, $\hat{\mathbf{f}}(k)$ and $\hat{\mathbf{y}}(k)$ are firstly introduced, which are the estimates of $\mathbf{x}(k)$, $\mathbf{f}(k)$ and $\mathbf{y}(k)$, respectively. Then the state

observer is described by

$$\begin{aligned}\hat{\mathbf{x}}(k+1) &= \mathbf{A}(k)\hat{\mathbf{x}}(k) + \mathbf{B}(k)\mathbf{u}(k) + \mathbf{E}_f(k)\hat{\mathbf{f}}(k) + \mathbf{L}(k)\mathbf{r}(k)\\ \hat{\mathbf{f}}(k+1) &= \hat{\mathbf{f}}(k) + \mathbf{G}(k)\mathbf{r}(k)\\ \hat{\mathbf{y}}(k) &= \mathbf{C}(k)\hat{\mathbf{x}}(k) + \mathbf{F}_f(k)\hat{\mathbf{f}}(k)\\ \mathbf{r}(k) &= \mathbf{y}(k) - \hat{\mathbf{y}}(k)\end{aligned} \tag{2.8}$$

where $\mathbf{r}(k)$ is the residual signal. The matrices $\mathbf{L}(k)$ and $\mathbf{G}(k)$ are the so-called observer and estimator gains, respectively. There are also other FE method for this type of faults, such as fast adaptive FE algorithm [29, 93]. By introducing the estimation errors $\mathbf{e}_x(k) = \mathbf{x}(k) - \hat{\mathbf{x}}(k)$, $\mathbf{e}_f(k) = \mathbf{f}(k) - \hat{\mathbf{f}}(k)$ and $\mathbf{e}(k) = \begin{bmatrix} \mathbf{e}_x'(k) & \mathbf{e}_f'(k) \end{bmatrix}'$, the error dynamics are shown as follows

$$\begin{aligned}\mathbf{e}(k+1) &= (\mathbf{A}_o(k) - \mathbf{L}_o(k)\mathbf{C}_o(k))\mathbf{e}(k) + (\mathbf{B}_o(k) - \mathbf{L}_o(k)\mathbf{D}_o(k))\mathbf{d}(k)\\ \mathbf{r}(k) &= \mathbf{C}_o(k)\mathbf{e}(k) + \mathbf{D}_o(k)\mathbf{d}(k)\end{aligned} \tag{2.9}$$

where

$$\mathbf{A}_o(k) = \begin{bmatrix} \mathbf{A}(k) & \mathbf{E}_f(k) \\ \mathbf{0} & \mathbf{I}(k) \end{bmatrix},\ \mathbf{L}_o(k) = \begin{bmatrix} \mathbf{L}(k) \\ \mathbf{G}(k) \end{bmatrix},\ \mathbf{B}_o(k) = \begin{bmatrix} \mathbf{E}_d(k) \\ \mathbf{0} \end{bmatrix},$$
$$\mathbf{C}_o(k) = \begin{bmatrix} \mathbf{C}(k) & \mathbf{F}_f(k) \end{bmatrix},\ \mathbf{D}_o(k) = \mathbf{F}_d(k).$$

The choice of the observer gain $\mathbf{L}_o(k)$ is to keep the eigenvalues of $(\mathbf{A}_o(k) - \mathbf{L}_o(k)\mathbf{C}_o(k))$ in a unit circle, then the estimation errors are asymptotically convergent. By properly selecting the observer gain, the performance of FE will be improved.

In recent years, FE of dynamic systems have attracted much attention. Although fruitful results of FE have been obtained, most of the achieved results focus only on AFs, the research of FE methods for MFs has not acquired enough results as that for AFs. In the literature, MFs are also considered as time-varying parameters, and the system with MFs is called parameter varying system [94]. The research activities of FE method for MFs or time-varying parameters have been ongoing for years and some results have been obtained. For example, [95] addressed a joint estimation problem of parameter and state in the presence of perturbation on observer gain of nonlinear continuous-time systems. [96] proposed an adaptive method of joint state-parameter estimation in linear time-varying (LTV) multiple input multiple output (MIMO) systems. Upon this, several extended contributions of FE or FD schemes for continuous- and discrete-time systems from this group have been published [97**?** , 98]. In the practical projects, the newest control commands are executed on the plant at discrete-time instants, therefore, the FE methods for discrete-time systems have a wider range of application than that for continuous-time

systems. A weight estimation method for discrete-time Neural Net systems is presented in [99]. Recently, some results of FD schemes based on [99] for systems with AFs and MFs have been developed by this group [100–102], where the Frobenius norm has been widely used to obtain boundary values. Nonetheless, the existence of convergence conditions isn't so convincing when the disturbance exists in the system. An adaptive observer for FD in nonlinear discrete-time systems was proposed in [103], in which an adaptive update law for the parameter estimate has also been proposed. Unfortunately, the assumption, that the whole states are measurable, severely restricts the extensive application of this method. Besides, [98] proposed an efficient adaptive observer for discrete-time LTV system with zero mean noises. So far, the development of FE scheme for discrete-time systems with MFs is still an attractive issue.

In practice, the newest control commands are implemented on the plant digitally. Hence the FE methods for discrete-time systems are more meaningful, due to the strong engineering background, for instance, the typical NCSs [9, 26, 104]. Nevertheless, research activities on FD of discrete-time systems have been ongoing for decades, most of the achievements relay on the first two steps of FD technology, only a few attention has been paid in the researches of FE schemes for discrete-time systems. In [105], an FE approach for linear multi-input-multi-output (MIMO) stochastic discrete-time systems was studied, but the on-line fault estimate at time k needed the output vector at time $k+1$. Due to the introduction of an estimation delay, this method may not be suitable for real-time practical situation. A learning approximation approach was proposed in [106, 107], which assumed the faults belonging to a special structure and didn't take the requirement of FE performance into account. [98] presented an efficient adaptive observer for discrete-time LTV system with zero mean noises. Besides, the existing methods are mostly demonstrated by numerical examples or simulation results, few literature has presented the application results on practical systems. Therefore, how to reduce the aforementioned constraints in the development of FE method is still a very interesting and promising topic.

2.2.4 FTC strategies

In the literature, FTC strategies are developed with an assumption of a successful FD, which offers the information about the faults, such as the type and the magnitude of the fault. Under certain conditions, there is $\mathbf{f}(k) = \lim_{k\to\infty} \hat{\mathbf{f}}(k)$ [94, 108], where $\hat{\mathbf{f}}(k)$ is the fault estimate of fault $\mathbf{f}(k)$. Once a fault occurs, the FTC strategy is to modify the nominal control law to compensate the effects of the faults and reduce the performance degradation. In the following, some typical FTC strategies for systems with AFs and

MFs are presented, respectively.

An FTC strategy for AFs

When the actuator AFs occur as in (2.2), the actuator fault estimate $\hat{\mathbf{f}}_a(k)$ will be applied to accommodate the actuator fault $\mathbf{f}_a(k)$. The FTC law is to be designed as $\mathbf{u}_{FTC}(k) = \mathbf{u}_{nom}(k) - \hat{\mathbf{f}}_a(k)$, where $\mathbf{u}_{nom}(k)$ and $\mathbf{u}_{FTC}(k)$ are the nominal and fault tolerant controllers, respectively. Substituting this FTC law into the process (2.2), there is

$$\begin{aligned}\mathbf{x}(k+1) &= \mathbf{A}(k)\mathbf{x}(k) + \mathbf{B}(k)\mathbf{u}_{FTC}(k) + \mathbf{B}(k)\mathbf{f}_a(k) \\ &= \mathbf{A}(k)\mathbf{x}(k) + \mathbf{B}(k)\mathbf{u}_{nom}(k) + \mathbf{B}(k)(\mathbf{f}_a(k) - \hat{\mathbf{f}}_a(k)),\end{aligned} \tag{2.10}$$

In the case with a perfect FE [108], i.e., $\lim_{k\to\infty} \hat{\mathbf{f}}_a(k) = \mathbf{f}_a(k)$, the system will be tolerant to the actuator AFs.

When the sensor AFs happen as in (2.3), the FTC strategy for the output is designed as

$$\mathbf{y}_{FTC}(k) = \mathbf{y}(k) - \mathbf{F}_s\hat{\mathbf{f}}_s(k),$$

where $\hat{\mathbf{f}}_s(k)$ is the fault estimate of the sensor fault $\mathbf{f}_s(k)$, $\mathbf{y}(k)$ is the measurement output, $\mathbf{y}_{FTC}(k)$ is the output handled by the FTC strategy.

An FTC strategy for MFs

When it comes to deal with the actuator MFs as stated in (2.6), a significantly valuable method has been proposed in [94]. The FTC law for the i-th actuator is designed as

$$\begin{aligned}&\text{if } \hat{\theta}_i(k) \neq 0 \quad \text{then } u^i_{FTC}(k) = \hat{\theta}_i^{-1}(k)u^i_{nom}(k), \\ &\text{if } \hat{\theta}_i(k) = 0 \quad \text{then } u^i_{FTC}(k) = 0,\ i = 1, \cdots, p\end{aligned}$$

where $\hat{\theta}_i(k)$ is the parameter estimate of $\theta_i(k)$ and $u^i_{FTC}(k)$ is the practical actuator signal accommodated by the FTC strategy. If $\hat{\theta}_i(k) \neq 0$, we define $\mathbf{f}^{-1}_{\hat{\theta}}(k) = diag\{\cdots, \hat{\theta}_i^{-1}, \cdots\}$, $i = 1, \cdots, p$. The FTC strategy for actuators with MFs is designed as

$$\mathbf{u}_{FTC}(k) = \mathbf{f}^{-1}_{\hat{\theta}}(k)\mathbf{u}_{nom}(k),$$

where $\mathbf{u}_{nom}(k)$ and $\mathbf{u}_{FTC}(k)$ are the nominal and fault tolerant controllers, respectively. Substituting this control law into (2.6), there is

$$\begin{aligned}\mathbf{x}(k+1) &= \mathbf{A}(k)\mathbf{x}(k) + \mathbf{B}(k)\mathbf{f}_\theta(k)\mathbf{u}_{FTC}(k) \\ &= \mathbf{A}(k)\mathbf{x}(k) + \mathbf{B}(k)\mathbf{f}_\theta(k)\mathbf{f}^{-1}_{\hat{\theta}}(k)\mathbf{u}_{nom}(k) \\ &= \mathbf{A}(k)\mathbf{x}(k) + \mathbf{B}(k)\begin{bmatrix} \ddots & & \\ & \theta_i(k)\hat{\theta}_i^{-1}(k) & \\ & & \ddots \end{bmatrix}\mathbf{u}_{nom}(k).\end{aligned} \tag{2.11}$$

With a commendable parameter estimation method, there is $\hat{\theta}_i(k) = \theta_i(k)$, so $\theta_i(k)\hat{\theta}_i^{-1}(k) = 1$ and $\mathbf{f}_\theta(k)\mathbf{f}_{\hat{\theta}}^{-1}(k) = \mathbf{I}$. Therefore, the system is tolerant to the actuator MFs.

2.3 FTC schemes for LTP systems

With the increasing complexity of industrial processes, the requirements of the sampling rates of components or subsystems may vary due to the different functionalities or locations. By employing the multirate sampling and control, the system is formulated into periodic systems, where the processing efficiency will be greatly increased. Although LTP systems have been encountered in many different industrial automotive fields, e.g., power supply [109], electronics [110]. Only a few results about LTP systems can be found in the literature [111, 112], the research on LTP systems deserves more attentions.

The discrete LTP systems with the consideration of disturbances are formulated by the following state-space representation

$$\begin{aligned} \mathbf{x}(k+1) &= \mathbf{A}(k)\mathbf{x}(k) + \mathbf{B}(k)\mathbf{u}(k) + \mathbf{E}_d(k)\mathbf{d}(k) \\ \mathbf{y}(k) &= \mathbf{C}(k)\mathbf{x}(k) + \mathbf{F}_d(k)\mathbf{d}(k) \end{aligned} \tag{2.12}$$

where $\mathbf{x} \in \Re^{n(k)}$, $\mathbf{u} \in \Re^{p(k)}$ and $\mathbf{y} \in \Re^{m(k)}$ are the system state vector, control input vector and measurement output vector with time-varying dimensions, respectively. $\mathbf{d}(k) \in \Re^{d(k)}$ denotes the disturbance. $\mathbf{A}(k)$, $\mathbf{B}(k)$, $\mathbf{C}(k)$, $\mathbf{E}_d(k)$ and $\mathbf{F}_d(k)$ are real periodic matrices with appropriate dimensions, which satisfy

$$\begin{aligned} \mathbf{A}(k) = \mathbf{A}(k+\mu),\ \mathbf{B}(k) = \mathbf{B}(k+\mu),\ \mathbf{C}(k) = \mathbf{C}(k+\mu), \\ \mathbf{E}_d(k) = \mathbf{E}_d(k+\mu),\ \mathbf{F}_d(k) = \mathbf{F}_d(k+\mu), \end{aligned}$$

where μ is a positive constant integer, which denotes the system time period.

To clearly distinguish the system period from the fragments within the period, model (2.12) can be further formulated [21] into

$$\begin{aligned} \mathbf{x}(k, j+1) &= \mathbf{A}(j)\mathbf{x}(k,j) + \mathbf{B}(j)\mathbf{u}(k,j) + \mathbf{E}_d(j)\mathbf{d}(k,j) \\ \mathbf{y}(k,j) &= \mathbf{C}(j)\mathbf{x}(k,j) + \mathbf{F}_d(j)\mathbf{d}(k,j),\ j = 1, \cdots, \mu \end{aligned} \tag{2.13}$$

where (k, j) denotes the j-th time segment in k-th system period T_p. The state observer for (2.13) is constructed as

$$\begin{aligned} \hat{\mathbf{x}}(k, j+1) &= \mathbf{A}(j)\hat{\mathbf{x}}(k,j) + \mathbf{B}(j)\mathbf{u}(k,j) + \mathbf{L}(j)\mathbf{r}(k,j) \\ \hat{\mathbf{y}}(k,j) &= \mathbf{C}(j)\hat{\mathbf{x}}(k,j),\ j = 1, \cdots, \mu \end{aligned} \tag{2.14}$$

$$\mathbf{r}(k,j) = \mathbf{y}(k,j) - \hat{\mathbf{y}}(k,j) \tag{2.15}$$

where $\hat{\mathbf{x}}(k,j)$ and $\hat{\mathbf{y}}(k,j)$ are the estimates of $\mathbf{x}(k,j)$ and $\mathbf{y}(k,j)$, respectively. $\mathbf{r}(k,j)$ is the residual signal. $\mathbf{L}(j)$ is the periodic observer gain.

We define the estimation error $\mathbf{e}(k,j) = \mathbf{x}(k,j) - \hat{\mathbf{x}}(k,j)$, then the error dynamics is

$$\begin{aligned} \mathbf{e}(k,j+1) &= (\mathbf{A}(j) - \mathbf{L}(j)\mathbf{C}(j))\mathbf{e}(k,j) + (\mathbf{E}_d(j) - \mathbf{L}(j)\mathbf{F}_d(j))\mathbf{d}(k,j) \\ \mathbf{r}(k,j) &= \mathbf{C}(j)\mathbf{e}(k,j) + \mathbf{F}_d(j)\mathbf{d}(k,j) \end{aligned} \tag{2.16}$$

The key issue of observer construction is to find the observer gain $\mathbf{L}(j)$, which keeps the eigenvalues of $(\mathbf{A}(j) - \mathbf{L}(j)\mathbf{C}(j))$ in a unit cycle and the convergence of the error dynamics system.

For a large-scale complex system, discrete LTP system model could distinctly express the behaviors of multirate sampling in the subsystems. Due to the distribution character of the subsystems and the limitation of the communication bandwidth in the large-scale complex system, it leads to the structure limitations in the observer gain $\mathbf{L}(j)$. When a fault occurs, it also requires a distributed FTC strategy, i.e., a structure-limited control law. Since the W-NCSs can be formulated as an integration of a scheduler and discrete LTP systems [21], where the scheduler plays a significant role in the development of FTC scheme for the discrete LTP systems, the design of FTC strategy for W-NCSs with an integrated scheduler will be the major research object in this thesis.

2.4 Summary

In this chapter, we briefly recall the wireless network scheduling schemes, including the wireless network protocols, time synchronization and scheduling algorithms (especially for TDMA mechanism). Time synchronization plays an important role in the realization of TDMA mechanism on wireless network for a given network topology. The principles of scheduling algorithms of wireless TDMA protocol are simply presented. The faults during the process can be classified as AFs and MFs. According to the types of faults, the corresponding FE and FTC strategies are broadly discussed. Based on these preliminary knowledge, the design of FTC strategies for W-NCSs with an integrated scheduler will be the major research object in the following chapters.

3 Modeling of W-NCS schedulers

This chapter introduces the procedures of reformulation from the information scheduler to a mathematical scheduler matrix with the consideration of QoS parameters, such as time delay and packet loss. In view of control theory, the mathematical scheduler matrix is restructured into a state-space representation in three cases.

3.1 Basic method of scheduler reformulation

The task of network scheduling for W-NCSs is to assign a transmission order (i.e., certain time slots) to all transmission entities (such as sensors, controllers and actuators) over the network based on a scheduling algorithm [113]. Following the scheduler, all the information generated by the transmission entities will be sent out onto the network at a scheduled starting time and arrive their destinations at a scheduled arriving time. According to the operation mechanism of W-NCSs, these information may include the sampled data from sensors to controller, the control commands from controller to actuators, synchronization and configuration messages, etc. Actually, in order to fulfill the requirement for deterministic transmission behaviors, as well as the high real-time ability and reliability, TDMA communication mode is widely adopted in industrial automatic control systems [21].

Since a great deal of research activities have been contributed to the study of scheduling design and quite rich outcomes have been achieved by now, see the survey papers [8, 9, 114] and the references therein, we are not going to reduplicate the procedure of this work. It is remarkable that the scheduler generated from the scheduling algorithms is called information scheduler and the design of information schedulers is usually limited in a fixed duration of time T, which is also considered as the period of the scheduler. The communication will continue strictly following this scheduler periodically. It is supposed that, the information scheduler used here has been scheduled off-line and is a static known scheduler, which is also identical to the requirement for deterministic transmission behaviors over wireless networks. The information scheduler is expressed as a Boolean matrix $\mathbf{S} \in \Re^{s_1 \times s_2}$ $(s_1, s_2 \in \mathrm{Z}^+)$. s_1 refers to the number of time slots for completing all the transmissions, s_2 is the number of transmission data. Normally, the duration for one hop in TDMA mode is considered as one T_{hop}. S_{ji} denotes the item of $\mathbf{S}$ at the j-th row

and the i-th column. $S_{ji} = 1$ means that the i-th datum has been scheduled one hop at the j-th T_{hop}. while, $S_{ji} = 0$ means that no mission has been scheduled at this T_{hop}.

Our subsequent study is based on a fault tolerant W-NCSs integrated with the scheduler. However, the information schedulers cannot be adopted directly. Some transformations of the information scheduler are required in advance.

In an industrial NCS, the time for generating a datum is usually in a fixed slot (according to the cycle of sampling and control). Due to the limited network communication resources, the new generated datum needs to wait for some slots before getting its permission to access the network. Sometimes, it has to wait on the network during its way to the destination. In order to describe the required time for the whole transmission of the i-th datum in the information schedule $\mathbf{S}$, we define h_i^w and h_i^t, $i = 1, \cdots, s_2$ as the numbers of required waiting and transmission hops for the i-th datum from its generation to the arrival of its destination, respectively. So the required time t_i for the i-th datum to complete the transmission can be achieved by $t_i = (h_i^w + h_i^t) \times T_{hop}$. The scheduler period T is divided as $T = rT_{slot}$, where r is a positive integer, T_{slot} is a unit of time slices. According to a control strategy, the controller will determine whether to handle the received data or not at the current T_{slot}. In the practical industrial processes, the handling interval is always bigger than one hop, so there exists $T_{hop} \leq T_{slot} \leq T$. In order to decide the effect of delay caused by the information scheduler, the delay decision logic is defined as follows

$$\tau_i = \lceil t_i / T_{slot} \rceil, (t_i > 0) \tag{3.1}$$

Notation $\lceil \bullet \rceil$ gets the nearest integers of $\bullet$ towards positive infinity. It is remarkable that if the datum arrives its destination before the handling, i.e., $0 < t_i < T_{slot}$, no delay will be considered. In this case we take τ_i as '1', for the convenience of our further study.

Define delay coefficient matrix $\mathbf{D_e} = \text{diag}\{\cdots, \tau_i, \cdots\}$ $(i = 1, \cdots, s_2)$ and packet loss coefficient matrix $\mathbf{P_l} = \text{diag}\{\cdots, P_{l,i}, \cdots\}$ $(i = 1, \cdots, s_2)$, where if packet loss happens, then $P_{l,i} = 0$, otherwise $P_{l,i} = 1$. So the scheduler-induced effect $\eta \in \Re^{s_2 \times s_2}$ is expressed as

$$\eta = \mathbf{P_l} \times \mathbf{D_e}. \tag{3.2}$$

Remark 3.1. *Here we have only considered time delay and packet loss. The other network induced effects, e.g., bit error, can also be defined as relevant coefficient matrices.*

It is obvious that η is a diagonal matrix. We denote η_i as the i-th item at the diagonal of η. With some logical conversion, the information scheduler will be expressed in a new matrix with the key information contained in η. This new matrix is named with the mathematical scheduler $\mathbf{S_m}$. The steps of logical conversion are described as follows:

Step 1: Define a zero matrix $\mathbf{O}_{r\times s_2}$. It is supposed that the i-th datum is generated at the g_i-th T_{slot}. According to η_i, set '1' to the item at the $(\eta_i + g_i - 1)$-th row and i-th column.

Step 2: compressing the Boolean matrix by deleting the full-zero rows. $\mathbf{S_m}$ denotes the finally compressed matrix.

Therefore, after transmitting following the information scheduler $\mathbf{S}$, a group of data $\{D_i\}$, $i = 1, \cdots, s_2$ will be in a new order and can be described as

$$\begin{bmatrix} \vdots \\ D_j \\ \vdots \end{bmatrix} = \mathbf{S_m} \begin{bmatrix} \vdots \\ D_i \\ \vdots \end{bmatrix}, \ i = 1, \cdots, s_2 \tag{3.3}$$

In the case with packet loss, the row of $\mathbf{S_m}$ is less than s_2, so does j. For the ease of reference, an example is given here.

Example 3.1. *See Fig.3.1, four data D_i, $i = 1, \cdots, 4$ (generated by the local nodes at the same time) are going to be transmitted to a central node. It is assumed that, each node works at a half-duplex mode, which means each node can only transmit or receive one datum at each hop. Due to these limitations, the information scheduler is designed as in $\mathbf{S}$. It is noted that 5 T_{hop}s are required to finish the transmissions for four data.*

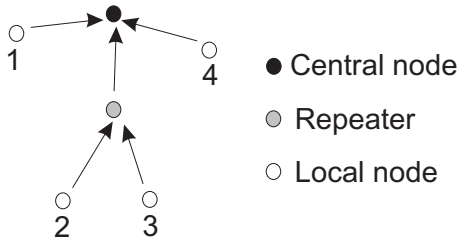

Figure 3.1: A scheduler for four data

$$\mathbf{S} = \begin{bmatrix} 1 & 1 & 0 & 0 \\ 0 & 0 & 0 & 1 \\ 0 & 1 & 0 & 0 \\ 0 & 0 & 1 & 0 \\ 0 & 0 & 1 & 0 \end{bmatrix}, \ \mathbf{D_e} = \begin{bmatrix} 1 & & & \\ & 3 & & \\ & & 5 & \\ & & & 2 \end{bmatrix}.$$

From $\mathbf{S}$ *we obtain the delay coefficient matrix* $\mathbf{D_e}$. *No packet loss happens,* $\mathbf{P_l} = \mathbf{I}_{4\times4}$. *So* $\eta = \mathbf{D_e}$. *Following the steps of logical conversion, we have*

$$\begin{bmatrix} 1 & 0 & 0 & 0 \\ 0 & 0 & 0 & 1 \\ 0 & 1 & 0 & 0 \\ 0 & 0 & 0 & 0 \\ 0 & 0 & 1 & 0 \end{bmatrix} \Rightarrow \mathbf{S_m} = \begin{bmatrix} 1 & 0 & 0 & 0 \\ 0 & 0 & 0 & 1 \\ 0 & 1 & 0 & 0 \\ 0 & 0 & 1 & 0 \end{bmatrix}.$$

Therefore, there is

$$\begin{bmatrix} D_1 \\ D_4 \\ D_2 \\ D_3 \end{bmatrix} = \mathbf{S_m} \begin{bmatrix} D_1 \\ D_2 \\ D_3 \\ D_4 \end{bmatrix}.$$

3.2 State-space representation of W-NCS schedulers

In the literature, the information scheduler has been expressed in terms of two modes:

(1) Matrix: with items '0' and '1' [24, 25], where '1' means some node has the right to access the communication medium at the corresponding slot, while '0' means no right to access at the current slot;

(2) State-space representation: The scheduler is considered as an LTI system [115] and the QoS parameters are reflected on the system matrices [116].

Although, the cores of these two forms are interconnected, the scheduler in the second mode is taken as a dynamic system, where the dynamics characters of network can be expressed better. Hence, the scheduler in the pattern of state-space representation is preferable to that in a matrix form during our study. However, details are lacked in the literature about how to obtain the state-space representation of the scheduler, which is very necessary for the process of integrating the scheduler into W-NCSs, so we're inspired to supplement this part of work.

We concentrate on the industrial control processes with wireless networks. The wireless network is demonstrated in the form of a scheduler. Fig.3.2 shows the basic structure of a feedback control system with an information scheduler, in which P, Sc and K denote the plant, the scheduler and the controller, respectively. The sampled data y (containing the information of the plant) are periodically sent to the controller via a wireless network. y_s is the output of the scheduler with input y. On the basis of the received data, a new

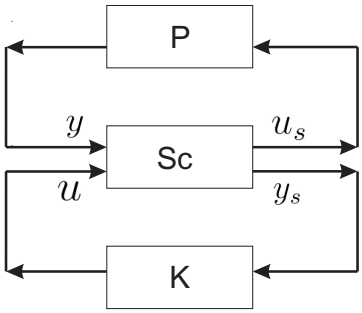

Figure 3.2: System structure with a scheduler

control command u will be produced by the controller and sent back to the plant through the wireless network. The plant is also controlled by the feedback control commands periodically. u_s is the output of the scheduler corresponding to the input u. The period of the whole feedback control system is set as T. There are two issues should be concerned in the design of information schedulers for one period T: one is the network topology, such as one-hop network, multi-hop network, etc; the other one is the communication requirement. there may be once or multiple samplings in one period. Meanwhile, once or multiple commands will be calculated and executed on the plant according to the system demands. Following the basic method of scheduler reformulation in the last subsection, a corresponding mathematical scheduler $\mathbf{S_m}$ is produced. Since the control command will always be calculated based on the received data and sent out after the calculation, from Fig.3.2, there is

$$\begin{bmatrix} y_s \\ u_s \end{bmatrix} = \mathbf{S_m} \begin{bmatrix} y \\ u \end{bmatrix}. \tag{3.4}$$

In view of control theory, we are going to construct the state-space representation of the scheduler with the help of the mathematical scheduler $\mathbf{S_m}$ from the following three cases: (1) once-sampling-once-control with single-hop network; (2) once-sampling-once-control with multi-hop network; (3) multi-sampling-multi-control with multi-hop network.

3.2.1 Once-sampling-once-control with single-hop network

In a single-hop wireless network, all local nodes surround the central node in one hop distance, see (a) in Fig.3.3, where only one transmission (sending or receiving) in one hop T_{hop} is allowed. In the case with once control in a period T, we have $T_{slot} = T$. For an once-sampling-once-control system, each local node only samples once and only one control command will be generated by the central node in each period T. After synchronization, all the local nodes sample their data at the k-th T. In this case, all the

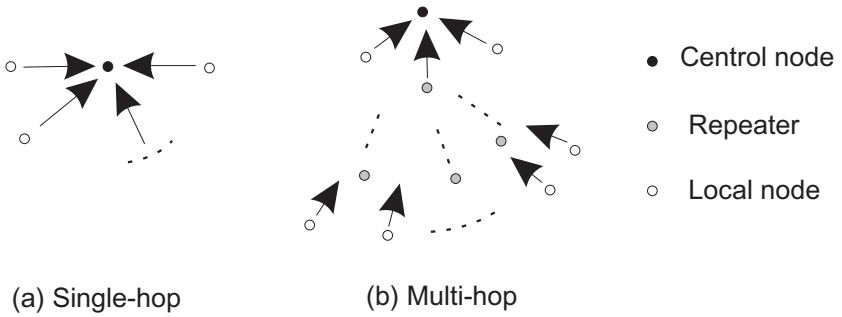

Figure 3.3: Network topologies

local nodes transmit their data to the central node one by one. Suppose n sampled data $\{y_1(k), y_2(k), \cdots, y_n(k)\}$ are scheduled to be transmitted to the central node. Obviously, the information scheduler $\mathbf{S^y} = \mathbf{I}_n$. Following the basic method of scheduler reformulation, the mathematical scheduler for the sampled data $\mathbf{S^y_m} = \mathbf{I}_n$. With the sampled data, a control command $u(k)$ will be generated and broadcast to the local nodes, so the information scheduler $S^u = 1$ and the mathematical scheduler for the control command $S^u_m = 1$. Therefore, we have

$$\mathbf{S_m} = \begin{bmatrix} \mathbf{S^y_m} & \\ & S^u_m \end{bmatrix} = \mathbf{I}_{n+1}.$$

Define $\mathbf{y}(k)$, $\mathbf{a}_i \in \Re^{n\times 1}$, $i = 1, \cdots, n$ and b as follows

$$\mathbf{y}(k) = \begin{bmatrix} y_1(k) \\ y_2(k) \\ \vdots \\ y_n(k) \end{bmatrix}, \mathbf{a}_1 = \begin{bmatrix} 1 \\ 0 \\ \vdots \\ 0 \end{bmatrix}, \mathbf{a}_2 = \begin{bmatrix} 0 \\ 1 \\ \vdots \\ 0 \end{bmatrix}, \cdots, \mathbf{a}_n = \begin{bmatrix} 0 \\ \vdots \\ 0 \\ 1 \end{bmatrix}, b = 1. \tag{3.5}$$

From equation (3.4), we have

$$\begin{aligned} \mathbf{y}_s(k) &= \begin{bmatrix} 1 & & & \\ & 1 & & \\ & & \ddots & 0 \\ & & & 1 \end{bmatrix} \begin{bmatrix} \mathbf{y}(k) \\ u(k) \end{bmatrix} \\ &= \mathbf{a}_1 y_1(k) + \mathbf{a}_2 y_2(k) + \cdots + \mathbf{a}_n y_n(k), \end{aligned} \tag{3.6}$$

$$u_s(k) = \begin{bmatrix} 0 & 1 \end{bmatrix} \begin{bmatrix} y(k) \\ u(k) \end{bmatrix} = bu(k). \tag{3.7}$$

Set $\psi_s(k) = \begin{bmatrix} y_1'(k-1) & \cdots & y_n'(k-1) & u'(k-1) \end{bmatrix}'$. The state equation for (3.4) in the case of once-sampling-once-control with single-hop network can be expressed as

$$\begin{aligned} \psi_s(k+1) &= \mathbf{A}_s\psi_s(k) + \mathbf{B}_s^y\mathbf{y}(k) + \mathbf{B}_s^u u(k) \\ \mathbf{y}_s(k) &= \mathbf{C}_s^y\psi_s(k) + \mathbf{D}_s^y\mathbf{y}(k) \\ u_s(k) &= \mathbf{C}_s^u\psi_s(k) + \mathbf{D}_s^u u(k) \end{aligned} \tag{3.8}$$

where

$$\mathbf{A}_s = \mathbf{O}_{(n+1)\times(n+1)}, \mathbf{B}_s^y = \begin{bmatrix} \mathbf{I}_{n\times n} \\ \mathbf{O}_{1\times n} \end{bmatrix}, \mathbf{B}_s^u = \begin{bmatrix} \mathbf{O}_{n\times 1} \\ 1 \end{bmatrix},$$
$$\mathbf{C}_s^y = \mathbf{O}_{n\times(n+1)}, \mathbf{C}_s^u = \mathbf{O}_{1\times(n+1)}, \mathbf{D}_s^y = \mathbf{I}_{n\times n}, \mathbf{D}_s^u = 1.$$

3.2.2 Once-sampling-once-control with multi-hop network

In this case, the positions of the local nodes are out of one hop distance from the central node, so the sampled data have to take multi-hops to arrive the central node, see (b) in Fig.3.3. Multi-hop TDMA scheduling is more challenging than one-hop scheduling, because of the possibility of spatial reuse in a T_{hop}. On one hand, more than one node can transmit at the same T_{hop}, if their receivers are in non-conflicting parts of the network. On the other hand, after the successful transmission of the first datum into the network, the next datum from the same node will be sent into the network when the receiver is in non-conflicting parts of the network. That means the latter datum will be sent into the wireless network not until the former datum arrives the central node.

Since the control command is required only once in this case, we still have $T_{slot} = T$. Although only one datum is generated by one local node in a T, the datum generated in the periods before k-th T may arrive the central node in the k-th T due to the long distance from the local node to the central node. The information scheduler for the sampled data $\mathbf{S^y}$, including the rich information of time delay and packet loss, will be much more complex than the one for the case with single-hop network. Therefore, the mathematical scheduler $\mathbf{S_m^y}$ might not be an identity matrix. Since only one control command will be generated in each T and broadcast to the local nodes, so the information scheduler $S^u = 1$ and the mathematical scheduler for the control command $S_m^u = 1$. Here we still have

$$\mathbf{S_m} = \begin{bmatrix} \mathbf{S_m^y} & \\ & S_m^u \end{bmatrix}.$$

The major difference from the case with single-hop network is that, the Boolean matrix $\mathbf{S_m^y}$ isn't an identity matrix. However, we still can construct the state-space representation in

a similar way as that in the former subsection. Considering the timeliness of the sampled data, only the data sampled in the $(k-1)$-th T will be taken into account in the k-th T.

It is assumed that n data $\{y_1(k), \cdots, y_n(k)\}$ are generated in the k-th T. n_d sampled data are scheduled to be delay in each T, and $(n-n_d)$ data generated in k-th T can arrive on time in k-th T. Denote $\mathbf{y_d}(k-1) \in \Re^{n_d}$ as the set of delayed data $\{y_i^d(k-1)\},\ i = 1, \cdots, n_d$ and $\mathbf{y_c}(k) \in \Re^{n-n_d}$ as the set of data $\{y_j^c(k)\},\ j = 1, \cdots, n-n_d$ which are generated and arrive the central node in the current k-th T. $u(k)$ is the control command.

It's obvious that $\mathbf{S_m} \in \Re^{(n+1)\times(n+1)}$ and $\mathbf{S_m^y} \in \Re^{n\times n}$. Denote $\mathbf{a}_i,\ i = 1, \cdots, n$ as the i-th column of $\mathbf{S_m^y}$ and $b = 1$. The mathematical scheduler $\mathbf{S_m}$ can be expressed as

$$\mathbf{S_m} = \begin{bmatrix} \mathbf{a}_1 & \mathbf{a}_2 & \cdots & \mathbf{a}_n & \mathbf{0} \\ 0 & 0 & \cdots & 0 & b \end{bmatrix}. \tag{3.9}$$

According to equation (3.4),

$$\begin{aligned} \mathbf{y}_s(k) &= \begin{bmatrix} \mathbf{a}_1 & \mathbf{a}_2 & \cdots & \mathbf{a}_n & \mathbf{0} \end{bmatrix} \begin{bmatrix} \mathbf{y_d}(k-1) \\ \mathbf{y_c}(k) \\ u(k) \end{bmatrix} \\ &= \mathbf{a}_1 y_1^d(k-1) + \cdots + \mathbf{a}_{n_d} y_{n_d}^d(k-1) + \mathbf{a}_{n_d+1} y_1^c(k) + \cdots + \mathbf{a}_n y_{n-n_d}^c(k), \end{aligned} \tag{3.10}$$

$$u_s(k) = \begin{bmatrix} 0 & \cdots & 0 & b \end{bmatrix} \begin{bmatrix} \mathbf{y_d}(k-1) \\ \mathbf{y_c}(k) \\ u(k) \end{bmatrix} = bu(k). \tag{3.11}$$

Define $\mathbf{y}(k) = \begin{bmatrix} y_1'(k) & \cdots & y_n'(k) \end{bmatrix}'$ and $\psi_s(k) = \begin{bmatrix} \mathbf{y}'(k-1) & u'(k-1) \end{bmatrix}'$. Similar to (3.8), we have the state-space representation as follows

$$\begin{aligned} \psi_s(k+1) &= \mathbf{A}_s \psi_s(k) + \mathbf{B}_s^y \mathbf{y}(k) + \mathbf{B}_s^u u(k) \\ \mathbf{y}_s(k) &= \mathbf{C}_s^y \psi_s(k) + \mathbf{D}_s^y \mathbf{y}(k) \\ u_s(k) &= \mathbf{C}_s^u \psi_s(k) + \mathbf{D}_s^u u(k) \end{aligned} \tag{3.12}$$

where

$$\mathbf{A}_s = \mathbf{O}_{(n+1)\times(n+1)}, \mathbf{B}_s^y = \begin{bmatrix} \mathbf{I}_{n\times n} \\ \mathbf{O}_{1\times n} \end{bmatrix}, \mathbf{B}_s^u = \begin{bmatrix} \mathbf{O}_{n\times 1} \\ 1 \end{bmatrix}, \mathbf{C}_s^u = \mathbf{O}_{1\times(n+1)}, \mathbf{D}_s^u = 1,$$

$\mathbf{C}_s^y \in \Re^{n\times(n+1)}$ and $\mathbf{D}_s^y \in \Re^{n\times n}$ are related to $\{\mathbf{a}_1, \cdots, \mathbf{a}_{n_d}\}$ and $\{\mathbf{a}_{n_d+1}, \cdots, \mathbf{a}_n\}$, respectively. It is remarkable that the scheduled delay reflects on $\mathbf{C}_s^y$. The role of $\mathbf{D}_s^y$ is to retain the data which are scheduled to arrive the central node in the current k-th T.

3.2.3 Multi-sampling-multi-control with multi-hop network

In a complex large-scale system, there are multiple samplings and multiple controls in a period T. The complicated topology of multi-hop network also brings a lot of complexity into the design of information schedulers. However, one rule still can been found in the scheduler: After several samplings, one control command will be generated. We suppose that n control commands are generated in each T. One period T has been divided into n time slices according to the transmission instants for control commands. So the information scheduler for each T can be noted as

$$\mathbf{S} = \begin{bmatrix} \vdots \\ \mathbf{S}(i) \\ \vdots \end{bmatrix} = \begin{bmatrix} \vdots & \\ \mathbf{S^y}(i) & \\ & \mathbf{S^u}(i) \\ \vdots & \end{bmatrix}, \ i = 1, \cdots, n$$

The corresponding mathematical scheduler is expressed as

$$\mathbf{S_m} = \begin{bmatrix} \vdots \\ \mathbf{S_m}(i) \\ \vdots \end{bmatrix} = \begin{bmatrix} \vdots & \\ \mathbf{S_m^y}(i) & \\ & \mathbf{S_m^u}(i) \\ \vdots & \end{bmatrix}, \ i = 1, \cdots, n$$

We denote n_i^s as the number of data which will be sampled during the i-th time slice. n_i^r is the number of data which will be received by the central node during the i-th time slice. Due to delay in the network, some of these data may have been sampled several time slices ago. Considering the timeliness, we only concern the data, which have been sampled in one period T before the generation of the i-th control command. The number of all the generated data (including sampled data and control commands) in one period T, $m = \sum_{i=1}^{n}(n_i^s + n)$. In the case with delay, there is $m = \sum_{i=1}^{n}(n_i^r + n)$. When the packet loss is scheduled in the scheduler, there is $m \geq \sum_{i=1}^{n}(n_i^r + n)$. Define $\mathbf{y}(k,i)$ and $u(k,i)$ as the sampled data and the control command in the i-th time slices of the k-th period T. Set $\psi_s(k,i) = \begin{bmatrix} \mathbf{y}'(k-1,i) & u'(k-1,i) & \cdots & \mathbf{y}'(k,i-1) & u'(k,i-1) \end{bmatrix}'$. Partitioning $\mathbf{S_m}(i)$ in a similar way as (3.10)-(3.11), we have the state-space representation as follows

$$\begin{aligned} \psi_s(k,i+1) &= \mathbf{A}_s(i)\psi_s(k,i) + \mathbf{B}_s^y(i)\mathbf{y}(k,i) + \mathbf{B}_s^u u(k,i) \\ \mathbf{y}_s(k,i) &= \mathbf{C}_s^y(i)\psi_s(k,i) + \mathbf{D}_s^y(i)\mathbf{y}(k,i) \\ u_s(k,i) &= \mathbf{C}_s^u(i)\psi_s(k,i) + \mathbf{D}_s^u(i)u(k,i) \end{aligned} \tag{3.13}$$

where $\mathbf{y}_s(k,i) \in \Re^{n_i^r \times 1}$, $\mathbf{y}(k,i) \in \Re^{n_i^s \times 1}$,

$$\mathbf{A}_s(i) = \begin{bmatrix} \mathbf{O}_{(m-n_i^s-1)\times(n_i^s+1)} & \mathbf{I}_{(m-n_i^s-1)\times(m-n_i^s-1)} \\ \mathbf{O}_{(n_i^s+1)\times(n_i^s+1)} & \mathbf{O}_{(n_i^s+1)\times(m-n_i^s-1)} \end{bmatrix},$$

$$\mathbf{B}_s^y(i) = \begin{bmatrix} \mathbf{O}_{(m-n_i^s-1)\times n_i^s} \\ \mathbf{I}_{n_i^s \times n_i^s} \\ \mathbf{O}_{1\times n_i^s} \end{bmatrix}, \mathbf{B}_s^u(i) = \begin{bmatrix} \mathbf{O}_{(m-n_i^s-1)\times 1} \\ \mathbf{O}_{n_i^s \times 1} \\ 1 \end{bmatrix},$$

$$\mathbf{C}_s^u(i) = \mathbf{O}_{1\times m},\ \mathbf{D}_s^u(i) = 1,$$

$\mathbf{C}_s^y(i) \in \Re^{n_i^r \times m}$ is related to the part of scheduled delay data which will be received in the i-th time slice. $\mathbf{D}_s^y(i) \in \Re^{n_i^r \times n_i^s}$ contains the scheduler for the data which will arrive the central node in the current T.

3.3 Summary

In this chapter, we have introduced the concept of a mathematical scheduler. The basic method of transformation from an information scheduler to a mathematical scheduler has been elaborated. In order to embody the control principle, the mathematical scheduler has been reformulated into a form of state-space representation. In view of control requirement and network topology, three cases have been concerned: 1) once sampling and once control in a period T with single-hop network; 2) once sampling and once control in a period T with multi-hop network; 3) multiple samplings and multiple controls in a period T with multi-hop network.

4 Modeling of W-NCSs

This chapter describes the modeling of W-NCSs with an integrated scheduler. The integrated systems are demonstrated in a form of discrete LTP systems. The scheduler is also formulated as a periodic system.

4.1 Communication mechanism on W-NCSs

During the last few years, there has being considerable interest in the development of NCSs. These developments have been advanced by technological progress in wired or wireless communications and real-time distributed algorithms, as well as by the demand for handling more complex large-scale systems of practical importance, such as manufacturing, transportation, power systems and mobile robotics, etc.

As an integrated design framework of fault tolerant W-NCSs for industrial automatic control applications, [21] has proposed a fault tolerant W-NCSs structure as shown in Fig.4.1 [21]. This structure aims at achieving high reliability and meeting the demands for control performances, as well as remaining the original process structure as much as possible. The fault tolerant W-NCSs structure consists of three functional layers: Execution layer, Coordination & Supervision layer and Management layer. Each layer supports a specific responsibility by its own communication mechanism.

4.1.1 Communication mechanism at Execution layer

This layer is located at the industrial field, where the process is divided into N subprocesses. For the i-th subprocess, M_i feedback local control loops, which are integrated by the local controllers (LCs) with the embedded sensors and actuators, are applied to regulate and achieve the technical requirements on the control performance.

For a complex large-scale systems, each subprocess might have different cycle. In one cycle, the time slots are reserved for (1) the transmissions of sensor data to the control stations (CSs); (2) the transmissions of control commands from the CSs to the LCs; (3) calculation and implementation of the communication strategies. All these communication actions can improve the W-NCSs reliability considerably and efficiently.

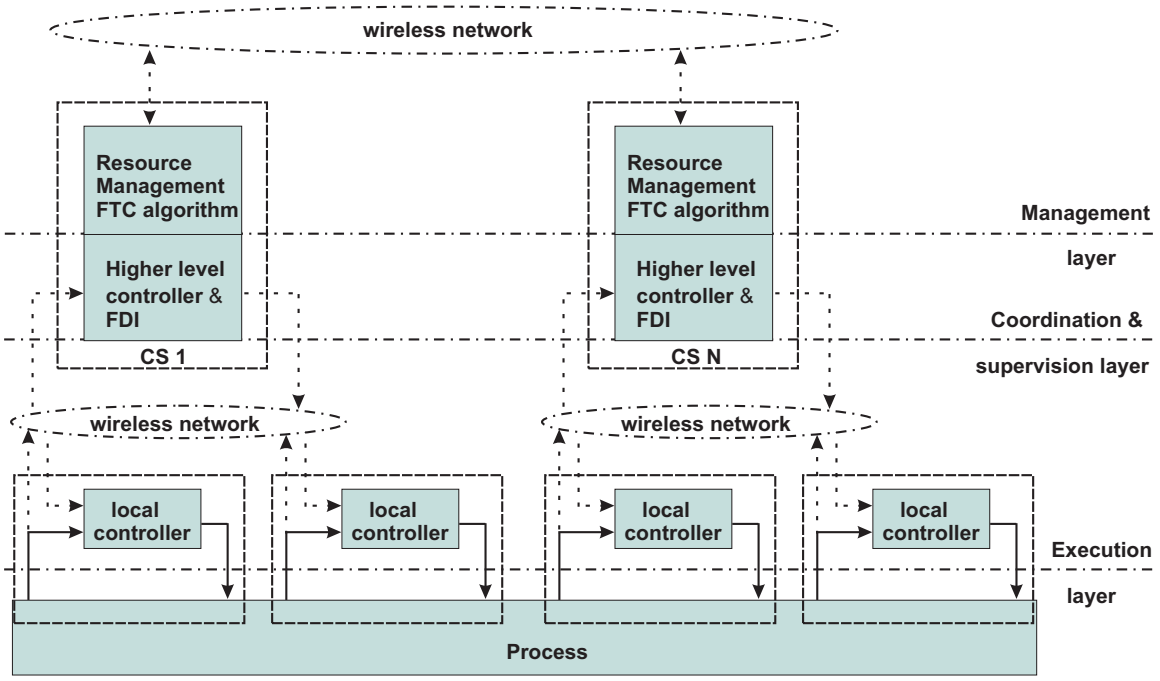

Figure 4.1: Structure of fault tolerant W-NCSs

Denote $T_{c,i}$ as the cycle of the i-th subprocess. During each $T_{c,i}$, all the sensors in the M_i local control loops will sample the local data and send them to their local controllers. Instead of delivering these sampled data directly to the higher layer, some primary processes will be done by the local controllers, such as obtaining the residuals and proceeding an early and simple fault detection and isolation (FDI), etc. Different from most theoretical and application studies in control systems, the residuals instead of the measurement outputs will be delivered to the CSs at the Coordination & Supervision layer immediately after they are generated. Since the value range of residuals are generally smaller than the originally sampled data, the transmission traffic will be reduced, meanwhile, more free communication channels will be offered for some critical data packets. Moreover, the residuals contains all the information needed for controllers and observers, therefore, transmitting residuals will not lose the needed information.

We assume that the states of the subprocesses are unaccessible or only partial available. The state estimate will be transmitted from the i-th CS via a wireless network and shared by the LCs of the i-th subprocess. It motivates us to write the state estimate from the i-th CS and other relative information (such as reference signal and fault estimate) in one packet, which will be multi-cast from the i-th CS to its LCs. After receiving the packet from the i-th CS, the LCs will decode this packet for the state estimate and the relative information. Following a local control strategy, the local feedback control loops ensure

the system stability in the totally decentralized mode.

4.1.2 Communication mechanism at Coordination & Supervision layer

The Coordination & Supervision layer comprises of N CSs. Each CS supervises a number of local feedback control loops at the Execution layer. Based on the received residuals from the M_i local controllers, the state of the i-th subprocess will be estimated by the i-th CS. Meanwhile, comprehensive FDI algorithms are executed in CSs for an advanced FDI, which will provide the occurrence information of the faults on the i-th subprocess. Afterwards, the state estimate, as well as other important information about the i-th subprocess (e.g., the fault estimate and the reference signals), will be packed together and multi-cast to its LCs.

Since the existence of coupling among subprocesses, the state of the i-th subprocess is also very important to the other CSs. Therefore, the i-th CS will share its state estimate with other CSs periodically. The state estimates from other CSs will also improve the state estimate of the i-the subprocess. Therefore, CSs are also considered as higher level controllers. For the sake of achieving the required control performance, another task of the CSs is to coordinate and synchronize the communication operations all over the W-NCSs.

We call the i-th CS and the i-th subprocess, as well as the M_i feedback local control loops as the i-th subsystem. $T_{c,i}$ is the cycle of the i-th subsystem. $T_{c,min}$ denotes the greatest common divisor (GCD) of $T_{c,i}$, $i = 1, \cdots, N$. The least common multiple (LCM) of $T_{c,i}$, $i = 1, \cdots, N$ is denoted as T_p, which is also the period of the overall W-NCSs. As a TDMA-based W-NCSs, the scheduler for the communication actions during one T_p all over the W-NCSs is very helpful to achieve the synchronization in the subsystems. An important definition has been presented in [21].

Definition 4.1. *[21] We denote all the time instants, $jT_{c,i},\ j = 1, \cdots, h/l_i,\ i = 1, \cdots, N$, by $\varsigma_1, \cdots, \varsigma_\mu,\ \mu \leq \sum_{i=1}^{N} h/l_i$, and order them as $\varsigma_j < \varsigma_{j+1},\ j = 1, \cdots, \mu$.*

Our sequel study on the design issues will rely closely on the definition of the time instants $\varsigma_1, \cdots, \varsigma_\mu$.

4.1.3 Communication mechanism at Management layer

In a complex large-scale industrial system, the occurrence of faults or failures during the process is unavoidable. The FTC strategy is very necessary and implemented at the Management layer in the context of resource management [117, 118]. As the system

resource, the components (such as sensors, actuators, controllers, etc) have been defined with a certain functionality. When a fault occurs, the component will be considered as a lose of partial or complete functionality to fulfill the system operation. In this case, the resource management and the FTC strategy integrated in CSs will be realized in a distributed manner. The specific information about the faults (i.e., fault estimate) will be offered to CSs. A frame containing the fault estimate will be generated and delivered to the LCs. Afterwards, a re-configuration of the controllers will be activated.

According to the practical requirement and purpose during the application, the resource management and the FTC strategy at the Management layer can be developed individually. The function of the Management layer can be formulated as an optimization algorithm of the resource management and re-allocation.

4.2 Modeling of decentralized W-NCSs

From the analysis of communication mechanisms at the three different layers in the last section, it is remarkable that the scheduler has been embedded into the decentralized W-NCSs. Although [21] has presented concrete processes of modeling the subsystems and the overall W-NCSs, the scheduler in [21] has been concerned in view of communication community. Following our previous study about scheduler reformulation in view of control community, the modeling of subsystems and the overall W-NCSs will be reintroduced in this section. It is remarkable that we will only consider the scheduler of wireless transmissions between the Coordination & Supervision layer and the Execution layer in this thesis. The updates of the state estimates periodically with other CSs in a broadcast mode are much more complex, which will not be considered in this work. Since our work is based on [21], only the procedures with revision, instead of the entire and repeated processes, will be stated in this section.

4.2.1 Modeling of a subsystem

It is assumed that the process under consideration consists of N subprocesses. Through discretization, the i-th subprocess with the sampling time $T_{c,i}$ is modeled as

$$\mathbf{x}_i((k+1)T_{c,i}) = \mathbf{A}_{d,ii}\mathbf{x}_i\left(kT_{c,i}\right) + \mathbf{B}_{d,i}\mathbf{u}_{s,i}(kT_{c,i}) + \sum_{j\neq i}^{N} \mathbf{A}_{d,ij}(kT_{c,i})\bar{\mathbf{x}}_j(kT_{c,i}) \tag{4.1}$$

$$\mathbf{y}_i(kT_{c,i}) = \mathbf{C}_{d,i}\mathbf{x}_i\left(kT_{c,i}\right) \tag{4.2}$$

where $\mathbf{x}_i(kT_{c,i}) \in \Re^{n_i}$ and $\mathbf{y}_i(kT_{c,i}) \in \Re^{m_i}$ denote the state vector and output vector of the i-th subprocess. $\mathbf{u}_{s,i}(kT_{c,i})$ is the input vector, which is constructed in the LCs with

the decoded information sent from the i-th CS. Due to the coupling among subprocesses, a lifted vector $\bar{\mathbf{x}}_j(kT_{c,i})$ [21] is defined, which contains all the updated states of other subprocesses during the time interval $[kT_{c,i}, (k+1)T_{c,i})$. After discretization, $\mathbf{A}_{d,ii}$, $\mathbf{B}_{d,i}$, $\mathbf{C}_{d,i}$ are known matrices of appropriate dimensions. It is notable that $\mathbf{A}_{d,ij}(kT_{c,i})$ is time-varying. Since the scheduler is restarted at the beginning of each T_p, which results in a periodic data transmissions, it holds

$$\mathbf{A}_{d,ij}(kT_{c,i}) = \mathbf{A}_{d,ij}(kT_{c,i} + T_p).$$

According to the communication mechanism at the Coordination & Supervision layer, during the time interval $[kT_{c,i}, (k+1)T_{c,i})$, the i-th CS acts as the receiver for two kinds of information: (1) residuals sent by the LCs; (2) state estimates sent by the other CSs. The residual signals, together with the available state estimate of the i-th CS, are used to improve the estimation performance. The state estimates from other CSs describes the coupling between the i-th CS and the other CSs.

Based on the discrete-time model of the i-th subprocess with the consideration of the scheduler, the observer embedded in the i-th CS can be constructed as follows

$$\begin{aligned}\hat{\mathbf{x}}_i((k+1)T_{c,i}) = {} & \mathbf{A}_{d,ii}\hat{\mathbf{x}}_i\left(kT_{c,i}\right) + \mathbf{B}_{d,i}\mathbf{u}_{s,i}(kT_{c,i}) \\ & + \sum_{j\neq i}^{N} \mathbf{A}_{d,ij}(kT_{c,i})\hat{\bar{\mathbf{x}}}_j(kT_{c,i}) + \mathbf{L}_i(kT_{c,i})\mathbf{r}_{s,i}(kT_{c,i}), \qquad (4.3)\end{aligned}$$

$$\hat{\mathbf{y}}_i(kT_{c,i}) = \mathbf{C}_{d,i}\hat{\mathbf{x}}_{s,i}(kT_{c,i}) \qquad (4.4)$$

where $\hat{\mathbf{x}}_i(kT_{c,i})$ and $\hat{\bar{\mathbf{x}}}_j(kT_{c,i})$ are the estimate vectors of $\mathbf{x}_i(kT_{c,i})$ and $\bar{\mathbf{x}}_j(kT_{c,i})$. Assume that the state estimate $\hat{\mathbf{x}}(kT_{c,i})_i$ is available at the beginning of the k-th cycle, and has been received by the LCs, we denote it as $\hat{\mathbf{x}}_{s,i}(kT_{c,i})$. $\hat{\mathbf{y}}_i(kT_{c,i})$ is the output estimate vector at the LCs. $\mathbf{r}_{s,i}(kT_{c,i})$ contains all the residuals that are received by the i-th CS. $\mathbf{L}_i(kT_{c,i})$ is the observer gain matrix to be designed.

Therefore, the residual vector generated by the LCs in the i-th subsystem is addressed as

$$\mathbf{r}_i(kT_{c,i}) = \mathbf{y}_i(kT_{c,i}) - \hat{\mathbf{y}}_i(kT_{c,i}) \qquad (4.5)$$

Considering the communication mechanism, it is remarkable that $\mathbf{r}_{s,i}(kT_{c,i})$ is actually the scheduler's output corresponding to the input $\mathbf{r}_i(kT_{c,i})$.

4.2.2 Modeling of the overall W-NCSs

In this subsection, we will model the overall W-NCSs based on the discrete-time models of the subprocesses and the scheduler among the subsystems. For our design purpose, we

introduce a vector $\mathbf{x}(k,j)$ $k=0,1,\cdots,$ $j=1,\cdots,\mu$ as defined in [21],

$$\mathbf{x}(k,j)=\begin{bmatrix}\mathbf{x}_j(kT_p+\varsigma_j)\\ \vdots\\ \mathbf{x}_\mu\left(kT_p+\varsigma_\mu\right)\\ \mathbf{x}_1((k+1)T_p+\varsigma_1)\\ \vdots\\ \mathbf{x}_{j-1}((k+1)T_p+\varsigma_{j-1})\end{bmatrix}, \tag{4.6}$$

where $\mathbf{x}_j(kT_p+\varsigma_j)$ denotes the vector which consists of all those state variables that have an update at the time instant $kT_p+\varsigma_j$. As stated in [21] that $\mathbf{x}(k,j)$ represents the vector of the whole process state variables with all their updates in the time interval $[kT_p+\varsigma_j,(k+1)T_p+\varsigma_j)$. It is remarkable that $\mathbf{x}(k,j)$ works like a buffer, which saves all the undated state variables during the time interval $[kT_p+\varsigma_j,(k+1)T_p+\varsigma_j)$. In the next time instant $kT_p+\varsigma_{j+1}$, the state variable $\mathbf{x}_j(kT_p+\varsigma_j)$ will be removed from $\mathbf{x}(k,j)$, meanwhile $\mathbf{x}_j((k+1)T_p+\varsigma_j)$ will be added. As a result, $\mathbf{x}(k,j+1)$ is constructed, which contains all the state variables during the time interval $[kT_p+\varsigma_{j+1},(k+1)T_p+\varsigma_{j+1})$. Following the steps in [21] and lifting the model of subprocesses in 4.1, we have

$$\mathbf{x}(k,j+1)=\mathbf{A}(j)\mathbf{x}(k,j)+\mathbf{B}(j)\mathbf{u}_s(k,j), \tag{4.7}$$

$$\mathbf{u}_s(k,j)=\begin{bmatrix}\mathbf{u}_{s,j}(kT_p+\varsigma_j)\\ \vdots\\ \mathbf{u}_{s,\mu}\left(kT_p+\varsigma_\mu\right)\\ \mathbf{u}_{s,1}((k+1)T_p+\varsigma_1)\\ \vdots\\ \mathbf{u}_{s,j-1}((k+1)T_p+\varsigma_{j-1})\end{bmatrix}, \tag{4.8}$$

where $\mathbf{u}_{s,j}(kT_p+\varsigma_j)$ denotes the input vector which contains all the input variables that have an update at the time instant $kT_p+\varsigma_j$. $\mathbf{A}(j)$ and $\mathbf{B}(j)$ are system matrices with appropriate dimensions, and the process of determining $\mathbf{A}(j)$ and $\mathbf{B}(j)$ has been presented in [21]. Moreover, it is noted that (4.7) is a discrete LTP system.

Remark 4.1. *As a μ-periodic discrete-time system, it is supposed here all the subsystems have once synchronization communication at the beginning of each T_p and all the states have the first updates at the first instant in each T_p, i.e. at $(k,1)$. In our subsequent study, without loss of generality, (k,j) will be widely applied to denote the j-th time instant during the k-th T_p. With the consideration of periodicity, in this thesis the instant $(k,\mu+1)$ is the actual instant $(k+1,1)$, $(k,-1)$ is the actual instant $(k-1,\mu)$.*

Follow the idea of observer algorithm (4.3) for the i-th subprocess embedded in the i-th CS, by lifting (4.3) it leads to the observer of (4.7) as follows

$$\hat{\mathbf{x}}(k,j+1) = \mathbf{A}(j)\hat{\mathbf{x}}(k,j) + \mathbf{B}(j)\mathbf{u}_s(k,j) + \mathbf{L}(j)\mathbf{r}_s(k,j) \tag{4.9}$$

$$\mathbf{r}_s(k,j) = \begin{bmatrix} \mathbf{r}_{s,j}(kT_p+\varsigma_j) \\ \vdots \\ \mathbf{r}_{s,\mu}(kT_p+\varsigma_\mu) \\ \mathbf{r}_{s,1}((k+1)T_p+\varsigma_1) \\ \vdots \\ \mathbf{r}_{s,j-1}((k+1)T_p+\varsigma_{j-1}) \end{bmatrix}, \mathbf{r}_{s,j}(kT_p+\varsigma_j) = \begin{bmatrix} \vdots \\ \mathbf{r}_{s,i}(kT_p+\varsigma-T_{c,i}) \\ \vdots \end{bmatrix},$$

where $\hat{\mathbf{x}}(k,j)$ is the estimate of $\mathbf{x}(k,j)$, $\mathbf{L}(j)$ is the structure-limited observer gain, as addressed in [21]. By confining the structure of $\mathbf{L}(j)$, a decentralized observer (4.9) can be constructed. Furthermore, developing a structure-limited controller for the decentralized W-NCSs is also a very interesting issue. It is notable that the W-NCSs and its observer have been formulated as discrete LTP systems. Observer/controller design schemes for discrete LTP systems are presented in [112, 119], which can also be applied for our purpose.

4.3 Scheduler model for W-NCSs

In the last section, the model of W-NCSs has been formulated into discrete LTP systems, where the effect of the scheduler's output acting on the model has been concerned. How the scheduler affects on the input information, which are delivered onto the wireless network, will be stated in view of control community in this section.

It is supposed that the scheduler has been scheduled off-line and is embedded into the structure of decentralized W-NCSs. It is remarkable that the scheduler considered in this thesis is a static scheduler which is also identical to the requirement for deterministic transmission behaviors. The schematic description of W-NCSs with an integrated scheduler is given in Fig.4.2, where $\mathbf{r}(k,j) \in \Re^{m_1(j)}$ denotes the residual, $\tilde{\mathbf{u}}(k,j) \in \Re^{p_2(j)}$ is the packet containing the essential signals (such as state and fault estimates) for controller design at the LCs. $\tilde{\mathbf{u}}(k,j)$ and $\mathbf{r}(k,j)$ are both time-driven. With the effect of the scheduler $\mathcal{S}$, they are realigned as $\tilde{\mathbf{u}}_s(k,j) \in \Re^{p_1(j)}$ and $\mathbf{r}_s(k,j) \in \Re^{m_2(j)}$, respectively. $\tilde{\mathbf{u}}_s(k,j)$ is the finally received packet by LCs corresponding to the input $\tilde{\mathbf{u}}(k,j)$, while $\mathbf{r}_s(k,j)$ is the actual residual signal received by the CSs corresponding to the input $\mathbf{r}(k,j)$. Following the construction steps of state-space representation of the scheduler in Chapter 3, the

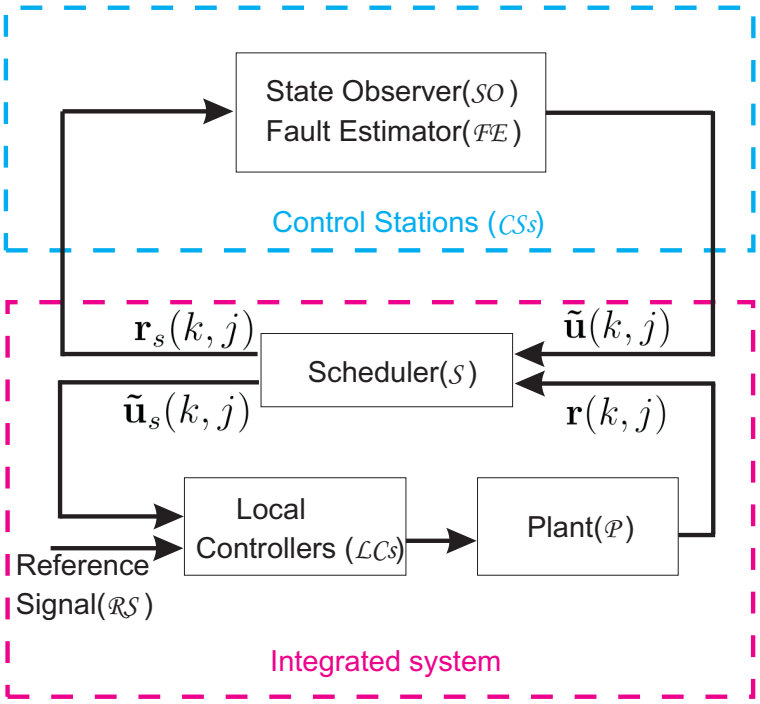

Figure 4.2: Schematic description of W-NCSs with an integrated scheduler

scheduler $\mathcal{S}$ is also addressed as μ-periodic discrete-time state-space representation

$$\begin{aligned}\psi_s(k,j+1) &= \mathbf{A}_s(j)\psi_s(k,j) + \mathbf{B}_{sr}(j)\mathbf{r}(k,j) + \mathbf{B}_{su}(j)\tilde{\mathbf{u}}(k,j)\\ \tilde{\mathbf{u}}_s(k,j) &= \mathbf{C}_{su}(j)\psi_s(k,j) + \mathbf{D}_{su}(j)\tilde{\mathbf{u}}(k,j)\\ \mathbf{r}_s(k,j) &= \mathbf{C}_{sr}(j)\psi_s(k,j) + \mathbf{D}_{sr}(j)\mathbf{r}(k,j), j = 1,\cdots,\mu\end{aligned} \tag{4.10}$$

where $\psi_s(k,j) \in \Re^{m_1(j)+p_2(j)}$ is the state of the scheduler. It should be pointed out that since the packet $\tilde{\mathbf{u}}(k,j)$ includes $\hat{\mathbf{x}}(k,j)$ and other information (for example, the fault estimate), which are written in one frame and multi-cast to the LCs, therefore, all the information packeted in $\tilde{\mathbf{u}}(k,j)$ will be transmitted following the same scheduler, i.e. using the same $\mathbf{C}_{su}(j)$ and $\mathbf{D}_{su}(j)$. All the system matrices are periodic with period μ, i.e., for each j,

$$\begin{aligned}&\mathbf{A}_s(j) = \mathbf{A}_s(j+\mu),\ \mathbf{B}_{sr}(j) = \mathbf{B}_{sr}(j+\mu),\ \mathbf{B}_{su}(j) = \mathbf{B}_{su}(j+\mu),\\ &\mathbf{C}_{su}(j) = \mathbf{C}_{su}(j+\mu),\ \mathbf{D}_{su}(j) = \mathbf{D}_{su}(j+\mu),\ \mathbf{C}_{sr}(j) = \mathbf{C}_{sr}(j+\mu),\ \mathbf{D}_{sr}(j) = \mathbf{D}_{sr}(j+\mu).\end{aligned}$$

Remark 4.2. *$\psi_s(k,j)$ works as a buffer and always saves all the data that have been generated during the last time τ. Considering the timeliness of the data, only the data in the last T_p will be used in the process, so here we have $\tau = T_p$. (1) In the case of ideal condition (i.e., without time delay and packet loss), the input is equal to the output,*

$\mathbf{C}_{su}(j)$ *and* $\mathbf{C}_{sr}(j)$ *are zero matrices,* $\mathbf{D}_{su}(j)$ *and* $\mathbf{D}_{sr}(j)$ *are identity matrices; (2) in the case with time delay, the transmission order of the data scheduled with delay will be reflected on* $\mathbf{C}_{su}(j)$ *and* $\mathbf{C}_{sr}(j)$*; (3) in the case with packet loss, the transmission order of the information scheduled with packet loss will be embodied in* $\mathbf{D}_{su}(j)$ *and* $\mathbf{D}_{sr}(j)$ *with zero matrices* $\mathbf{C}_{su}(j)$ *and* $\mathbf{C}_{sr}(j)$*. An experimental study of the cases with delay or packet loss have been presented in [116].*

Remark 4.3. *In the case of ensuring the system with acceptable control performance, the scheduler with time delay and packet loss has also been taken into account. In the case (1) of the ideal condition (i.e., without time delay and packet loss) and (2) with packet loss, the conditions* $m_2(j) \leq m_1(j)$ *and* $p_1(j) \leq p_2(j)$ *hold. While in the case (3) with time delay, there are* $m_2(j) > m_1(j)$ *or* $p_1(j) > p_2(j)$ *at the* j*-th instant scheduled with delayed information, in other case the conditions* $m_2(j) \leq m_1(j)$ *and* $p_1(j) \leq p_2(j)$ *are still logical.*

4.4 Summary

This chapter introduced a fault tolerant W-NCS structure, which consists of three functional layers: Execution layer, Coordination & Supervision layer and Management layer. The communication mechanisms at these three layers are described. After that, based on the model and observer for a subsystem, the model and observer of the overall W-NCSs are constructed in the form of μ-periodic systems. Finally, the scheduler of the overall W-NCSs is also expressed as a μ-periodic system.

5 An FTC scheme for W-NCSs with AFs

For additive sensor and actuator faults, an FTC scheme based on the FE technology will be developed for the W-NCSs with an integrated scheduler.

With the development of large-scale complex and physically distributed systems, faults in embedded system components are unavoidable, which leads to an interruption to the systems of performing a required function under specified operating conditions and may cause great economic loss and even severe danger to the operators and the environment. In recent years, FTC study has become a very active research area, and many contributions have been reported. However, there is still a blank gap in the design of FTC strategies for W-NCSs with integrated schedulers for the AF case. This motivates the study in this chapter.

5.1 System model with AFs

Following the schematic description of W-NCSs with an integrated scheduler $\mathcal{S}$ presented in Fig.4.2, the plant $\mathcal{P}$ is described by the following μ-periodic discrete time state-space representation

$$\mathbf{x}(k, j+1) = \mathbf{A}(j)\mathbf{x}(k, j) + \mathbf{B}(j)\mathbf{u}_s(k, j) + \mathbf{E}_d(j)\mathbf{d}(k, j) + \mathbf{E}_f(j)\mathbf{f}(k, j) \tag{5.1}$$

$$\mathbf{y}(k, j) = \mathbf{C}(j)\mathbf{x}(k, j) + \mathbf{F}_d(j)\mathbf{d}(k, j) + \mathbf{F}_f(j)\mathbf{f}(k, j) \ (j = 1, \cdots, \mu) \tag{5.2}$$

where $\mathbf{x}(k, j) \in \Re^n$, $\mathbf{u}_s(k, j) \in \Re^{p_1(j)}$ and $\mathbf{y}(k, j) \in \Re^{m_1(j)}$ are the plant state, control input and measurement output variables, respectively. $\mathbf{d}(k, j) \in \Re^{d(j)}$ is the disturbance vector which belongs to $l_2[0, \infty)$. The system matrices $\mathbf{A}(j)$, $\mathbf{B}(j)$, $\mathbf{C}(j)$, $\mathbf{E}_d(j)$, $\mathbf{F}_d(j)$, $\mathbf{E}_f(j)$ and $\mathbf{F}_f(j)$ are all μ-periodic matrices with appropriate dimensions, i.e., for each j,

$$\begin{aligned}
&\mathbf{A}(j) = \mathbf{A}(j+\mu),\ \mathbf{B}(j) = \mathbf{B}(j+\mu),\ \mathbf{C}(j) = \mathbf{C}(j+\mu),\ \mathbf{E}_d(j) = \mathbf{E}_d(j+\mu),\\
&\mathbf{F}_d(j) = \mathbf{F}_d(j+\mu),\ \mathbf{E}_f(j) = \mathbf{E}_f(j+\mu),\ \mathbf{F}_f(j) = \mathbf{F}_f(j+\mu),\\
&p_2(j) = p_2(j+\mu),\ m_1(j) = m_1(j+\mu).
\end{aligned}$$

$\mathbf{f}(k,j) \in \Re^{f(j)}$ denotes the fault vector and is divided into $\mathbf{f}(k,j) = [\mathbf{f}^a(k,j)' \ \mathbf{f}^s(k,j)']'$, where $\mathbf{f}^a(k,j) \in \Re^{f_a(j)}$ and $\mathbf{f}^s(k,j) \in \Re^{f_s(j)}$ are the actuator fault and sensor fault vectors, respectively. We denote $\mathbf{f}_i^a(k,j)$ and $\mathbf{f}_i^a(k,l)$ as the actuator faults of the i-th actuator at the time instant (k,j) and (k,l), respectively. The time instant (k,l) is one control cycle of the i-th actuator later than (k,j). And we define $\mathbf{f}_r^s(k,j)$ and $\mathbf{f}_r^s(k,t)$ as the sensor faults of the r-th sensor at (k,j) and (k,t), respectively. The time instant (k,t) is one sampling cycle of the r-th sensor later than (k,j).

Assumption 5.1. *There exist four constants $\mathbf{f}_{0,i}^a$, $\mathbf{f}_{1,i}^a$, $\mathbf{f}_{0,r}^s$ and $\mathbf{f}_{1,r}^s$ such that*

$$\|\mathbf{f}_i^a(k,j)\|_2 \le \mathbf{f}_{0,i}^a, \|\mathbf{f}_i^a(k,l) - \beta_i^a \mathbf{f}_i^a(k,j)\|_2 \le \mathbf{f}_{1,i}^a,$$
$$\|\mathbf{f}_r^s(k,j)\|_2 \le \mathbf{f}_{0,r}^s, \|\mathbf{f}_r^s(k,t) - \beta_r^s \mathbf{f}_r^s(k,j)\|_2 \le \mathbf{f}_{1,r}^s,$$

where β_i^a and β_r^s are positive reals as close as possible to 1.

From the described properties of the faults, we can rewrite the faults as follows

$$\mathbf{f}_i^a(k,l) = \beta_i^a \mathbf{f}_i^a(k,j) + \mathbf{\Delta}_i^a(k,j), \tag{5.3}$$
$$\mathbf{f}_r^s(k,t) = \beta_r^s \mathbf{f}_r^s(k,j) + \mathbf{\Delta}_r^s(k,j). \tag{5.4}$$

By augmenting (5.3) and (5.4) respectively, we have

$$\mathbf{f}^a(k,j+1) = \mathbf{A}_f^a(j)\mathbf{f}^a(k,j) + \mathbf{S}^a(j)\mathbf{\Delta}^a(k,j), \tag{5.5}$$
$$\mathbf{f}^s(k,j+1) = \mathbf{A}_f^s(j)\mathbf{f}^s(k,j) + \mathbf{S}^s(j)\mathbf{\Delta}^s(k,j), \tag{5.6}$$
$$\mathbf{A}_f^a(j) = \begin{bmatrix} \mathbf{O}_{\bar{n}_a(j)\times n_a(j)} & \mathbf{I}_{\bar{n}_a(j)\times \bar{n}_a(j)} \\ \mathbf{A}_{f,1}^a(j) & \mathbf{A}_{f,2}^a(j) \end{bmatrix}, \mathbf{S}^a(j) = \begin{bmatrix} \mathbf{O}_{\bar{n}_a(j)\times f_a(j)} \\ \mathbf{S}_f^a(j) \end{bmatrix},$$
$$\mathbf{A}_f^s(j) = \begin{bmatrix} \mathbf{O}_{\bar{n}_s(j)\times n_s(j)} & \mathbf{I}_{\bar{n}_s(j)\times \bar{n}_s(j)} \\ \mathbf{A}_{f,1}^s(j) & \mathbf{A}_{f,2}^s(j) \end{bmatrix}, \mathbf{S}^s(j) = \begin{bmatrix} \mathbf{O}_{\bar{n}_s(j)\times f_s(j)} \\ \mathbf{S}_f^s(j) \end{bmatrix},$$

where $\mathbf{\Delta}^a(k,j) \in \Re^{f_a(j)}$ and $\mathbf{\Delta}^s(k,j) \in \Re^{f_s(j)}$ are augmented vectors with the items $\mathbf{\Delta}_i^a(k,j)$ and $\mathbf{\Delta}_r^s(k,j)$ in (5.3) and (5.4), respectively. And $\mathbf{A}_{f,1}^a(j)$, $\mathbf{A}_{f,2}^a(j)$, $\mathbf{A}_{f,1}^s(j)$, $\mathbf{A}_{f,2}^s(j)$, $\mathbf{S}_f^a(j)$, $\mathbf{S}_f^s(j)$ are all μ-periodic matrices with proper dimensions. $n_a(j)$ (or $n_s(j)$) denotes the number of actuator (or sensor) faults that appear at the j-th slot of a period T_p. $r_a(j)$ (or $r_s(j)$) denotes the row number of actuator fault vector $\mathbf{f}^a(k,j)$ (or sensor fault vector $\mathbf{f}^s(k,j)$). $\bar{n}_a(j) = r_a(j) - n_a(j)$, $\bar{n}_s(j) = r_s(j) - n_s(j)$. Furthermore, from (5.3)-(5.4), it leads to

$$\mathbf{f}(k,j+1) = \mathbf{A}_f(j)\mathbf{f}(k,j) + \mathbf{S}(j)\mathbf{\Delta}_f(k,j), \tag{5.7}$$
$$\mathbf{A}_f(j) = \begin{bmatrix} \mathbf{A}_f^a(j) & \mathbf{O}_{r_a(j)\times r_s(j)} \\ \mathbf{O}_{r_s(j)\times r_a(j)} & \mathbf{A}_f^s(j) \end{bmatrix}, \mathbf{S}(j) = \begin{bmatrix} \mathbf{S}^a(j) & \\ & \mathbf{S}^s(j) \end{bmatrix},$$

where $\mathbf{\Delta}_f(k,j) = \begin{bmatrix} \mathbf{\Delta}^a(k,j)' & \mathbf{\Delta}^s(k,j)' \end{bmatrix}'$. $\mathbf{S}(j)$, as well as $\mathbf{S}^a(j)$ and $\mathbf{S}^s(j)$, is a Boolean matrix. For the convenience of our further study, an assumption about $\mathbf{\Delta}_f(k,j)$ is given as follows.

Assumption 5.2. *$\mathbf{\Delta}_f(k,j)$ belongs to $l_2[0,\infty)$.*

5.2 Problem formulation

Since the active FTC strategy is based on an assumption of a successful FD, in particular of FE, which offers the information of faults. The estimated information of faults will be used to accommodate the controller so as to compensate the effects caused by faults. So the fault estimator should be developed in advance. Besides, the system states are considered unmeasurable, hence, design of the state observer is also required.

The μ-periodic state observer of the plant $\mathcal{P}$ (5.1) is constructed as

$$\hat{\mathbf{x}}(k,j+1) = \mathbf{A}(j)\hat{\mathbf{x}}(k,j) + \mathbf{B}(j)\mathbf{u}_s(k,j) + \mathbf{E}_f(j)\hat{\mathbf{f}}(k,j) + \mathbf{L}(j)\mathbf{r}_s(k,j), \tag{5.8}$$

$$\hat{\mathbf{y}}(k,j) = \mathbf{C}(j)\hat{\mathbf{x}}_s(k,j) + \mathbf{F}_f(j)\hat{\mathbf{f}}_s(k,j)\ (j = 1,\cdots,\mu), \tag{5.9}$$

$$\mathbf{r}(k,j) = \mathbf{y}(k,j) - \hat{\mathbf{y}}(k,j), \tag{5.10}$$

where $\hat{\mathbf{x}}(k,j) \in \Re^n$ is the estimate of $\mathbf{x}(k,j)$. $\hat{\mathbf{f}}(k,j) = \begin{bmatrix} \hat{\mathbf{f}}^a(k,j)' & \hat{\mathbf{f}}^s(k,j)' \end{bmatrix}'$. $\hat{\mathbf{f}}^a(k,j) \in \Re^{f_a(j)}$ and $\hat{\mathbf{f}}^s(k,j) \in \Re^{f_s(j)}$ are the estimates of actuator fault vector $\mathbf{f}^a(k,j)$ and sensor fault vector $\mathbf{f}^s(k,j)$. $\hat{\mathbf{x}}_s(k,j)$ and $\hat{\mathbf{f}}_s(k,j)$ are the outputs of the scheduler $\mathcal{S}$ corresponding to the inputs $\hat{\mathbf{x}}(k,j)$ and $\hat{\mathbf{f}}(k,j)$. $\mathbf{r}(k,j) \in \Re^{m_1(j)}$ denotes the residual vector generated at the LCs. $\mathbf{r}_s(k,j) \in \Re^{m_2(j)}$ with $m_2(j) = m_2(j+\mu)$ is the residual vector which has been sent from LCs to CSs and coordinated by the scheduler $\mathcal{S}$. $\hat{\mathbf{y}}(k,j) \in \Re^{m_1(j)}$ denotes the estimate of $\mathbf{y}(k,j)$ at the LCs. $\mathbf{L}(j)$ is the structure-limited observer gain matrix [21], which needs to be designed.

The fault estimation algorithms for (5.3)-(5.4) are constructed as follows

$$\hat{\mathbf{f}}_i^a(k,l) = \beta_i^a \hat{\mathbf{f}}_i^a(k,j) + \mathbf{G}_i^a(j)\mathbf{r}_s(k,j), \tag{5.11}$$

$$\hat{\mathbf{f}}_r^s(k,t) = \beta_r^s \hat{\mathbf{f}}_r^s(k,j) + \mathbf{G}_r^s(j)\mathbf{r}_s(k,j), \tag{5.12}$$

where $\mathbf{G}_i^a(j)$ and $\mathbf{G}_r^s(j)$ are gain matrices of fault estimators. By augmenting (5.11)-(5.12), the FE algorithms for the actuator fault vector $\mathbf{f}^a(k,j)$ and sensor fault vector $\mathbf{f}^s(k,j)$ are addressed as

$$\hat{\mathbf{f}}^a(k,j+1) = \mathbf{A}_f^a(j)\hat{\mathbf{f}}^a(k,j) + \mathbf{G}^a(j)\mathbf{r}_s(k,j),$$

$$\hat{\mathbf{f}}^s(k,j+1) = \mathbf{A}_f^s(j)\hat{\mathbf{f}}^s(k,j) + \mathbf{G}^s(j)\mathbf{r}_s(k,j),$$

where

$$\mathbf{G}^a(j) = \begin{bmatrix} \mathbf{O}_{\bar{n}_a(j)\times m_2(j)} \\ \mathbf{G}_f^a(j) \end{bmatrix}, \mathbf{G}^s(j) = \begin{bmatrix} \mathbf{O}_{\bar{n}_s(j)\times m_2(j)} \\ \mathbf{G}_f^s(j) \end{bmatrix}.$$

And $\mathbf{G}_f^a(j)$, $\mathbf{G}_f^s(j)$ are all μ-periodic matrices composed of $\mathbf{G}_i^a(j)$ and $\mathbf{G}_r^s(j)$, respectively, as well as zero matrices. For achieving the concrete structures of $\mathbf{G}_f^a(j)$ and $\mathbf{G}_f^s(j)$, please refer to the procedure of obtaining the system matrices in [21].

Therefore, the FE algorithm for (5.7) can be described by

$$\hat{\mathbf{f}}(k, j+1) = \mathbf{A}_f(j)\hat{\mathbf{f}}(k, j) + \mathbf{G}(j)\mathbf{r}_s(k, j), \tag{5.13}$$

where

$$\mathbf{G}(j) = \begin{bmatrix} \mathbf{G}^a(j) \\ \mathbf{G}^s(j) \end{bmatrix}.$$

We define $\mathbf{e}_x(k, j) = \mathbf{x}(k, j) - \hat{\mathbf{x}}(k, j)$, $\mathbf{e}_f(k, j) = \mathbf{f}(k, j) - \hat{\mathbf{f}}(k, j)$, and

$$\mathbf{e}(k, j) = \begin{bmatrix} \mathbf{e}_x'(k, j) & \mathbf{e}_f'(k, j) \end{bmatrix}', \mathbf{v}(k, j) = \begin{bmatrix} \mathbf{d}'(k, j) & \mathbf{\Delta}_f'(k, j) \end{bmatrix}'. \tag{5.14}$$

Due to the decentralization of W-NCSs and the limitation of communication bandwidth [21], the state observer and fault estimator have structure-limited gains $\mathbf{L}(j)$ and $\mathbf{G}(j)$. Our main objective is to find the feasible solutions for a set of structure-limited gains $\mathbf{L}(j)$ and $\mathbf{G}(j)$ such that a set of the H_∞ performance indices

$$||\mathbf{e}(k, j)||_2 \leq \gamma_{1,j}||\mathbf{v}(k, j)||_2, \ j = 1, \cdots, \mu \tag{5.15}$$

are satisfied, where $\gamma_{1,j}$, $j = 1, \cdots, \mu$ are a set of given scalars.

According to the basic form of controllers for periodic systems in [21], combining with the communication mechanism in Fig.4.2, our FTC strategy for (5.1)-(5.2) is to be developed with the received $\hat{\mathbf{x}}(k, j)$ and $\hat{\mathbf{f}}(k, j)$, i.e., $\hat{\mathbf{x}}_s(k, j)$ and $\hat{\mathbf{f}}_s(k, j)$. The fault tolerant controller at the LCs is constructed as follows

$$\mathbf{u}_s(k, j) = \mathbf{K}_1(j)\phi_1(j)\hat{\mathbf{x}}_s(k, j) + \mathbf{K}_2(j)\phi_2(j)\hat{\mathbf{f}}_s(k, j) + \mathbf{R}_{ef}(j) \ (j = 1, \cdots, \mu), \tag{5.16}$$

where $\mathbf{K}_1(j)$ and $\mathbf{K}_2(j)$ are feedback gains, which also have limited structures [21]. $\mathbf{R}_{ef}(j)$ is the reference signal vector. In the case with scheduled delay or packet loss, the latest update will be used to design the controller. $\phi_1(j)$ and $\phi_2(j)$ are Boolean matrices, which will choose a proper update to proceed the calculation of controller. The key issue in the development of FTC strategy for W-NCSs is to find the feedback control gains $\mathbf{K}_1(j)$ and $\mathbf{K}_2(j)$ such that a set of the H_∞ performance indices

$$||\mathbf{y}_{FTC}(k, j)||_2 \leq \gamma_{2,j}||\mathbf{v}(k, j)||_2, \ j = 1, \cdots, \mu \tag{5.17}$$

are fulfilled, where $\mathbf{y}_{FTC}(k,j)$ denotes the real output after applying the FTC strategy on the process, $\gamma_{1,j}$, $j = 1, \cdots, \mu$ are a set of given scalars.

Therefore, our major objective in this chapter is to find feasible solutions for the estimation gains $\mathbf{L}(j)$ and $\mathbf{G}(j)$, as well as the feedback control gains $\mathbf{K}_1(j)$ and $\mathbf{K}_2(j)$, which have limited structures and ensure the system (5.1)-(5.2) satisfying the performance indices (5.15) and (5.17).

5.3 An FE scheme for LTP systems with AFs

When we describe LTI systems with AFs, $\mathbf{E}_f(j)$ and $\mathbf{F}_f(j)$ shouldn't be zero matrices, simultaneously. Otherwise, it makes no sense. However, this is not the case with LTP systems. As we know, the W-NCS model has been formulated as discrete LTP systems according to the time instants $j = 1, \cdots, \mu$ [21]. During the process, faults appear and vary slowly. With a proper FDI technology [92] applied to this model, it's easy to know when and where the fault has occurred. However, not all devices (sensors or actuators) are considered with faults during the process. For example, the abrasion or offset on some newly installed devices is still very small. To save the calculation, only the devices, that have been diagnosed with faults or potential faults, are taken into account. Due to the multirate sampling mechanism applied in W-NCSs, at some time instants during one period T_p, no faults are considered. As a result, $\mathbf{E}_f(j)$ and $\mathbf{F}_f(j)$ in (5.1)-(5.2) are zero matrices at these time instants. This situation has a significant influence on the design of FE algorithms for discrete LTP systems. In this section, we are going to introduce the design methods of state observer and fault estimator from two cases:

> Case I: $\mathbf{E}_f(j)$ and $\mathbf{F}_f(j)$ are nonzero matrices at all the time instants during one period T_p.
>
> Case II: $\mathbf{E}_f(j)$ and $\mathbf{F}_f(j)$ are zero matrices at partial time instants during one period T_p.

5.3.1 An FE scheme for case I

We will start the design of the state observer and fault estimator from case I. With the consideration of the scheduler (4.10), the residual (5.10) can be expressed as

$$\begin{aligned}\mathbf{r}(k,j) = {} & \mathbf{C}(j)\mathbf{x}(k,j) + \mathbf{F}_d(j)\mathbf{d}(k,j) + \mathbf{F}_f(j)\mathbf{f}(k,j) - \mathbf{C}(j)\mathbf{C}_{su}(j)\mathbf{x}_s(k,j) \\ & - \mathbf{C}(j)\mathbf{D}_{su}(j)\hat{\mathbf{x}}(k,j) - \mathbf{F}_f(j)\mathbf{C}_{su}(j)\mathbf{x}_s(k,j) - \mathbf{F}_f(j)\mathbf{D}_{su}(j)\hat{\mathbf{f}}(k,j). \end{aligned} \tag{5.18}$$

Considering (5.1), (5.8) and (5.18), we have

$$\begin{aligned}\mathbf{e}_x(k,j+1) = &(\mathbf{A}(j)-\mathbf{L}(j)\mathbf{D}_{sr}(j)\mathbf{C}(j)\mathbf{D}_{su}(j))\mathbf{e}_x(k,j)\\ &+(\mathbf{E}_d(j)-\mathbf{L}(j)\mathbf{D}_{sr}(j)\mathbf{F}_d(j))\mathbf{d}(k,j)\\ &+\mathbf{L}(j)(\mathbf{D}_{sr}(j)\mathbf{C}(j)\mathbf{C}_{su}(j)+\mathbf{D}_{sr}(j)\mathbf{F}_f(j)\mathbf{C}_{su}(j)-\mathbf{C}_{sr}(j))\mathbf{x}_s(k,j)\\ &+(\mathbf{E}_f(j)-\mathbf{L}(j)\mathbf{D}_{sr}(j)\mathbf{F}_f(j)\mathbf{D}_{su}(j))\mathbf{e}_f(k,j)+\mathbf{L}(j)\mathbf{D}_{sr}(j)\mathbf{C}(j)(\mathbf{D}_{su}(j)\\ &-\mathbf{I}(j))\mathbf{x}(k,j)+\mathbf{L}(j)\mathbf{D}_{sr}(j)\mathbf{F}_f(j)(\mathbf{D}_{su}(j)-\mathbf{I}(j))\mathbf{f}(k,j) \qquad (5.19)\end{aligned}$$

From (5.7) and (5.13), there is

$$\begin{aligned}\mathbf{e}_f(k,j+1) = &(\mathbf{A}_f(j)-\mathbf{G}(j)\mathbf{D}_{sr}(j)\mathbf{F}_f(j)\mathbf{D}_{su}(j))\mathbf{e}_f(k,j)\\ &-\mathbf{G}(j)\mathbf{D}_{sr}(j)\mathbf{C}(j)\mathbf{D}_{su}(j)\mathbf{e}_x(k,j)\\ &+\mathbf{G}(j)(\mathbf{D}_{sr}(j)\mathbf{C}(j)\mathbf{C}_{su}(j)+\mathbf{D}_{sr}(j)\mathbf{F}_f(j)\mathbf{C}_{su}(j)-\mathbf{C}_{sr}(j))\mathbf{x}_s(k,j)\\ &-\mathbf{G}(j)\mathbf{D}_{sr}(j)\mathbf{F}_d(j)\mathbf{d}(k,j)+\mathbf{G}(j)\mathbf{D}_{sr}(j)\mathbf{C}(j)(\mathbf{D}_{su}(j)-\mathbf{I}(j))\mathbf{x}(k,j)\\ &+\mathbf{G}(j)\mathbf{D}_{sr}(j)\mathbf{F}_f(j)(\mathbf{D}_{su}(j)-\mathbf{I}(j))\mathbf{f}(k,j)+\mathbf{S}(j)\boldsymbol{\Delta}_f(k,j) \qquad (5.20)\end{aligned}$$

According to the definition (5.14) and combining equations (5.19) and (5.20) together, the error dynamics are obtained as follows

$$\begin{aligned}\mathbf{e}(k,j+1) = &(\mathbf{A}_o(j)-\mathbf{L}_o(j)\mathbf{C}_o(j))\mathbf{e}(k,j)+(\mathbf{B}_o(j)-\mathbf{L}_o(j)\mathbf{D}_o(j))\mathbf{v}(k,j)\\ &+\mathbf{L}_o(j)(\xi_1(k,j)+\xi_2(k,j)+\xi_3(k,j)), \qquad (5.21)\\ \mathbf{r}(k,j) = &\mathbf{E}_o(j)\mathbf{e}(k,j)+\mathbf{F}_o(j)\mathbf{v}(k,j)-(\mathbf{C}(j)+\mathbf{F}_f(j))\xi_4(k,j)\\ &-\mathbf{C}(j)\xi_5(k,j)-\mathbf{F}_f(j)\xi_6(k,j), \qquad (5.22)\end{aligned}$$

where

$$\begin{aligned}&\mathbf{A}_o(j)=\begin{bmatrix}\mathbf{A}(j) & \mathbf{E}_f(j)\\ \mathbf{0} & \mathbf{A}_f(j)\end{bmatrix},\mathbf{B}_o(j)=\begin{bmatrix}\mathbf{E}_d(j) & \mathbf{0}\\ \mathbf{0} & \mathbf{S}(j)\end{bmatrix},\mathbf{L}_o(j)=\begin{bmatrix}\mathbf{L}(j)\\ \mathbf{G}(j)\end{bmatrix},\\ &\mathbf{C}_o(j)=\begin{bmatrix}\mathbf{D}_{sr}(j)\mathbf{C}(j)\mathbf{D}_{su}(j) & \mathbf{D}_{sr}(j)\mathbf{F}_f(j)\mathbf{D}_{su}(j)\end{bmatrix},\mathbf{D}_o(j)=\begin{bmatrix}\mathbf{D}_{sr}(j)\mathbf{F}_d(j) & \mathbf{0}\end{bmatrix},\\ &\mathbf{E}_o(j)=\begin{bmatrix}\mathbf{C}(j)\mathbf{D}_{su}(j) & \mathbf{F}_f(j)\mathbf{D}_{su}(j)\end{bmatrix},\mathbf{F}_o(j)=\begin{bmatrix}\mathbf{F}_d(j) & \mathbf{0}\end{bmatrix},\\ &\mathbf{M}_1(j)=\mathbf{D}_{sr}(j)\mathbf{C}(j)\mathbf{C}_{su}(j)+\mathbf{D}_{sr}(j)\mathbf{F}_f(j)\mathbf{C}_{su}(j)-\mathbf{C}_{sr}(j),\\ &\mathbf{M}_2(j)=\mathbf{D}_{sr}(j)\mathbf{C}(j)\mathbf{M}_4(j),\ \mathbf{M}_3(j)=\mathbf{D}_{sr}(j)\mathbf{F}_f(j)\mathbf{M}_4(j),\ \mathbf{M}_4(j)=\mathbf{D}_{su}(j)-\mathbf{I}(j),\\ &\xi_1(k,j)=\mathbf{M}_1(j)\mathbf{x}_s(k,j),\ \xi_2(k,j)=\mathbf{M}_2(j)\mathbf{x}(k,j),\ \xi_3(k,j)=\mathbf{M}_3(j)\mathbf{f}(k,j),\\ &\xi_4(k,j)=\mathbf{C}_{su}(j)\mathbf{x}_s(k,j),\ \xi_5(k,j)=\mathbf{M}_4(j)\mathbf{x}(k,j),\ \xi_6(k,j)=\mathbf{M}_4(j)\mathbf{f}(k,j).\end{aligned}$$

It is obvious that the existence of the ξ group ($\xi_i(k,j),\ i=1,\cdots,6$) lies tightly on the scheduler $\mathcal{S}$. A brief discussion on their existence based on the scheduler (4.10) is

stated as follows. (1) In the case with an ideal condition, both $\mathbf{C}_{su}(j)$ and $\mathbf{C}_{sr}(j)$ are zero matrices, $\mathbf{D}_{sr}(j)$ and $\mathbf{D}_{su}(j)$ are identity matrices with proper dimensions, therefore the ξ group are zero vectors. That means the ξ group doesn't exist. (2) In the case with delay, either $\mathbf{C}_{su}(j)$ or $\mathbf{C}_{sr}(j)$ are not zero matrices, either $\mathbf{D}_{sr}(j) \neq \mathbf{I}(j)$ or $\mathbf{D}_{su}(j) \neq \mathbf{I}(j)$, hence the ξ group will exist. (3) In the case with packet loss, both $\mathbf{C}_{su}(j)$ and $\mathbf{C}_{sr}(j)$ are still zero matrices, but there maybe $\mathbf{D}_{su}(j) \neq \mathbf{I}(j)$, so $\xi_1(k,j)$ and $\xi_4(k,j)$ will not exist, while $\xi_i(k,j),\ i = 2,3,5,6$ will. Considering the practicability of the scheduler, the scheduled slots for delay or packet loss shouldn't occupy too much proportion in a period T_p.

In the following, we consider the wireless network under an ideal condition, in other words, the ξ group will not exist. The cases with delay and packet loss will be one of our future research directions.

Until now, the error dynamics can be rewritten as

$$\mathbf{e}(k,j+1) = (\mathbf{A}_o(j) - \mathbf{L}_o(j)\mathbf{C}_o(j))\mathbf{e}(k,j) + (\mathbf{B}_o(j) - \mathbf{L}_o(j)\mathbf{D}_o(j))\mathbf{v}(k,j), \tag{5.23}$$

$$\mathbf{r}(k,j) = \mathbf{E}_o(j)\mathbf{e}(k,j) + \mathbf{F}_o(j)\mathbf{v}(k,j), \tag{5.24}$$

Assumption 5.3. *$(\mathbf{A}_o(j), \mathbf{C}_o(j)),\ j = 1, \cdots, \mu$ is observable.*

In the following theorem, a multi-constrained FE method for discrete LTP systems under an H_∞ performance specification with a regional pole constraint is proposed to achieve a robust fault estimator.

Theorem 5.1. *Given a set of prescribed H_∞ performance levels $\gamma_{1,j},\ j = 1, \cdots, \mu$ and a circular region $\mathcal{D}_1(\alpha_1, r_1)$, error dynamics (5.23)-(5.24) satisfy the H_∞ performance index $||\mathbf{e}(k,j)||_2 \leq \gamma_{1,j}||\mathbf{v}(k,j)||_2$, and the eigenvalues of $\mathbf{A}_o(j) - \mathbf{L}_o(j)\mathbf{C}_o(j)$ belong to $\mathcal{D}_1(\alpha_1, r_1)$, if there exist a μ-periodic symmetric positive definite matrix $\mathbf{P}_1(j)$ and a μ-periodic gain matrix $\mathbf{L}_o(j)$ such that the following conditions hold for each j:*

$$\begin{bmatrix} -\mathbf{P}_1^{-1}(j+1) & \mathbf{A}_o(j) - \mathbf{L}_o(j)\mathbf{C}_o(j) & \mathbf{B}_o(j) - \mathbf{L}_o(j)\mathbf{D}_o(j) & \mathbf{0} \\ * & -\mathbf{P}_1(j) & \mathbf{0} & \mathbf{I}(j) \\ * & * & -\gamma_{1,j}\mathbf{I}(j) & \mathbf{0} \\ * & * & * & -\gamma_{1,j}\mathbf{I}(j) \end{bmatrix} \leq 0, \tag{5.25}$$

$$\begin{bmatrix} -\mathbf{P}_1^{-1}(j+1) & \mathbf{A}_o(j) - \mathbf{L}_o(j)\mathbf{C}_o(j) - \alpha_1\mathbf{I}(j) \\ * & -r_1^2\mathbf{P}_1(j) \end{bmatrix} \leq 0. \tag{5.26}$$

Proof. Define a quadratic Lyapunov function $V(k,j) = \mathbf{e}'(k,j)\mathbf{P}_1(j)\mathbf{e}(k,j)$, and $\mathbf{P}_1(j)$ is

a μ-periodic symmetric positive definite matrix. There is

$$\begin{aligned} V(k,j+1)-V(k,j) &= \mathbf{e}'(k,j+1)\mathbf{P}_1(j+1)\mathbf{e}(k,j+1)-\mathbf{e}'(k,j)\mathbf{P}_1(j)\mathbf{e}(k,j) \\ &= \begin{bmatrix} \mathbf{e}(k,j) \\ \mathbf{v}(k,j) \end{bmatrix}' \left(\begin{bmatrix} (\mathbf{A}_o(j)-\mathbf{L}_o(j)\mathbf{C}_o(j))' \\ (\mathbf{B}_o(j)-\mathbf{L}_o(j)\mathbf{D}_o(j))' \end{bmatrix} \mathbf{P}_1(j+1) \right. \\ &\quad \left. \times \begin{bmatrix} (\mathbf{A}_o(j)-\mathbf{L}_o(j)\mathbf{C}_o(j))' \\ (\mathbf{B}_o(j)-\mathbf{L}_o(j)\mathbf{D}_o(j))' \end{bmatrix}' - \begin{bmatrix} \mathbf{P}_1(j) & \\ & \mathbf{0} \end{bmatrix} \right) \begin{bmatrix} \mathbf{e}(k,j) \\ \mathbf{v}(k,j) \end{bmatrix} \end{aligned}$$

According to (5.25), it leads to

$$\mathbf{e}'(k,j)\mathbf{e}(k,j)-\gamma_{1,j}^2\mathbf{v}'(k,j)\mathbf{v}(k,j)+V(k,j+1)-V(k,j)\le 0$$

For a μ-periodic system, there is

$$\begin{aligned} &\sum_{j=1}^{\mu}(\mathbf{e}'(k,j)\mathbf{e}(k,j)-\gamma_{1,j}^2\mathbf{v}'(k,j)\mathbf{v}(k,j)+V(k,j+1)+V(k,j))\le -V(k,1)\le 0 \\ \Leftrightarrow &\sum_{j=1}^{\mu}(\mathbf{e}'(k,j)\mathbf{e}(k,j)-\gamma_{1,j}^2\mathbf{v}'(k,j)\mathbf{v}(k,j))\le -V(k+1,1)+V(k,1)-V(k,1) \\ \Leftrightarrow &\sum_{j=1}^{\mu}(\mathbf{e}'(k,j)\mathbf{e}(k,j)-\gamma_{1,j}^2\mathbf{v}'(k,j)\mathbf{v}(k,j))\le -V(k+1,1)\le 0 \end{aligned} \tag{5.27}$$

Therefore, the H_∞ performance index $||\mathbf{e}(k,j)||_2\le\gamma_{1,j}||\mathbf{v}(k,j)||_2$ can be satisfied. The proof of bounded eigenvalues (5.26) for discrete LTP systems can refer to [112, 120] and is omitted here. □

As it is pointed in [21] that $\mathbf{L}_o(j)$ is a set of structure-limited matrices, it's not easy to achieve a feasible solution for a μ-periodic $\mathbf{L}_o(j)$ taking into account of the limitations of $\mathbf{P}_1(j)$ and the high-dimensional of matrices in equation (5.25). To solve this problem, we present an improved theorem.

Theorem 5.2. *Given H_∞ performance levels $\gamma_{1,j}$, $j=1,\cdots,\mu$ and a circular region $\mathcal{D}_1(\alpha_1,r_1)$. If there exist a μ-periodic symmetric positive definite matrix $\mathbf{P}_1(j)$ and a μ-periodic gain matrix $\mathbf{L}_o(j)$ such that the following conditions hold for each j:*

$$\begin{bmatrix} \mathbf{P}_1(j+1)-2\mathbf{I}(j) & \mathbf{A}_o(j)-\mathbf{L}_o(j)\mathbf{C}_o(j) & \mathbf{B}_o(j)-\mathbf{L}_o(j)\mathbf{D}_o(j) & \mathbf{0} \\ * & -\mathbf{P}_1(j) & \mathbf{0} & \mathbf{I}(j) \\ * & * & -\gamma_{1,j}\mathbf{I}(j) & \mathbf{0} \\ * & * & * & -\gamma_{1,j}\mathbf{I}(j) \end{bmatrix} \le 0, \tag{5.28}$$

$$\begin{bmatrix} \mathbf{P}_1(j+1)-2\mathbf{I}(j) & \mathbf{A}_o(j)-\mathbf{L}_o(j)\mathbf{C}_o(j)-\alpha_1\mathbf{I}(j) \\ * & -r_1^2\mathbf{P}_1(j) \end{bmatrix} \le 0, \tag{5.29}$$

then the error dynamics (5.23)-(5.24) satisfy the H_∞ performance index $||\mathbf{e}(k,j)||_2 \leq \gamma_{1,j}||\mathbf{v}(k,j)||_2$, the eigenvalues of $(\mathbf{A}_o(j) - \mathbf{L}_o(j)\mathbf{C}_o(j))$ belong to $\mathcal{D}_1(\alpha_1, r_1)$.

Proof. Consider that for any matrix $\mathbf{P} > 0$: there is

$$(\mathbf{P}-\mathbf{I})^2 \geq \mathbf{0} \Rightarrow \mathbf{P}^2 - 2\mathbf{P} + \mathbf{I} \geq \mathbf{0}$$
$$\Rightarrow \mathbf{P} - 2\mathbf{I} + \mathbf{P}^{-1} \geq \mathbf{0} \Rightarrow \mathbf{P} - 2\mathbf{I} \geq -\mathbf{P}^{-1}$$

As a result, for a symmetric positive definite matrix $\mathbf{P}_1(j)$, it holds for each j:

$$\mathbf{P}_1(j+1) - 2\mathbf{I}(j) \geq -\mathbf{P}_1^{-1}(j+1) \tag{5.30}$$

Thus, by substituting (5.30) into (5.25) and (5.26), we can achieve (5.28) and (5.29). The proof of this theorem is obvious and omitted here. □

5.3.2 An FE scheme for case II

If $\mathbf{E}_f(j)$ and $\mathbf{F}_f(j)$ are zero matrices in (5.1)-(5.2) at partial time instants in a T_p during the process, identity matrices will appear directly at the diagonal of matrices $A_f(j)$, $j = 1, \cdots, T$ for balancing the error dynamics (5.21). Identity matrices on the diagonal of $A_f(j)$ result in the absolute eigenvalues of $A_o(j) - L_o(j)C_o(j)$ equal to 1, which means a marginal stability of (5.23). Consequently, some modifications should be implemented to the definition of $e(k,j)$ in (5.14).

We recall the structure of $\mathbf{x}(k,j)$ in (4.6), which contains all the state variables during the time interval $((k-1,j),(k,j)]$. Therefore, $\mathbf{e}_x(k,j)$ and $\mathbf{e}_f(k,j)$ include all the state and fault estimation error variables during the time interval $((k-1,j),(k,j)]$. We denote $\mathbf{e}_{x,l}(k-1,l)$ and $\mathbf{e}_{x,t}(k,t)$ are the vectors which consist of all those state estimation error variables that have an update at the time instant $(k-1,l)$ and (k,t), respectively. $\mathbf{e}_{f,l}(k-1,l)$ and $\mathbf{e}_{f,t}(k,t)$ as the vectors which consist of all those fault estimation error variables that have an update at the time instant $(k-1,l)$ and (k,t), respectively. Now we define $\mathbf{e}(k,j)$ with all the items of $\mathbf{e}_x(k,j)$ and $\mathbf{e}_f(k,j)$ during the interval $((k-1,j),(k,j)]$ in a new order. $\mathbf{e}(k,j)$ is defined as

$$\mathbf{e}(k,j) = \begin{bmatrix} \cdots & \mathbf{e}'_{x,l}(k-1,l) & \mathbf{e}'_{f,l}(k-1,l) & \cdots & \mathbf{e}'_{x,t}(k,t) & \mathbf{e}'_{f,t}(k,t) & \cdots \end{bmatrix}', \\ (j+1 \leq l \leq \mu, 1 \leq t \leq j) \tag{5.31}$$

With the newly defined $\mathbf{e}(k,j)$, deduce again the error dynamics (5.23)-(5.24) with a new set of parameter matrices $\mathbf{A}_o(j)$, $\mathbf{B}_o(j)$, $\mathbf{C}_o(j)$, $\mathbf{D}_o(j)$, $\mathbf{E}_o(j)$, $\mathbf{F}_o(j)$ and $\mathbf{L}_o(j)$. The rest derivation of FE method for this case is similar as that for case I, so please refer to Theorem 5.1 and Theorem 5.2. Actually, case I is just a special situation of case II, so the definition for case II is also suitable for case I.

Remark 5.1. *It is known that* $\mathbf{L}_o(k,j)$ *has a strict structure limitations which is one of the biggest difficulties during the way to reach a feasible solution. With our robust FE method in Theorem 5.2,* $\mathbf{L}_o(k,j)$ *has been taken as one of the unknown parameters and defined intuitively with a limited structure. MATLAB LMI toolbox is considered as a popular computation tool during the research. With the help of LMI toolbox, a structure-limited solution for* $\mathbf{L}_o(k,j)$ *can be obtained directly.*

5.4 An FTC scheme for LTP systems with AFs

Now, our object is to develop a fault tolerant controller which ensures the integrated discrete LTP systems satisfying the required FTC performance under the fault. With the help of fault estimator constructed in the last section, the effects caused by the sensor faults can be restrained by subtracting the sensor fault estimate from the output, i.e.,

$$\mathbf{y}_{FTC}(k,j) = \mathbf{y}(k,j) - \mathbf{F}_f(j)\hat{\mathbf{f}}(k,j) \tag{5.32}$$

where $\mathbf{y}_{FTC}(k,j)$ is the real output after applying FTC strategy on the process. In the following, our object mainly focuses on the development of a fault tolerant controller, which will make the system (5.1)-(5.2) to be tolerant to the actuator faults. According to the structure of the fault tolerant controller for AFs proposed in (5.16), our task is to achieve the structure-limited feedback control gains $\mathbf{K}_1(j)$ and $\mathbf{K}_2(j)$ to satisfy the performance index (5.17).

5.4.1 An FTC scheme for case I

Assumption 5.4. $rank(\mathbf{B}(j), \mathbf{E}_f(j)(\phi_2(j)\mathbf{D}_{su}(j))^\dagger) = rank(\mathbf{B}(j)),\ j = 1, \cdots, \mu$ *[121].*

Remark 5.2. *Assumption 5.4 is satisfied for the actuator fault case with the consideration of the effects of the scheduler* $\mathcal{S}$*. It means* $I_m(\mathbf{E}_f(j)(\phi_2(j)\mathbf{D}_{su}(j))^\dagger) \subseteq I_m(\mathbf{B}(j))$*, which leads to the existence of* $\mathbf{B}^*(j)$ *such that* $(\mathbf{I} + \mathbf{B}(j)\mathbf{B}^*(j))\mathbf{E}_f(j)(\phi_2(j)\mathbf{D}_{su}(j))^\dagger = \mathbf{0}$*.*

We set $\mathbf{R}_{ef}(j) = \mathbf{0}$ and choose $\mathbf{K}_2(j) = \mathbf{B}^*(j)\mathbf{E}_f(j)(\phi_2(j)\mathbf{D}_{su}(j))^\dagger$, so the state equation of the discrete LTP systems (5.1) is transformed into

$$\begin{aligned}
\mathbf{x}(k,j+1) &= (\mathbf{A}(j) + \mathbf{B}(j)\mathbf{K}_1(j)\phi_1(j)\mathbf{D}_{su}(j))\mathbf{x}(k,j) + \mathbf{E}_d(j)\mathbf{d}(k,j) \\
&\quad + \mathbf{B}(j)(\mathbf{K}_1(j)\phi_1(j) + \mathbf{K}_2(j)\phi_2(j))\mathbf{C}_{su}(j)\mathbf{x}_s(k,j) \\
&\quad - \mathbf{B}(j)\mathbf{K}_1(j)\phi_1(j)\mathbf{D}_{su}(j)\mathbf{e}_x(k,j) - \mathbf{B}(j)\mathbf{K}_2(j)\phi_2(j)\mathbf{D}_{su}(j)\mathbf{e}_f(k,j) \\
&= \mathbf{E}_d(j)\mathbf{d}(k,j) + \mathbf{B}(j)(\mathbf{K}_1(j)\phi_1(j) + \mathbf{K}_2(j)\phi_2(j))\xi_7(k,j) \\
&\quad - \mathbf{B}(j)\mathbf{K}_1(j)\phi_1(j)\mathbf{D}_{su}(j)\mathbf{e}_x(k,j) - \mathbf{B}(j)\mathbf{K}_2(j)\phi_2(j)\mathbf{D}_{su}(j)\mathbf{e}_f(k,j) \\
&\quad + (\mathbf{A}(j) + \mathbf{B}(j)\mathbf{K}_1(j)\phi_1(j)\mathbf{D}_{su}(j))\mathbf{x}(k,j)
\end{aligned} \tag{5.33}$$

where $\xi_7(k,j) = \mathbf{C}_{su}(j)\mathbf{x}_s(k,j)$. Considering the case with an ideal network environment, i.e., no delay or packet loss, so $\mathbf{C}_{su}(j)$ is zero matrix and $\xi_7(k,j)$ will be zero vector.

We will consider case I firstly and let

$$\mathbf{e}_c(k,j) = \begin{bmatrix} \mathbf{x}'(k,j) & \mathbf{e}'_x(k,j) & \mathbf{e}'_f(k,j) \end{bmatrix}', \tag{5.34}$$

and $\mathbf{v}(k,j)$ is defined in (5.14). It follows from the equation (5.33) and the error dynamics (5.23)-(5.24) under an ideal network condition that

$$\begin{aligned} \mathbf{e}_c(k,j+1) &= (\mathbf{A}_c(j) + \mathbf{B}_c(j)\mathbf{K}_1(j)\mathbf{C}_c(j))\mathbf{e}_c(k,j) \\ &\quad + (\mathbf{D}_c(j) + \mathbf{E}_c(j)\mathbf{K}_1(j)\mathbf{F}_c(j))\mathbf{v}(k,j), \qquad (5.35) \\ \mathbf{y}_{FTC}(k,j) &= \mathbf{G}_c(j)\mathbf{e}_c(k,j) + \mathbf{H}_c(j)\mathbf{v}(k,j), \qquad (5.36) \end{aligned}$$

where

$$\mathbf{A}_c(j) = \begin{bmatrix} \mathbf{A}(j) & \mathbf{0} & -\mathbf{B}(j)\mathbf{K}_2(j)\phi_2(j)\mathbf{D}_{su}(j) \\ \mathbf{L}(j)\mathbf{M}_2(j) & \mathbf{A}(j) - \mathbf{L}(j)\mathbf{A}_{c,1}(j) & \mathbf{E}_f(j) - \mathbf{L}(j)\mathbf{D}_{sr}(j)\mathbf{F}_f(j)\mathbf{D}_{su}(j) \\ \mathbf{G}(j)\mathbf{M}_2(j) & -\mathbf{G}(j)\mathbf{A}_{c,1}(j) & \mathbf{A}_f(j) - \mathbf{G}(j)\mathbf{D}_{sr}(j)\mathbf{F}_f(j)\mathbf{D}_{su}(j) \end{bmatrix},$$

$$\mathbf{B}_c(j) = \begin{bmatrix} \mathbf{B}'(j) & -\mathbf{B}'(j) & \mathbf{0} \end{bmatrix}', \ \mathbf{C}_c(j) = \begin{bmatrix} \phi_1(j)\mathbf{D}_{su}(j) & \phi_1(j)\mathbf{D}_{su}(j) & \mathbf{0} \end{bmatrix},$$

$$\mathbf{D}_c(j) = \begin{bmatrix} \mathbf{E}_d(j) & \mathbf{0} \\ \mathbf{E}_d(j) - \mathbf{L}(j)\mathbf{D}_{sr}(j)\mathbf{F}_d(j) & \mathbf{0} \\ -\mathbf{G}(j)\mathbf{D}_{sr}(j)\mathbf{F}_d(j) & \mathbf{S}(j) \end{bmatrix},$$

$$\mathbf{G}_c(j) = \begin{bmatrix} \mathbf{C}(j) & \mathbf{0} & \mathbf{F}_f(j)\mathbf{p}hi_2(j)\mathbf{D}_{su}(j) \end{bmatrix},$$

$$\mathbf{H}_c(j) = \begin{bmatrix} \mathbf{F}_d(j) & \mathbf{0} \end{bmatrix}, \mathbf{A}_{c,1}(j) = \mathbf{D}_{sr}(j)\mathbf{C}(j)\mathbf{D}_{su}(j).$$

The method of fault-tolerant controller design for μ-periodic linear systems is given by the following theorem.

Theorem 5.3. *There are a set of H_∞ performance levels $\gamma_{2,j}$, $j = 1, \cdots, \mu$ and a circular region $\mathcal{D}_2(\alpha_2, r_2)$. The eigenvalues of $(\mathbf{A}_c(j) + \mathbf{B}_c(j)\mathbf{K}_1(j)\mathbf{C}_c(j))$ belong to $\mathcal{D}_2(\alpha_2, r_2)$, and the error dynamics (5.35)-(5.36) fulfill the H_∞ performance index $||\mathbf{y}_{FTC}(k,j)||_2 \leq \gamma_{2,j}||\mathbf{v}(k,j)||_2$, if there are a μ-periodic symmetric positive definite matrix $\mathbf{P}_2(j)$ and a μ-periodic gain matrix $\mathbf{K}_1(j)$ such that the following conditions hold for each j:*

$$\begin{bmatrix} -\mathbf{P}_2^{-1}(j+1) & \mathbf{A}_c(j) + \mathbf{B}_c(j)\mathbf{K}_1(j)\mathbf{C}_c(j) & \mathbf{D}_c(j) & \mathbf{0} \\ * & -\mathbf{P}_2(j) & \mathbf{0} & \mathbf{G}'_c(j) \\ * & * & -\gamma_{2,j}\mathbf{I}(j) & \mathbf{H}'_c(j) \\ * & * & * & -\gamma_{2,j}\mathbf{I}(j) \end{bmatrix} \leq 0, \tag{5.37}$$

$$\begin{bmatrix} -\mathbf{P}_2^{-1}(j+1) & \mathbf{A}_c(j) + \mathbf{B}_c(j)\mathbf{K}_1(j)\mathbf{C}_c(j) - \alpha_2\mathbf{I}(j) \\ * & -r_2^2\mathbf{P}_2(j) \end{bmatrix} \leq 0. \tag{5.38}$$

Proof. Define a quadratic Lyapunov function $V(k,j) = \mathbf{e}_c'(k,j)\mathbf{P}_2(j)\mathbf{e}_c(k,j)$, and $\mathbf{P}_2(j)$ is a μ-periodic symmetric positive definite matrix.

$$\begin{aligned} V(k,j+1) - V(k,j) &= \mathbf{e}_c'(k,j+1)\mathbf{P}_2(j+1)\mathbf{e}_c(k,j+1) - \mathbf{e}_c'(k,j)\mathbf{P}_2(j)\mathbf{e}_c(k,j) \\ &= \begin{bmatrix} \mathbf{e}_c(k,j) \\ \mathbf{v}(k,j) \end{bmatrix}' \left(\begin{bmatrix} (\mathbf{A}_c(j) + \mathbf{B}_c(j)\mathbf{K}_1(j)\mathbf{C}_c(j))' \\ \mathbf{D}_c'(j) \end{bmatrix} \mathbf{P}_2(j+1) \right. \\ &\quad \left. \times \begin{bmatrix} (\mathbf{A}_c(j) + \mathbf{B}_c(j)\mathbf{K}_1(j)\mathbf{C}_c(j))' \\ \mathbf{D}_c'(j) \end{bmatrix}' - \begin{bmatrix} \mathbf{P}_2(j) & \\ & \mathbf{0} \end{bmatrix} \right) \begin{bmatrix} \mathbf{e}_c(k,j) \\ \mathbf{v}(k,j) \end{bmatrix} \end{aligned}$$

From condition (5.37), we have

$$\mathbf{y}_{FTC}'(k,j)\mathbf{y}_{FTC}(k,j) - \gamma_{2,j}^2\mathbf{v}'(k,j)\mathbf{v}(k,j) + V(k,j+1) - V(k,j) \le 0$$

For a μ-periodic system, there is

$$\begin{aligned} &\sum_{j=1}^{\mu}(\mathbf{y}_{FTC}'(k,j)\mathbf{y}_{FTC}(k,j) - \gamma_{2,j}^2\mathbf{v}'(k,j)\mathbf{v}(k,j) + V(k,j+1) + V(k,j)) \le -V(k,1) \le 0 \\ \Leftrightarrow &\sum_{j=1}^{\mu}(\mathbf{y}_{FTC}'(k,j)\mathbf{y}_{FTC}(k,j) - \gamma_{2,j}^2\mathbf{v}'(k,j)\mathbf{v}(k,j)) \le -V(k+1,1) + V(k,1) - V(k,1) \\ \Leftrightarrow &\sum_{j=1}^{\mu}(\mathbf{y}_{FTC}'(k,j)\mathbf{y}_{FTC}(k,j) - \gamma_{2,j}^2\mathbf{v}'(k,j)\mathbf{v}(k,j)) \le -V(k+1,1) \le 0 \end{aligned} \tag{5.39}$$

Therefore, the H_∞ performance index $||\mathbf{y}_{FTC}(k,j)||_2 \le \gamma_{2,j}||\mathbf{v}(k,j)||_2$ can be satisfied. The proof of the bounded eigenvalues (5.38) for discrete LTP systems can refer to [112, 120] and is omitted here. □

It has been remarked in [21] that $\mathbf{K}_1(j)$ is a structure-limited periodic matrix, which causes great difficulty in gaining a feasible solution for the fault tolerant controller of a μ-periodic systems. As proved in Theorem 5.2, there exists $-\mathbf{P}_2^{-1}(j+1) \le \mathbf{P}_2(j+1) - 2\mathbf{I}(j)$ for a symmetric positive definite matrix $\mathbf{P}_2(j)$, and an improved theorem is presented as follows.

Theorem 5.4. *For a set of H_∞ performance levels $\gamma_{2,j}$, $j = 1, \cdots, \mu$ and a circular region $\mathcal{D}_2(\alpha_2, r_2)$, if there are a μ-periodic symmetric positive definite matrix $\mathbf{P}_2(j)$ and a μ-periodic gain matrix $\mathbf{K}_1(j)$ such that the following conditions hold for each j:*

$$\begin{bmatrix} \mathbf{P}_2(j+1) - 2\mathbf{I}(j) & \mathbf{A}_c(j) + \mathbf{B}_c(j)\mathbf{K}_1(j)\mathbf{C}_c(j) & \mathbf{D}_c(j) & \mathbf{0} \\ * & -\mathbf{P}_2(j) & \mathbf{0} & \mathbf{G}_c'(j) \\ * & * & -\gamma_{2,j}\mathbf{I}(j) & \mathbf{H}_c'(j) \\ * & * & * & -\gamma_{2,j}\mathbf{I}(j) \end{bmatrix} \le 0, \tag{5.40}$$

$$\begin{bmatrix} \mathbf{P}_2(j+1) - 2\mathbf{I}(j) & \mathbf{A}_c(j) + \mathbf{B}_c(j)\mathbf{K}_1(j)\mathbf{C}_c(j) - \alpha_2\mathbf{I}(j) \\ * & -r_2^2\mathbf{P}_2(j) \end{bmatrix} \le 0, \tag{5.41}$$

thus the eigenvalues of $(\mathbf{A}_c(j) + \mathbf{B}_c(j)\mathbf{K}_1(j)\mathbf{C}_c(j))$ *belong to* $\mathcal{D}_2(\alpha_2, r_2)$*, and the error dynamics (5.35)-(5.36) satisfy the* H_∞ *performance index* $||\mathbf{y}_{FTC}(k,j)||_2 \leq \gamma_{2,j}||\mathbf{v}(k,j)||_2$.

Proof. The proof of this theorem is obvious and omitted here. □

5.4.2 An FTC scheme for case II

In case II, we define

$$\mathbf{e}_c(k,j) = \Big[\begin{array}{cccc} \mathbf{x}'(k,j) & \cdots & \mathbf{e}'_{x,l}(k-1,l) & \mathbf{e}'_{f,l}(k-1,l) \\ \cdots & \mathbf{e}'_{x,t}(k,t) & \mathbf{e}'_{f,t}(k,t) & \cdots \end{array} \Big]' (j+1 \leq l \leq \mu, 1 \leq t \leq j),$$

where $\mathbf{e}_c(k,j)$ includes all the items of $\mathbf{x}(k,j)$, $\mathbf{e}_x(k,j)$ and $\mathbf{e}_f(k,j)$ during the interval $((k-1,j),(k,j)]$ in a new order.

With the newly defined $\mathbf{e}_c(k,j)$, the error dynamics (5.35)-(5.36) will be derived again with a new set of system matrices $\mathbf{A}_c(j)$, $\mathbf{B}_c(j)$, $\mathbf{C}_c(j)$, $\mathbf{D}_c(j)$, $\mathbf{G}_c(j)$ and $\mathbf{H}_c(j)$. Then the derivation of obtaining a fault tolerant controller for μ-periodic system in this situation is similar as the one in case I, so please refer to Theorem 5.3 and Theorem 5.4.

5.5 Summary

In this chapter, based on the decentralized W-NCS model with an integrated scheduler, an FTC scheme is proposed for the integrated systems (in the form of discrete LTP systems) with AFs. Due to the limitation of the accessibility to the entire system states, the controller is designed to be related to the state and fault estimates. Therefore, a theorem is proposed to achieve the robust state observer and fault estimator firstly. When the state-space representations are not described with faults at all the time instants in a period T_p, structural adjustment is required in the pursuit of a feasible solution for the state and fault estimates. With the achieved state and fault estimates, corresponding FTC strategy is presented. Due to the decentralized structure of W-NCSs, the problem of structure limitations on the gains of the estimators and the controller is unavoidable. Therefore, improved theorems are put forward to obtain feasible solutions.

6 An FTC scheme for W-NCSs with MFs

This chapter focuses on the development of FTC schemes for the integrated W-NCSs with actuator MFs. An adaptive observer is constructed for the estimation of the state and fault vectors. Afterwards, an FTC strategy based on the adaptive observer is proposed.

The control law for a plant is often required not only to ensure stability and desired performance during normal operating conditions, but also to guarantee suitable behaviors at the occurrence of faults in the system. Besides AFs that have been discussed in the last chapter, MFs are also quite common in the process. The study of FD and FTC with MFs have risen great interest in the control community during last years. However, to the best of our knowledge, the research activities haven't covered FTC schemes for the decentralized W-NCSs integrated with the scheduler in the occurrence of MFs. This motivates strongly our current work. In this chapter we only consider the integrated systems with actuator MFs, as well as system noises.

6.1 System model with MFs

The schematic description of W-NCSs integrated with scheduler $\mathcal{S}$ has been sketched in Fig.4.2. With the consideration of the communication mechanism, a μ-periodic discrete-time plant $\mathcal{P}$ with actuator MFs is addressed as follows

$$\mathbf{x}(k, j+1) = \mathbf{A}(j)\mathbf{x}(k, j) + \mathbf{B}(j)\mathbf{f}_\theta(k, j)\mathbf{u}_s(k, j) + \mathbf{E}(j)\mathbf{w}(k, j) \tag{6.1}$$

$$\mathbf{y}(k, j) = \mathbf{C}(j)\mathbf{x}(k, j) + \mathbf{F}(j)\mathbf{v}(k, j) \ (j = 1, \cdots, \mu) \tag{6.2}$$

where $\mathbf{x}(k, j) \in \Re^n$, $\mathbf{u}_s(k, j) \in \Re^{p_1}$ and $\mathbf{y}(k, j) \in \Re^{m_1(j)}$ are the plant state, control input and measurement output variables, respectively. p_1 is the number of all the actuators in W-NCSs. The noises $\mathbf{w}(k, j) \in \Re^{w(j)}$ and $\mathbf{v}(k, j) \in \Re^{v(j)}$ have zero means. The system

matrices $\mathbf{A}(j)$, $\mathbf{B}(j)$, $\mathbf{C}(j)$, $\mathbf{E}(j)$ and $\mathbf{F}(j)$ are all μ-periodic matrices, i.e., for each j,

$$\begin{aligned}&\mathbf{A}(j)=\mathbf{A}(j+\mu),\ \mathbf{B}(j)=\mathbf{B}(j+\mu),\ \mathbf{C}(j)=\mathbf{C}(j+\mu),\\&\mathbf{E}(j)=\mathbf{E}(j+\mu),\ \mathbf{F}(j)=\mathbf{F}(j+\mu).\end{aligned}$$

$\mathbf{f}_\theta(k,j)\in\Re^{p_1\times p_1}$ is the MF coefficient matrix, expressed as

$$\mathbf{f}_\theta(k,j)=\ \mathrm{diag}\left\{\ \cdots\quad\theta_i(k,j)\quad\cdots\ \right\}.$$

where i is an integer of the interval $[1,p_1]$, and $\theta_i(k,j)$ is the MF coefficient impacting on $u_{s,i}(k,j)$ (the i-th item of $u_s(k,j)$). The physical meaning of $\theta_i(k,j)$ is defined as follows

$$\begin{cases}\text{if}\quad\theta_i(k,j)=0 & :\text{ the actuator is shut down;}\\ \text{if}\quad 0<\theta_i(k,j)<1 & :\text{ the fault deminishes the nominal input;}\\ \text{if}\quad\theta_i(k,j)=1 & :\text{ no fault occurs;}\\ \text{if}\quad 1<\theta_i(k,j)\le\theta_i^o(j) & :\text{ the fault amplifies the nominal input.}\end{cases}\tag{6.3}$$

where $\theta_i^o(j)$ is the possible amplification factor of the input $u_{s,i}(k,j)$. It is assumed that the faults vary slowly during a period T_p in the real-time process, and can be expressed as

$$\theta_i(k+1,j)=\ \theta_i(k,j),\ (1\le j\le\mu,1\le i\le p_1)\tag{6.4}$$

By augmenting (6.4), it holds

$$\theta(k+1,j)=\theta(k,j),\tag{6.5}$$

where $\theta(k,j)\in\Re^{p_1}$ is a column vector consisting of $\theta_i(k,j)$.

For the convenience of our consequent study, we define

$$\begin{aligned}\phi_{s,u}(k,j)&=\mathrm{diag}\left\{\mathbf{u}_s(k,j)\right\}=\ \mathrm{diag}\left\{\ \cdots\quad u_{s,i}(k,j)\quad\cdots\ \right\}\\ \phi_s(k,j)&=\mathbf{B}(j)\phi_{s,u}(k,j),\end{aligned}$$

where $\phi_{s,u}(k,j)\in\Re^{p_1\times p_1}$ and $\phi_s(k,j)\in\Re^{n\times p_1}$.

Assumption 6.1. *The norm of the matrix $\phi_s(k,j)$ is uniformly bounded by a constant $\phi_s(j)$, i.e.,*

$$\|\phi_s(k,j)\|_2\le\phi_s(j),j=1,\ldots,\mu$$

This condition can be satisfied for a wide class of matrix $\phi_s(k,j)$, under the assumption that $\mathbf{u}(k,j)$ and $\mathbf{u}_s(k,j)$ remain bounded even in the presence of faults.

Following the previous analysis, the state-space representation (6.1) can be reformulated as

$$\mathbf{x}(k,j+1)=\mathbf{A}(j)\mathbf{x}(k,j)+\phi_s(k,j)\theta(k,j)+\mathbf{E}(j)\mathbf{w}(k,j).\tag{6.6}$$

6.2 Adaptive estimation method

For the convenience of our further study, we introduce the adaptive estimation method proposed in [96, 98].

Consider the discrete-time stochastic MIMO LTV systems

$$\theta(k+1) = \theta(k) \tag{6.7}$$
$$\mathbf{x}(k+1) = \mathbf{A}(k)\mathbf{x}(k) + \phi(k)\theta(k) + \mathbf{w}(k) \tag{6.8}$$
$$\mathbf{y}(k) = \mathbf{C}(k)\mathbf{x}(k) + \mathbf{v}(k) \tag{6.9}$$

where $\mathbf{x}(k) \in \Re^n$ and $\mathbf{y}(k) \in \Re^m$ are the state vector and output vector, respectively. $\mathbf{A}(k)$ and $\mathbf{C}(k)$ are known time varying matrices with appropriate dimensions. $\theta(k) \in \Re^p$ is an unknown parameter vector, $\phi(k) \in \Re^{n\times p}$ is a matrix of known signals, $\mathbf{w}(k)$ and $\mathbf{v}(k)$ are noises with zero means.

The adaptive observer for (6.7)-(6.9) is constructed as follows

$$\boldsymbol{\Upsilon}(k+1) = (\mathbf{A}(k) - \mathbf{L}(k)\mathbf{C}(k))\boldsymbol{\Upsilon}(k) + \phi(k) \tag{6.10}$$
$$\hat{\mathbf{x}}(k+1) = \mathbf{A}(k)\hat{\mathbf{x}}(k) + \phi(k)\hat{\theta}(k) + \mathbf{L}(k)\mathbf{r}(k) + \boldsymbol{\Upsilon}(k+1)(\hat{\theta}(k+1) - \hat{\theta}(k)) \tag{6.11}$$
$$\hat{\theta}(k+1) = \hat{\theta}(k) + \mu(k)\boldsymbol{\Upsilon}'(k)\mathbf{C}'(k)\mathbf{r}(k) \tag{6.12}$$
$$\hat{\mathbf{y}}(k) = \mathbf{C}(k)\hat{\mathbf{x}}(k) \tag{6.13}$$
$$\mathbf{r}(k) = \mathbf{y}(k) - \hat{\mathbf{y}}(k) \tag{6.14}$$

where matrix $\boldsymbol{\Upsilon}(k) \in \Re^{n\times p}$, $\hat{\mathbf{x}}(k)$, $\hat{\mathbf{y}}(k)$ and $\hat{\theta}(k)$ are the state, output and parameter estimates, respectively. $\mathbf{L}(k)$ is the observer gain and $\mathbf{r}(k)$ is the residual vector. $\mu(k) > 0$ is a bounded scalar gain satisfying the following assumption.

Assumption 6.2. *[98] For all $k \geq 0$, the scalar gain $\mu(k) > 0$ is small enough such that*

$$\left\| \sqrt{\mu(k)}\mathbf{C}(k)\boldsymbol{\Upsilon}(k) \right\|_2 \leq 1$$

For the convenience of the proof of adaptive estimation method, one definition and two lemmas are presented as follows.

Definition 6.1. *[98] The linear discrete-time varying system*

$$\mathbf{z}(k+1) = \mathbf{A}(k)\mathbf{z}(k), \mathbf{z} \in \Re^{n_l}, \mathbf{A} \in \Re^{n_l\times n_l} \tag{6.15}$$

is exponentially stable, if there exist two constants $r > 0$ and $0 < q < 1$ such that

$$\left\| \prod_{i=k_0}^{k-1} A(i) \right\|_2 \leq rq^{k-k_0}, \ (k > k_0)$$

Lemma 6.1. *[98, 122] If the linear discrete-time varying system (6.15) is exponentially stable, then*

1. *for any bounded signal* $\mathbf{v}(k) \in \Re^{n_l}$, $\mathbf{z}(k)$ *is bounded in the sense of* $\mathbf{z}(k+1) = \mathbf{A}(k)\mathbf{z}(k) + \mathbf{v}(k)$;

2. *for any* $\mathbf{v}(k)$ *tending to zero exponentially, the state vector* $\mathbf{z}(k)$ *constructed as above also tends to zero exponentially.*

Lemma 6.2. *[98] A matrix* $\varphi(k) \in \Re^{m_l \times n_l}$ *satisfies that* $\|\varphi(k)\|_2 \leq 1$ *for* $k \geq 0$. *If there exist a real constant* $\alpha > 0$ *and an integer* $l > 0$ *such that the following inequality holds*

$$\frac{1}{l}\sum_{i=k}^{k+l-1} \varphi'(i)\varphi(i) \geq \alpha \mathbf{I},$$

then the linear discrete-time varying system $\mathbf{z}(k+1) = (\mathbf{I} - \varphi'(k)\varphi(k))\mathbf{z}(k)$ *is exponentially stable.*

6.3 Problem formulation

The basic idea of FTC strategy for the system model (6.1)-(6.2) with actuator MFs is divided into two steps:

(1) achieving the estimation model of $\mathbf{f}_\theta(k, j)$ in (6.1);

(2) developing a fault tolerant controller and compensating the effects caused by $\mathbf{f}_\theta(k, j)$ with its estimation model.

Since the system model (6.1) has been reformulated into (6.6) with faults as unknown parameters, the first step of FTC strategy turns to construct the estimator of the parameter $\theta(k, j)$. Besides, the state vector $\mathbf{x}(k, j)$ is also considered unmeasurable. For such a problem of joint state-parameter estimation in (6.6), it seems natural to use the adaptive estimation method proposed in [98]. However, it should be pointed out that, due to the decentralization of W-NCSs, the structures of system matrices in (6.1)-(6.2) are all limited [21]. By applying the adaptive estimation method directly to the system model in (6.6), it requires that $\mathbf{\Upsilon}(k)$ has to be a structure-limited matrix, which cannot be guaranteed by this way. To solve this problem, we will reconstruct the system model (6.6) by a lifting technology, meanwhile, increase the communication volume among CSs to loosen the structure limitations. After that, we apply the adaptive estimation method to the lifted system model to estimate the system state and the unknown parameter vectors.

In order to develop a fault tolerant controller, we will start from the design of a nominal controller for the system in the fault-free case. Due to the inaccessibility of the system states $\mathbf{x}(k,j)$, the controller will be developed to be related with $\hat{\mathbf{x}}(k,j)$ (the estimate of $\mathbf{x}(k,j)$). Hence the fault-free controller $\mathbf{u}_{nom,s}(k,j)$ is designed by LCs as

$$\mathbf{u}_{nom,s}(k,j) = \mathbf{K}(j)\hat{\mathbf{x}}_s(k,j) + \mathbf{R}_{ef}(j),\ j = 1,\cdots,\mu \tag{6.16}$$

where $\hat{\mathbf{x}}_s(k,j)$ denotes the state estimate $\hat{\mathbf{x}}(k,j)$ received by LCs. With the consideration of the limit traffic load in the i-th subsystem, sometimes only the state estimates of the i-th subprocess will be transmitted from the i-th CS to its LCs. Of course, if enough bandwidth can be supported by the network, the received state estimates from other CSs could also be delivered by the i-th CS to its LCs. Such limitation can be managed by the feedback gain $\mathbf{K}(j)$, which is a structure-limited μ-periodic matrix as stated in [21]. $\mathbf{R}_{ef}(j)$ is the reference signal vector. To obtain the nominal controller (6.16), a suitable $\mathbf{K}(j)$ should be found to keep the stability of Plant $\mathcal{P}$.

When the actuator MFs occur as in (2.4), the following FTC strategy is developed to compensate the effects caused by the faults

$$\mathbf{u}_{FTC,s}(k,j) = \mathbf{f}_{\hat{\theta}}^{-1}(k,j)\mathbf{u}_{nom,s}(k,j),\ j = 1,\cdots,\mu \tag{6.17}$$

where $\mathbf{f}_{\hat{\theta}}(k,j)$ is the estimate of $\mathbf{f}_{\theta}(k,j)$, $\mathbf{u}_{FTC,s}(k,j)$ is the fault tolerant controller.

Therefore, the FTC scheme for W-NCSs with actuator MFs consists of four steps:

(1) modeling (6.6) with a lifting technology;

(2) applying adaptive estimation method to the lifted system to estimate the system state and fault vectors;

(3) constructing the fault-free controller (6.16) and finding the solution for the μ-periodic feedback gain $\mathbf{K}(j)$ with a limited structure, to ensure the stability of the system (6.1);

(4) compensating the effects caused by faults with the fault estimate vector.

6.4 An FE scheme for LTP systems with MFs

In this section, the lifting technology will be applied on the discrete LTP systems, firstly. After that, an adaptive observer will be constructed based on the lifted system.

6.4.1 Lifting of LTP systems

Considering the periodicity in equation (6.6), a lifting computation will be implemented on it. Let $\mathbf{\Phi}(\tau_1, \tau_0)$ be the state transition matrix defined by

$$\mathbf{\Phi}(\tau_1, \tau_0) = \begin{cases} \mathbf{I} & , \text{ if } \tau_1 = \tau_0; \\ \mathbf{A}(\tau_1 - 1)\mathbf{A}(\tau_1 - 2)\cdots\mathbf{A}(\tau_0) & , \text{ if } \tau_1 > \tau_0. \end{cases}$$

where τ_1 and τ_0 are arbitrary integers among $[1, \mu]$. Considering the periodicity of the system model, there is $\mathbf{\Phi}(\tau_1 + \mu, \tau_0 + \mu) = \mathbf{\Phi}(\tau_1, \tau_0)$ [112]. Select an arbitrary integer j $(1 \leq j \leq \mu)$ as the initial time instant and define $\mathbf{x}_j(k) = \mathbf{x}(k, j)$, $\theta_j(k) = \theta(k, j)$. An augmented vector $\mathbf{y}_j(k) \in \Re^{m_1}$ $(m_1 = \sum_{j=1}^{\mu} m_1(j))$ is constructed by

$$\mathbf{y}_j(k) = \begin{bmatrix} \mathbf{y}(k, j) \\ \vdots \\ \mathbf{y}(k+1, j-1) \end{bmatrix} \tag{6.18}$$

Besides, $\mathbf{w}_j(k) \in \Re^{w}$ $(w = \sum_{j=1}^{\mu} w(j))$ and $\mathbf{v}_j(k) \in \Re^{v}$ $(v = \sum_{j=1}^{\mu} v(j))$ are built in the same way as $\mathbf{y}(k)$, by replacing the items $\mathbf{y}$ with $\mathbf{w}$ and $\mathbf{v}$, respectively. It is remarkable that $\mathbf{w}_j(k)$ and $\mathbf{v}_j(k)$ also have zero means. According to [111, 112], the models of the periodic systems (6.6)-(6.2) and the fault (6.5) can be lifted into a discrete LTV system

$$\mathbf{x}_j(k+1) = \mathbf{A}_j\mathbf{x}_j(k) + \psi_{1,j}(k)\theta_j(k) + \mathbf{E}_j\mathbf{w}_j(k), \tag{6.19}$$

$$\mathbf{y}_j(k) = \mathbf{C}_j\mathbf{x}_j(k) + \psi_{2,j}(k)\theta_j(k) + \mathbf{F}_j\mathbf{v}_j(k), \tag{6.20}$$

$$\theta_j(k+1) = \theta_j(k), \tag{6.21}$$

where the system matrices $\mathbf{A}_j$, $\mathbf{E}_j$, $\mathbf{C}_j$ and $\mathbf{F}_j$ are known matrices for certain j and

$$\mathbf{A}_j = \mathbf{\Phi}(j+\mu, j),\ \psi_{1,j}(k) = \sum_{i=1}^{\mu} \mathbf{\Phi}(j+\mu, j+i)\phi_s(k, j+i-1)$$

$$\mathbf{E}_j = \Big[\ \mathbf{\Phi}(j+\mu, j+1)\mathbf{E}(j) \quad \mathbf{\Phi}(j+\mu, j+2)\mathbf{E}(j+1) \quad \cdots$$
$$\mathbf{\Phi}(j+\mu, j-2+\mu)\mathbf{E}(j-2) \quad \mathbf{E}(j-1)\ \Big],$$

$$\mathbf{C}_j = \begin{bmatrix} \mathbf{C}(j) \\ \mathbf{C}(j+1)\mathbf{\Phi}(j+1, j) \\ \vdots \\ \mathbf{C}(j-1+\mu)\mathbf{\Phi}(j-1+\mu, j) \end{bmatrix},$$

$$\psi_{2,j}(k)=\begin{bmatrix}\psi_1\\ \psi_2\\ \vdots\\ \psi_\mu\end{bmatrix},\mathbf{F}_j=\begin{bmatrix}\mathbf{F}_{1,1} & \mathbf{O} & \cdots & \mathbf{O}\\ \mathbf{F}_{2,1} & \mathbf{F}_{2,2} & \ddots & \vdots\\ \vdots & \vdots & \vdots & \mathbf{O}\\ \mathbf{F}_{\mu,1} & \cdots & \mathbf{F}_{\mu,\mu-1} & \mathbf{F}_{\mu,\mu}\end{bmatrix},$$

$$\psi_p=\begin{cases}\mathbf{O} & ,\text{ if } p=1;\\ \sum_{i=1}^{p-1}\mathbf{C}(j-1+p)\mathbf{\Phi}(j+p,j+i)\phi_s(k,j+i-1) & ,\text{ if } p>1.\end{cases}$$

$$\mathbf{F}_{p,q}=\begin{cases}\mathbf{F}(j) & ,\text{ if } p=q;\\ \mathbf{C}(j-1+p)\mathbf{\Phi}(j-1+p,j+q)\mathbf{E}(j+q-1) & ,\text{ if } 2\le p\le\mu.\end{cases}$$

$$(p,q=1,\cdots,\mu).$$

Remark 6.1. *It should be pointed out that in $\psi_{1,j}(k)$ and $\psi_{2,j}(k)$, the item $\phi_s(k,j+i-1)$ denotes actually $\phi_s(k+1,j+i-1-\mu)$ for $j+i-1>\mu$.*

6.4.2 Design of an adaptive observer

In order to realize the design of fault tolerant controller in the sequels, it is required to estimate the state vector $\mathbf{x}(k)$ and fault vector $\theta(k)$ in (6.19)-(6.20) primarily. An adaptive observer is proposed in [96], which considers the joint estimation of states and unknown parameters. This method have received lots of contribution both for linear systems [96, 98, 123–126] and nonlinear systems [97, 127–130]. In these references, the unknown parameters are assumed to be embedded either in state equations or in output equations. Recently, [131] extended the adaptive algorithm for the system with unknown parameters in both state and output equations. However, this algorithm is developed only for continue-time systems. In the following, we will present an adaptive observer for linear discrete-time systems with unknown parameters in both state and output equations.

Firstly, we give an assumption, which is the basis of the development of adaptive observer for the system (6.19)-(6.21).

Assumption 6.3. *For a certain time instant $j\in[1,\mu]$, the matrix pair $(\mathbf{A}_j,\mathbf{C}_j)$ in (6.19)-(6.20) is observable, and there exists matrix $\mathbf{L}_j\in\Re^{n\times m_2}$, such that the LTI system*

$$\mathbf{x}(k+1)=(\mathbf{A}_j-\mathbf{L}_j\mathbf{C}_j)\mathbf{x}(k)$$

is exponentially stable.

For the joint estimation of state and fault vectors in linear discrete-time varying systems

(6.19)-(6.21), the adaptive observer is proposed as follows

$$\boldsymbol{\Upsilon}_j(k+1) = (\mathbf{A}_j - \mathbf{L}_j\mathbf{C}_j)\boldsymbol{\Upsilon}_j(k) + \psi_{1,j}(k) - \mathbf{L}_j\psi_{2,j}(k) \tag{6.22}$$

$$\hat{\mathbf{x}}_j(k+1) = \mathbf{A}_j\hat{\mathbf{x}}_j(k) + \psi_{1,j}(k)\hat{\theta}_j(k) + \mathbf{L}_j\mathbf{r}_{s,j}(k) + \boldsymbol{\Upsilon}_j(k+1)(\hat{\theta}_j(k+1) - \hat{\theta}_j(k)) \tag{6.23}$$

$$\hat{\theta}_j(k+1) = \hat{\theta}_j(k) + \mu_j(k)(\mathbf{C}_j\boldsymbol{\Upsilon}_j(k) + \psi_{2,j}(k))'\mathbf{r}_{s,j}(k) \tag{6.24}$$

where $\hat{\mathbf{x}}_j(k) \in \Re^n$ and $\hat{\theta}_j(k) \in \Re^{p_1}$ are the estimates of $\mathbf{x}_j(k)$ and $\theta_j(k)$, respectively. $\mathbf{r}_{s,j}(k) \in \Re^{m_2}$ is the residual which has been coordinated by the scheduler $\mathcal{S}$ and received by the CSs. Matrix $\boldsymbol{\Upsilon}_j(k) \in \Re^{n\times p_1}$, scalar gain $\mu_j(k) > 0$. $\mathbf{L}_j$ is the observer gain matrix with limited structure [21].

Following the communication mechanism in [21], the state estimate will be transmitted back to the LCs through the wireless network. Due to the effects of the scheduler $\mathcal{S}$, the output estimate of (6.2) at the LCs will be

$$\hat{\mathbf{y}}(k,j) = \mathbf{C}(j)\hat{\mathbf{x}}_s(k,j)\ (j = 1, \cdots, \mu), \tag{6.25}$$

where $\hat{\mathbf{y}}(k,j) \in \Re^{m_1(j)}$ is the estimates of $\mathbf{y}(k,j)$, and $\hat{\mathbf{x}}_s(k,j) \in \Re^n$ is the output of the state estimate $\hat{\mathbf{x}}(k,j)$ transmitting through the network. With an ideal wireless network, there is $\hat{\mathbf{x}}_s(k,j) = \hat{\mathbf{x}}(k,j)$. Following the lifting process for (6.20) and considering the ideal wireless network, there is

$$\hat{\mathbf{y}}_j(k) = \mathbf{C}_j\hat{\mathbf{x}}_j(k) + \psi_{2,j}(k)\hat{\theta}_j(k) \tag{6.26}$$

where $\hat{\mathbf{y}}_j(k)$ is the estimate of $\mathbf{y}_j(k)$. So the residual vector $\mathbf{r}_j(k) \in \Re^{m_1}$ at the LCs is obtained by

$$\mathbf{r}_j(k) = \mathbf{y}_j(k) - \hat{\mathbf{y}}_j(k). \tag{6.27}$$

Moreover, the received residual vector at the CSs in the ideal wireless network satisfies

$$\mathbf{r}_{s,j}(k) = \mathbf{r}_j(k) \tag{6.28}$$

To prove the convergence of the proposed adaptive algorithm (6.22)-(6.24), the following two assumptions are required.

Assumption 6.4. *The scalar gain $\mu_j(k) > 0$ is small enough such that*

$$\left\| \sqrt{\mu_j(k)}(\mathbf{C}_j\boldsymbol{\Upsilon}_j(k) + \psi_{2,j}(k)) \right\|_2 \leq 1$$

where $\boldsymbol{\Upsilon}_j(k)$ is constructed by (6.22).

Assumption 6.5. *The matrices of signals $\psi_{1,j}(k)$ and $\psi_{2,j}(k)$ are persistently exciting such that, for some constant $\alpha > 0$ and integer $l > 0$, the matrix $\boldsymbol{\Upsilon}_j(k)$ in (6.22) and the gain $\mu_j(k)$ satisfy the following inequality*

$$\frac{1}{l}\sum_{i=k}^{k+l-1}\mu_j(i)(\mathbf{C}_j\boldsymbol{\Upsilon}_j(i)+\psi_{2,j}(i))'(\mathbf{C}_j\boldsymbol{\Upsilon}_j(i)+\psi_{2,j}(i)) \geq \alpha\mathbf{I}$$

The property of the adaptive observer (6.22)-(6.24) for the state-space representation (6.19)-(6.21) in the noise-free case is stated in the following theorem.

Theorem 6.1. *Under an ideal wireless network and for a certain initial time instant j, $j = 1, \cdots, \mu$, if the noises are absent in the system models (6.19)-(6.21), i.e., $\mathbf{w}_j(k) = \mathbf{0}$ and $\mathbf{v}_j(k) = \mathbf{0}$ with all $k \geq 0$, then the algorithm (6.22)-(6.24) under Assumptions 6.3-6.5 is a globally exponential adaptive observer.*

Proof. Define the state estimation error $\mathbf{e}_{x,j}(k) = \mathbf{x}_j(k) - \hat{\mathbf{x}}_j(k)$, and the fault estimation error $\mathbf{e}_{\theta,j}(k) = \theta_j(k) - \hat{\theta}_j(k)$. From (6.19) and (6.23) without noises, as well as equation (6.21) and the residual in (6.28), it's easy to obtain the error dynamics of the state estimation as follows

$$\begin{aligned}\mathbf{e}_{x,j}(k+1) = {} & (\mathbf{A}_j - \mathbf{L}_j\mathbf{C}_j)\mathbf{e}_{x,j}(k) + (\psi_{1,j}(k) - \mathbf{L}_j\psi_{2,j}(k))\mathbf{e}_{\theta,j}(k) \\ & + \boldsymbol{\Upsilon}_j(k+1)(\mathbf{e}_{\theta,j}(k+1) - \mathbf{e}_{\theta,j}(k))\end{aligned} \tag{6.29}$$

Now, we define a linearly combined error $\eta(k) = \mathbf{e}_{x,j}(k) - \boldsymbol{\Upsilon}_j(k)\mathbf{e}_{\theta,j}(k)$. The dynamic equation of $\eta(k)$ is addressed as

$$\begin{aligned}\eta(k+1) = {} & (\mathbf{A}_j - \mathbf{L}_j\mathbf{C}_j)\eta(k) \\ & + \left[(\mathbf{A}_j - \mathbf{L}_j\mathbf{C}_j)\boldsymbol{\Upsilon}_j(k) + \psi_{1,j}(k) - \mathbf{L}_j\psi_{2,j}(k) - \boldsymbol{\Upsilon}_j(k+1)\right]\mathbf{e}_{\theta,j}(k)\end{aligned}$$

From the equation (6.22), the last equation simply becomes

$$\eta(k+1) = (\mathbf{A}_j - \mathbf{L}_j\mathbf{C}_j)\eta(k) \tag{6.30}$$

According to Assumption 6.3, the combined error $\eta(k)$ tends to zero exponentially.

Following equations (6.21) and (6.24), there is

$$\mathbf{e}_{\theta,j}(k+1) = \mathbf{e}_{\theta,j}(k) - \mu_j(k)(\mathbf{C}_j\boldsymbol{\Upsilon}_j(k)+\psi_{2,j}(k))'(\mathbf{C}_j\mathbf{e}_{x,j}(k)+\psi_{2,j}(k)\mathbf{e}_{\theta,j}(k)) \tag{6.31}$$

Considering the definition of $\eta(k)$, (6.31) is rewritten as

$$\begin{aligned}\mathbf{e}_{\theta,j}(k+1) = {} & \left[\mathbf{I} - \mu_j(k)(\mathbf{C}_j\boldsymbol{\Upsilon}_j(k)+\psi_{2,j}(k))'(\mathbf{C}_j\boldsymbol{\Upsilon}_j(k)+\psi_{2,j}(k))\right]\mathbf{e}_{\theta,j}(k) \\ & - \mu_j(k)(\mathbf{C}_j\boldsymbol{\Upsilon}_j(k)+\psi_{2,j}(k))'\mathbf{C}_j\eta(k)\end{aligned} \tag{6.32}$$

According to Lemma 6.2 and Assumption 6.5, we finally have that the linear discrete-time varying system (6.33) is exponentially stable.

$$\mathbf{z}(k+1) = [\mathbf{I} - \mu_j(k)(\mathbf{C}_j\boldsymbol{\Upsilon}_j(k) + \psi_{2,j}(k))'(\mathbf{C}_j\boldsymbol{\Upsilon}_j(k) + \psi_{2,j}(k))]\,\mathbf{z}(k) \tag{6.33}$$

In the lifted model (6.19)-(6.21), $\mathbf{C}_j$ is known, while $\psi_{1,j}(k)$ and $\psi_{2,j}(k)$ are bounded following Assumption 6.1. Therefore, $\boldsymbol{\Upsilon}_j(k)$ constructed in (6.22) is also bounded. According to Lemma 6.2 and Assumption 6.4, as well as the property of $\eta(k)$ in (6.30), the fault estimation error $\mathbf{e}_{\theta,j}(k)$ in (6.32) driven by $-\mu_j(k)(\mathbf{C}_j\boldsymbol{\Upsilon}_j(k)+\psi_{2,j}(k))'\mathbf{C}_j\eta(k)$ tends to zero exponentially.

Consequently, the state estimation error $\mathbf{e}_{x,j}(k) = \eta(k)+\boldsymbol{\Upsilon}_j(k)\mathbf{e}_{\theta,j}(k)$ tends also to zero exponentially. □

Now we will concern the properties of the proposed adaptive estimation method applied to the system models with noises.

Theorem 6.2. *Under Assumptions 6.3-6.5 with an ideal wireless network, when the adaptive observer (6.22)-(6.24) is applied to the system models (6.19)-(6.21), where the noises* $\mathbf{w}_j(k)$ *and* $\mathbf{v}_j(k)$ *have zero means, then along with* $k \to \infty$*, the mathematical expectations of the state and fault estimation errors are convergent exponentially as* $\mathbf{E}\mathbf{e}_{x,j}(k) \to 0$, $\mathbf{E}\mathbf{e}_{\theta,j}(k) \to 0$.

Proof. The proof of this theorem is based on the result of the noise-free case. In the case with noises in the system models (6.19)-(6.21), the error dynamics are addressed as

$$\begin{aligned}\mathbf{e}_{x,j}(k+1) = {} & (\mathbf{A}_j - \mathbf{L}_j\mathbf{C}_j)\mathbf{e}_{x,j}(k) + (\psi_{1,j}(k) - \mathbf{L}_j\psi_{2,j}(k))\mathbf{e}_{\theta,j}(k) \\ & + \boldsymbol{\Upsilon}_j(k+1)(\mathbf{e}_{\theta,j}(k+1) - \mathbf{e}_{\theta,j}(k)) + \mathbf{E}_j\mathbf{w}_j(k) - \mathbf{L}_j\mathbf{F}_j\mathbf{v}_j(k) \qquad (6.34)\\ \mathbf{e}_{\theta,j}(k+1) = {} & \mathbf{e}_{\theta,j}(k) - \mu_j(k)(\mathbf{C}_j\boldsymbol{\Upsilon}_j(k) + \psi_{2,j}(k))'(\mathbf{C}_j\mathbf{e}_{x,j}(k) + \psi_{2,j}(k)\mathbf{e}_{\theta,j}(k)) \\ & - \mu_j(k)(\mathbf{C}_j\boldsymbol{\Upsilon}_j(k) + \psi_{2,j}(k))'\mathbf{F}_j\mathbf{v}_j(k) \qquad (6.35)\end{aligned}$$

In the case without noises in the system models, the error dynamics (6.34)-(6.35) are exponentially stable, which is concordant with the Theorem 6.1.

When it comes to the case with the consideration of noises in the system models (6.22)-(6.24), some mathematical processes are implemented on the error dynamics (6.34)-(6.35). Since the noises are all with zero means, by taking the mathematical expectation on both sides of the error dynamics (6.34)-(6.35), we have

$$\begin{aligned}\mathbf{E}\mathbf{e}_{x,j}(k+1) = {} & (\mathbf{A}_j - \mathbf{L}_j\mathbf{C}_j)\mathbf{E}\mathbf{e}_{x,j}(k) + (\psi_{1,j}(k) - \mathbf{L}_j\psi_{2,j}(k))\mathbf{E}\mathbf{e}_{\theta,j}(k) \\ & + \boldsymbol{\Upsilon}_j(k+1)(\mathbf{E}\mathbf{e}_{\theta,j}(k+1) - \mathbf{E}\mathbf{e}_{\theta,j}(k)) \qquad (6.36)\\ \mathbf{E}\mathbf{e}_{\theta,j}(k+1) = {} & \mathbf{E}\mathbf{e}_{\theta,j}(k) - \mu_j(k)(\mathbf{C}_j\boldsymbol{\Upsilon}_j(k) + \psi_{2,j}(k))'(\mathbf{C}_j\mathbf{E}\mathbf{e}_{x,j}(k) + \psi_{2,j}(k)\mathbf{E}\mathbf{e}_{\theta,j}(k)) \qquad (6.37)\end{aligned}$$

which are identical as the error dynamics (6.29)-(6.31) in the noise-free case, except that the estimation errors $\mathbf{e}_{x,j}(k)$ and $\mathbf{e}_{\theta,j}(k)$ are replaced by their mathematical expectation $\mathbf{E}\mathbf{e}_{x,j}(k)$ and $\mathbf{E}\mathbf{e}_{\theta,j}(k)$, respectively. Following the same procedure as in the proof of Theorem 6.1, the mathematical expectations $\mathbf{E}\mathbf{e}_{x,j}(k)$ and $\mathbf{E}\mathbf{e}_{\theta,j}(k)$ tend to zero exponentially. □

6.4.3 Realization of the adaptive observer

The proposed adaptive estimation method is proceeded on a lifted system, which also can be taken as the model of W-NCSs with period T_p. Considering the distribution of W-NCSs, no central node is supposed to carry out this estimation algorithm. Therefore, all the CSs are required to execute the adaptive estimation method at each T_p. According to the operation mechanism of sampling and communication described in chapter 4, the i-th subsystem $i = 1, \cdots, N$ in view of discrete-time systems has a state update at each $T_{c,i}$, so l_i $(= T_p/T_{c,i})$ state updates will be generated in each T_p. With this lifted system model before the time kT_p, the i-th CS will estimate the l_i state updates during $[kT_p, (k+1)T_p)$ simultaneously. After that, the i-th CS will share the l_i new state estimates with other CSs. These state estimates will arrive other CSs as soon as possible and help them to improve their state estimation, which is executed also before $(k+1)T_p$. As is well known that, the control commands executed by the LCs on the i-th subprocess are calculated based on the state estimates generated by the i-th CS. Hence, with the received state estimates from the i-th CS, the other CSs will obtain the control information which will be implemented on the i-th subprocess during $[kT_p, (k+1)T_p)$. In other words, the control commands will be shared among CSs, which will be very necessary for the realization of equation (6.22).

In the event of actuator MFs on W-NCSs, the fault estimates will be generated by the CSs in a similar way as the state estimation. Afterwards, the fault estimates of the i-th CS will be packed with its state estimates and shared among all the CSs before kT_p. Since this fault estimates will be very helpful for the design of fault tolerant controller, this share of fault estimates will bring more specific control information to other CSs.

After the state have been estimated, the i-th CS will send its newest state estimates immediately to its LCs for the residual generation. Although the state estimation of the i-th CS is executed only once in each T_p and completed before kT_p, the residuals during $[kT_p, (k+1)T_p)$ are generated still at each $T_{c,i}$. Since the adaptive observer method is based on a lifted system, it required the share of residuals among CSs, which has been considered as an advanced design issue in [21]. Therefore, the problem of structure limitations on $\mathbf{L}_j$ is avoided here.

6.5 An FTC scheme for LTP systems with MFs

In this section, an FTC strategy will be developed to ensure the discrete LTP systems to be tolerant to actuator MFs.

6.5.1 Design of a fault-free controller

We will start from the μ-periodic discrete-time plant $\mathcal{P}$ (6.1)-(6.2) without MFs, which are expressed as follows:

$$\mathbf{x}(k, j+1) = \mathbf{A}(j)\mathbf{x}(k, j) + \mathbf{B}(j)\mathbf{u}_s(k, j) + \mathbf{E}(j)\mathbf{w}(k, j) \tag{6.38}$$

$$\mathbf{y}(k, j) = \mathbf{C}(j)\mathbf{x}(k, j) + \mathbf{F}(j)\mathbf{v}(k, j) \ (j = 1, \cdots, \mu) \tag{6.39}$$

Define $\mathbf{u}_{s,j}(k)$ in a similar way as $\mathbf{y}_j(k)$ in (6.18).

$$\mathbf{u}_{s,j}(k) = \begin{bmatrix} \mathbf{u}_s(k, j) \\ \vdots \\ \mathbf{u}_s(k+1, j-1) \end{bmatrix} \tag{6.40}$$

Following the lifting procedure in equations (6.19)-(6.20), we have a discrete LTI system

$$\mathbf{x}_j(k+1) = \mathbf{A}_j\mathbf{x}_j(k) + \mathbf{B}_j\mathbf{u}_{s,j}(k) + \mathbf{E}_j\mathbf{w}_j(k), \tag{6.41}$$

$$\mathbf{y}_j(k) = \mathbf{C}_j\mathbf{x}_j(k) + \mathbf{D}_j\mathbf{u}_{s,j}(k) + \mathbf{F}_j\mathbf{v}_j(k), \tag{6.42}$$

where

$$\mathbf{B}_j = \begin{bmatrix} \mathbf{\Phi}(j+\mu, j+1)\mathbf{B}(j) & \mathbf{\Phi}(j+\mu, j+2)\mathbf{B}(j+1) & \cdots \\ \mathbf{\Phi}(j+\mu, j-2+\mu)\mathbf{B}(j-2) & \mathbf{B}(j-1) \end{bmatrix},$$

$$\mathbf{D}_j = \begin{bmatrix} \mathbf{D}_{1,1} & \mathbf{O} & \cdots & \mathbf{O} \\ \mathbf{D}_{2,1} & \mathbf{D}_{2,2} & \ddots & \vdots \\ \vdots & \vdots & \vdots & \mathbf{O} \\ \mathbf{D}_{\mu,1} & \cdots & \mathbf{D}_{\mu,\mu-1} & \mathbf{D}_{\mu,\mu} \end{bmatrix},$$

$$\mathbf{D}_{p,q} = \begin{cases} \mathbf{O} & , \text{if } p = q; \\ \mathbf{C}(j-1+p)\mathbf{\Phi}(j-1+p, j+q)\mathbf{B}(j+q-1) & , \text{if } p > q. \end{cases}$$

$(p, q = 1, \cdots, \mu)$.

Under an ideal network environment, an nominal controller for (6.38)-(6.39) has been proposed in (6.16). In the case with scheduled delay or packet loss, the latest update will be adopted to develop the controller. Therefore, the fault-free controller is designed as

$$\mathbf{u}_{nom,s}(k, j) = \mathbf{K}(j)\phi(j)\hat{\mathbf{x}}_{s,j}(k) + \mathbf{R}_{ef}(j), \ j = 1, \cdots, \mu \tag{6.43}$$

where $\phi(j)$ is a Boolean matrix, which will choose a proper state update to proceed the calculation of the controller. $\phi(j)$ relies closely on the scheduler $\mathcal{S}$: (1) in the case with ideal condition, $\phi(j)$ is an identity matrix, so (6.43) is identical as (6.16); (2) in the case with delay or packet loss, the former received information will be considered, the latest update of state estimates will be chosen by $\phi(j)$ and assigned as $\hat{\mathbf{x}}_s(k,j)$ for calculation.

For our purpose of designing the controller, we first set $\mathbf{R}_{ef}(j) = \mathbf{0}$ and define $\mathbf{K}_j$ as

$$\mathbf{K}_j = \begin{bmatrix} \mathbf{K}(j)\phi(j) \\ \mathbf{K}(j+1)\phi(j+1) \\ \vdots \\ \mathbf{K}(j-1+\mu)\phi(j-1+\mu) \end{bmatrix} \tag{6.44}$$

Now the controller $\mathbf{u}_{nom,s}(k,j)$ can be rewritten as

$$\mathbf{u}_{nom,s}(k,j) = \mathbf{K}_j \hat{\mathbf{x}}_{s,j}(k). \tag{6.45}$$

Substituting (6.45) in (6.41) with the consideration of an ideal wireless network, we have

$$\mathbf{x}_j(k+1) = (\mathbf{A}_j + \mathbf{B}_j\mathbf{K}_j)\mathbf{x}_j(k) - \mathbf{B}_j\mathbf{K}_j\mathbf{e}_{x,j}(k) + \mathbf{E}_j\mathbf{w}_j(k) \tag{6.46}$$

Since $\mathbf{w}_j(k)$ has zero mean and the expectation of $\mathbf{e}_{x,j}(k)$ tends to zero exponentially according to Theorem 6.2, we only need to find a suitable $\mathbf{K}_j$ to satisfy the stability of Plant $\mathcal{P}$.

It has been mentioned before that $\mathbf{K}_j$ is a structure-limited matrix, which increases the difficulty of gaining a feasible solution for the controller gain $\mathbf{K}_j$. To achieve this controller for the lifted system, we present the following theorem.

Theorem 6.3. *Give a certain initial time instant j, $j = 1, \cdots, \mu$ and a circular region $\mathcal{D}(\alpha, r)$. The eigenvalues of $(\mathbf{A}_j + \mathbf{B}_j\mathbf{K}_j)$ belong to $\mathcal{D}(\alpha, r)$, if there exist a symmetric positive definite matrix $\mathbf{P}_j$ and a gain matrix $\mathbf{K}_j$ such that the following condition holds:*

$$\begin{bmatrix} \mathbf{P}_j - 2\mathbf{I} & \mathbf{A}_j + \mathbf{B}_j\mathbf{K}_j - \alpha\mathbf{I} \\ * & -r^2\mathbf{P}_j \end{bmatrix} < 0, \tag{6.47}$$

Proof. The proof of this theorem is similar as that of Theorem 5.4 and omitted here. □

Whether faults have happened during the process, with the proposed adaptive estimation method, specific information of the faults can be achieved during the process. For our purpose of designing the fault tolerant controller at LCs, the fault estimate vector $\hat{\theta}_j(k)$ will be packed with the state estimate $\hat{\mathbf{x}}_j(k)$ and transmitted to LCs. We denote $\hat{\theta}_{s,j}(k)$ as the output of $\hat{\theta}_j(k)$ transmitting through the scheduler $\mathcal{S}$, i.e., $\hat{\theta}_{s,j}(k) = \mathbf{H}(j)\hat{\theta}_j(k)$, where

a Boolean matrix $\mathbf{H}(j) \in \Re^{p_1 \times p_1}$ will decide which part of the fault estimate vector $\hat{\theta}_j(k)$ will be transmitted. For example, considering the limit network bandwidth, only the fault estimates of the actuators, which belong to the i-th subprocess, will be transmitted from the i-th CS to its LCs. In this case, $\mathbf{H}(j)$ should be chosen according to the concrete situation. Of course, if there is enough network bandwidth, all the fault estimate vector $\hat{\theta}_j(k)$ could be transmitted to LCs, which will offer a better fault tolerant controller and finally improve the whole FTC performance. In such case, $\mathbf{H}(j) = \mathbf{I}$.

6.5.2 Fault accommodation

The fault tolerant controller for actuator MFs at LCs is developed based on the fault-free controller. According to the physical meaning of $\theta_i(k,j)$ in (6.3), we concern that $\theta_i(k,j) > 0$, therefore, $\hat{\theta}_i(k,j)$, as well as $\hat{\theta}_j(k)$ and $\hat{\theta}_{s,j}(k)$, should also be greater than 0. We define $\mathbf{f}_{\hat{\theta}}(k,j) = \text{diag}\left\{\hat{\theta}_{s,j}(k)\right\}$, denote $\hat{\theta}_{s,i}(k,j)$ as the i-th item of $\hat{\theta}_{s,j}(k)$, and construct $\mathbf{f}_{\hat{\theta}}^{-1}(k,j)$ as

$$\mathbf{f}_{\hat{\theta}}^{-1}(k,j) = \text{diag}\left\{ \cdots \quad \theta_{t,i}(k,j) \quad \cdots \right\}$$

$$\theta_{t,i}(k,j) = \begin{cases} 0 & , \text{ if } \hat{\theta}_{s,i}(k,j) \leq 0; \\ \hat{\theta}_{s,i}^{-1}(k,j) & , \text{ if } \hat{\theta}_{s,i}(k,j) > 0. \end{cases}$$

Consequently, for the purpose of compensating the effect caused by the MFs, the FTC strategy for actuator MFs is developed as follows

$$\mathbf{u}_{FTC,s}(k,j) = \mathbf{f}_{\hat{\theta}}^{-1}(k,j)\mathbf{u}_{nom,s}(k,j),\ j = 1, \cdots, \mu \tag{6.48}$$

where $\mathbf{u}_{FTC,s}(k,j)$ is the fault tolerant controller.

Following Theorem 6.2 we know that, by using the proposed adaptive estimation method, if the noises in the systems are distributed with zero means, there is $\mathbf{E}(\theta_{s,j}(k) - \hat{\theta}_{s,j}(k)) \to 0$ when $k \to \infty$. In other words, $\hat{\theta}_{s,j}(k)$ is convergent exponentially to $\theta_{s,j}(k)$ when $k \to \infty$. Therefore, with fault tolerant controller (6.48), the effects caused by MFs to the systems will be accommodated.

6.6 Summary

In this chapter, the integrated system of W-NCSs and scheduler is modeled as a μ-periodic system with actuator MFs. The lifting technology is applied to model the integrated LTP systems. Due to the unavailability of the full information about the system state, an adaptive observer is constructed to estimate the state and fault vectors simultaneously.

Finally, an FTC strategy for W-NCSs with actuator MFs is developed based on a nominal controller.

7 Application to WiNC platform

In this chapter, we will verify the proposed FTC schemes for W-NCSs with AFs and MFs on WiNC platform, respectively.

7.1 Experimental setup

In this chapter, the proposed methods will be verified on an advanced experimentation platform WiNC which was developed by the faculties of Automatic Control and Complex Systems (AKS) and Communication Systems (NTS) of Duisburg-Essen university (UDE), and is now located in the faculty of AKS. Before starting our verification experiments, we'd like to give a brief introduction about the experimentation platform WiNC.

The experimentation platform WiNC is constructed to explore the control, FD, FTC and communication issues based on real-time reliable W-NCSs. The whole WiNC contains two well-known laboratory benchmarks acting as subsystems (namely the three-tank system and the inverted pendulum system), a remote controller, wireless communication facilities, as well as a protocol optimized for industrial real-time wireless communication.

WiNC is built on Linux operating system with KDevelop, which is an open source software with integrated development environment (IDE), so it is quite accessible for the integration of new FTC or FD algorithms. It also provides harmonious graphic user interface (GUI) and significant parameters, e.g., controller parameters, time slot duration, antenna transmission power and so on, which can be set during the process.

The wireless facilities support IEEE 802.11a/b/g protocol standards and provides the possibility of choosing different modulation methods and frequency bands, which means less interference, therefore potential for more reliable transmissions. TDMA method is adopted in WiNC to ensure the deterministic transmission behaviors. SoftMAC, which supports a flexible wireless research platform, is used to design a new MAC protocol optimized for industrial wireless network communication. In order to satisfy the requirements of transmission speed in data exchange and make the best usage of network resources, the transmission scheduler has a great demand of being optimized, especially for large-scale networks. The scheduling approach for real-time decentralized network in WiNC has been reported in [21, 132].

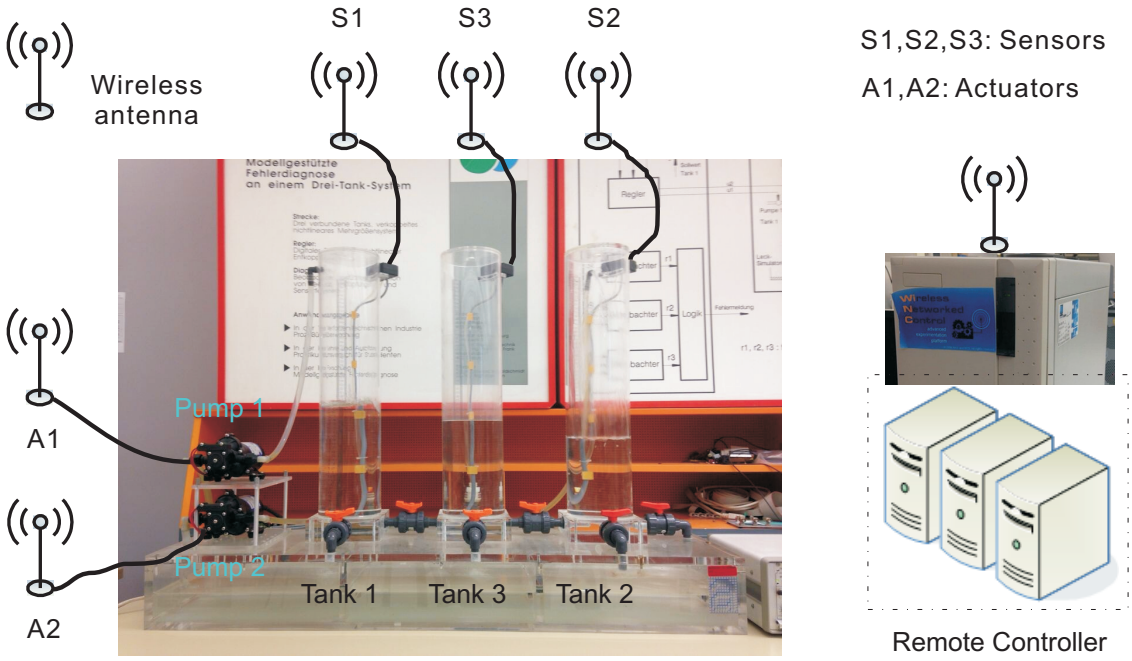

Figure 7.1: WiNC platform with three-tank system

In our experiment, the three-tank subsystem will be discretized into a linear 4-periodic system in which sensors work with different sampling rates and actuators implement with periodic time-varying rates, namely multirate sampling and multiple control (MSMC) in one period. The scheduler is also periodic with the period time coordinating with the discretized system. During the experiment, all the communication will be implemented between the remote controller and the three-tank system, the inverted pendulum subsystem will not participate this experiment.

7.2 Modeling of three-tank system with AFs

In this section, the proposed FE method and FTC algorithms for AFs will be tested on the WiNC platform. The system structure is shown in Fig.7.1. The three-tank system includes 3 water level gauges as sensors and 2 pumps as actuators, and is controlled via wireless network by a remote controller which comprises of three virtual CSs with information shared among them. Each tank acts as one subprocess and each attaches to one virtual CS. The actuators, sensors and the remote controller act as wireless nodes embedded with wireless cards. Therefore, the communications from sensors to remote controller and from remote controller to actuators all rely on the wireless network.

Nonlinear model

Applying the incoming and outgoing mass flows under consideration of Torricelli's law [133], the dynamics of three-tank system is modeled by

$$
\begin{aligned}
S\dot{h}_1(t) &= Q_1(t) - Q_{13}(t) \\
S\dot{h}_2(t) &= Q_2(t) + Q_{32}(t) - Q_{20}(t) \\
S\dot{h}_3(t) &= Q_{13}(t) - Q_{32}(t) \\
Q_{13}(t) &= a_1 s_{13} \mathrm{sgn}(h_1(t) - h_3(t)) \sqrt{2g|h_1(t) - h_3(t)|} \\
Q_{32}(t) &= a_3 s_{23} \mathrm{sgn}(h_3(t) - h_2(t)) \sqrt{2g|h_3(t) - h_2(t)|} \\
Q_{20}(t) &= a_2 s_0 \sqrt{2g h_2(t)}
\end{aligned}
$$

where

- $Q_i(t),\ i = 1, 2$, are incoming flow (cm^3/s) of pump i;
- $Q_{ij}(t),\ i = 1, 2, 3,\ j = 0, 2, 3$, are the mass flow ($\mathrm{cm}^3/\mathrm{s}$) from the i-th tank to the j-th tank;
- $h_i(t),\ i = 1, 2, 3$, are the water level (cm) of each tank;
- $s_{13},\ s_{23},\ s_0$ are cross section area (cm^2) of circular pipes, that interconnect the three circular tanks;
- $\mathrm{sgn}(h(t))$ is an odd mathematical function that extracts the sign of $h(t)$.

The parameters of this model are given in Table 7.1.

Table 7.1: Parameters of the three-tank system

Parameters	Symbol	Value	Unit
cross section area of tanks	S	154	cm^2
cross section area of pipes	s_{13}, s_{23}, s_0	0.5	cm^2
maximum height of tanks	H_{max}	62	cm
maximum flow rate of pump 1	$Q_{1,max}$	124.165	cm^3/s
maximum flow rate of pump 2	$Q_{2,max}$	121.882	cm^3/s
coefficient of flow for pipe 1	a_1	0.399	
coefficient of flow for pipe 2	a_2	0.799	
coefficient of flow for pipe 3	a_3	0.520	
acceleration due to gravity	g	980.7	cm/s^2

Linear model

After a linearization at operating point $h_{10} = 30$ cm, $h_{20} = 20$ cm and $h_{30} = 25$ cm, we have the following linear (nominal) model

$$\begin{bmatrix} \dot{x}_1(t) \\ \dot{x}_2(t) \\ \dot{x}_3(t) \end{bmatrix} = \begin{bmatrix} -A_{13} & 0 & A_{13} \\ 0 & -A_2 - A_{32} & A_{32} \\ A_{13} & A_{32} & -A_{32} - A_{13} \end{bmatrix} \begin{bmatrix} x_1(t) \\ x_2(t) \\ x_3(t) \end{bmatrix} + \frac{1}{S} \begin{bmatrix} 1 & 0 \\ 0 & 1 \\ 0 & 0 \end{bmatrix} \begin{bmatrix} u_{s,1}(t) \\ u_{s,2}(t) \end{bmatrix}$$
$$\begin{bmatrix} y_1(t) \\ y_2(t) \\ y_3(t) \end{bmatrix} = \begin{bmatrix} 1 & 0 & 0 \\ 0 & 1 & 0 \\ 0 & 0 & 1 \end{bmatrix} \begin{bmatrix} x_1(t) \\ x_2(t) \\ x_3(t) \end{bmatrix} \tag{7.1}$$

where

$$x_i = y_i = h_i,\ i = 1, 2, 3,$$
$$u_{s,i} = Q_i,\ i = 1, 2,$$
$$A_{13} = \frac{1}{S} a_1 s_{13} \sqrt{\frac{g}{2(h_{10} - h_{30})}}\ ,\ A_2 = \frac{1}{S} a_2 s_{20} \sqrt{\frac{g}{2h_{20}}}\ ,\ A_{32} = \frac{1}{S} a_3 s_{32} \sqrt{\frac{g}{2(h_{30} - h_{20})}}\ .$$

By allocating the three sensors with different sampling rates, the system is formulated as a periodic system. The multirate sampling mechanism applied here is $T_{c,1} = 0.008$ s, $T_{c,2} = 0.012$ s, $T_{c,3} = 0.024$ s where $T_{c,i},\ i = 1, 2, 3$, is the sampling cycle of the i-th sensor, as shown in Fig.7.2. The LCM of sensors' sampling cycles is the period of the whole system T_p ($= 0.024$ s). The control signal is calculated on account of the received data and broadcast from remote controller to actuators with a periodic time-varying rate.

The scheduling scenario is under the assumption that the length of each transmission signal doesn't exceed the packet maximal length, which is defined by protocol, so the transmission of every signal can be completed in one time slot. $T_{c,min}$ is the greatest common divisor of sensors' sampling cycles and is treated as basic process unit. In this case, $T_{c,min} = 0.004$ s. For the sake of simple notation, $\varsigma_j,\ j = 1, 2, 3, 4$, denote the time instants, which have transmission tasks during the k-th T_p. In this case, $\varsigma_1 = 0,\ \varsigma_2 = 2T_{c,min},\ \varsigma_3 = 3T_{c,min},\ \varsigma_4 = 4T_{c,min}$.

The discrete-time system with multi-rate sampling in the k-th period T_p is modeled as follows,

$$\begin{aligned}
x_1(kT_p + T_{s1}) &= x_2(k, 2) = A_{d1} x_1(k, 1) + A_{d13} x_3(k, 1) + B_{d1} u_{s,1}(k, 1), \\
x_2(kT_p + T_{s2}) &= x_2(k, 3) = A_{d2} x_2(k, 1) + A_{d23} x_3(k, 1) + B_{d2} u_{s,2}(k, 1), \\
x_1(kT_p + 2T_{s1}) &= x_1(k, 4) = A_{d1} x_1(k, 2) + A_{d13} x_3(k, 1) + B_{d1} u_{s,1}(k, 2), \\
x_1(kT_p + 3T_{s1}) &= x_1(k + 1, 1) = A_{d1} x_1(k, 4) + A_{d13} x_3(k, 1) + B_{d1} u_{s,1}(k, 4), \\
x_2(kT_p + 2T_{s2}) &= x_2(k + 1, 1) = A_{d2} x_2(k, 3) + A_{d23} x_3(k, 1) + B_{d2} u_{s,2}(k, 3),
\end{aligned}$$

$$x_3(kT_p + T_{s3}) = x_3(k+1,1) = A_{d3}x_3(k,1) + A_{d311}x_1(k,1) + A_{d312}x_1(k,2) + A_{d313}x_1(k,4) + A_{d321}x_2(k,1) + A_{d322}x_2(k,3),$$

where $x_i(k,j),\ i = 1,2,3,\ j = 1,2,3,4$, are the water level of i-th tank at time instant $kT_p + \varsigma_j$, and

$$\begin{aligned}
&A_{d1} = e^{-A_{13}T_{s1}},\ A_{d2} = e^{-(A_2+A_{32})T_{s2}},\ A_{d3} = e^{-(A_{32}+A_{13})T_{s3}},\\
&e_{13} = \int_0^{T_{s1}} e^{-A_{13}(T_{s1}-\tau)}d\tau,\ e_{23} = \int_0^{T_{s2}} e^{-(A_2+A_{32})(T_{s2}-\tau)}d\tau,\ A_{d13} = e_{13}A_{13},\\
&e_3 = \int_0^{T_{s3}} e^{-(A_{32}+A_{13})(T_{s3}-\tau)}d\tau,\ A_{d23} = e_{23}A_{32},\ B_1 = 1/S,\ B_2 = 1/S,\\
&e_{311} = \int_0^{T_{s1}} e^{-(A_{32}+A_{13})(T_{s3}-\tau)}d\tau,\ A_{d311} = e_{311}A_{13},\ B_{d1} = e_{13}B_1,\ B_{d2} = e_{23}B_2,\\
&e_{312} = \int_{T_{s1}}^{2T_{s1}} e^{-(A_{32}+A_{13})(T_{s3}-\tau)}d\tau,\ A_{d312} = e_{312}A_{13},\\
&e_{313} = \int_{2T_{s1}}^{T_{s3}} e^{-(A_{32}+A_{13})(T_{s3}-\tau)}d\tau,\ A_{d313} = e_{313}A_{13},\\
&e_{321} = \int_0^{T_{s2}} e^{-(A_{32}+A_{13})(T_{s3}-\tau)}d\tau,\ A_{d321} = e_{321}A_{32},\\
&e_{322} = \int_{T_{s2}}^{T_{s3}} e^{-(A_{32}+A_{13})(T_{s3}-\tau)}d\tau,\ A_{d322} = e_{322}A_{32}.
\end{aligned} \tag{7.2}$$

According to (4.6) and the scheduler in Fig.7.2, the system states of the whole three-tank system in one T_p are addressed as follows [116].

$$\mathbf{x}(k,1) = \begin{bmatrix} x_1(k-1,2)\\ x_2(k-1,3)\\ x_1(k-1,4)\\ x_1(k,1)\\ x_2(k,1)\\ x_3(k,1) \end{bmatrix}, \mathbf{x}(k,2) = \begin{bmatrix} x_2(k-1,3)\\ x_1(k-1,4)\\ x_1(k,1)\\ x_2(k,1)\\ x_3(k,1)\\ x_1(k,2) \end{bmatrix},$$

$$\mathbf{x}(k,3) = \begin{bmatrix} x_1(k-1,4)\\ x_1(k,1)\\ x_2(k,1)\\ x_3(k,1)\\ x_1(k,2)\\ x_2(k,3) \end{bmatrix}, \mathbf{x}(k,4) = \begin{bmatrix} x_1(k,1)\\ x_2(k,1)\\ x_3(k,1)\\ x_1(k,2)\\ x_2(k,3)\\ x_1(k,4) \end{bmatrix}. \tag{7.3}$$

Now the periodic system model is described as

$$\begin{aligned} \mathbf{x}(k,j+1) &= \mathbf{A}(j)\mathbf{x}(k,j) + \mathbf{B}(j)\mathbf{u}_s(k,j) + \mathbf{E}(j)\mathbf{d}(k,j) \\ \mathbf{y}(k,j) &= \mathbf{C}(j)\mathbf{x}(k,j) + \mathbf{F}(j)\mathbf{d}(k,j),\ j = 1,2,3,4 \end{aligned} \tag{7.4}$$

where $\mathbf{x}(k,j) \in \Re^6$ is the system state vector containing all the three tank levels at different sampling instants during one period T_p. $\mathbf{y}(k,j) \in \Re^6$ is the system output vector, working as a first input first output (FIFO) buffer updated with the latest water levels of 3 tanks. $\mathbf{d}(k,j) \in \Re^6$ is the process disturbance vector. The control signals are defined as

$$\begin{aligned} &\mathbf{u}_s(k,1) = u_{s,1}(k,1),\ \mathbf{u}_s(k,2) = u_{s,2}(k,1), \\ &\mathbf{u}_s(k,3) = u_{s,1}(k,2),\ \mathbf{u}_s(k,4) = \begin{bmatrix} u'_{s,1}(k,4) & u'_{s,2}(k,3) \end{bmatrix}'. \end{aligned} \tag{7.5}$$

where $u_{s,i}(k,j),\ i = 1,2;\ j = 1,2,3,4$, denotes the local pump input of the tank i at the time instant (k,j).

According to the physical parameters given in Table 7.1, the system matrices of 4-periodic system are listed as follows,

$$\mathbf{A}(1) = \begin{bmatrix} \mathbf{O}_{5\times1} & & \mathbf{I}_{5\times5} & & & \\ 0 & 0 & 0 & 0.9999 & 0 & 0.0001 \end{bmatrix},\ \mathbf{B}(1) = \mathbf{B}(3) = \begin{bmatrix} \mathbf{O}_{5\times1} \\ 0.5195 \end{bmatrix},$$

$$\mathbf{A}(2) = \begin{bmatrix} \mathbf{O}_{5\times1} & & \mathbf{I}_{5\times5} & & & \\ 0 & 0 & 0 & 0.9997 & 0.0002 & 0 \end{bmatrix},\ \mathbf{B}(2) = \begin{bmatrix} \mathbf{O}_{5\times1} \\ 0.7791 \end{bmatrix},$$

$$\mathbf{A}(3) = \begin{bmatrix} \mathbf{O}_{5\times1} & & \mathbf{I}_{5\times5} & & & \\ 0 & 0 & 0 & 0.0001 & 0.9999 & 0 \end{bmatrix},\ \mathbf{B}(4) = \begin{bmatrix} \mathbf{O}_{3\times2} \\ 0.5195 & 0 \\ 0 & 0.7791 \\ 0 & 0 \end{bmatrix},$$

$$\mathbf{A}(4) = \begin{bmatrix} \mathbf{O}_{3\times3} & & & \mathbf{I}_{3\times3} & & \\ 0 & 0 & 0.0001 & 0 & 0 & 0.9999 \\ 0 & 0 & 0.0002 & 0 & 0.9997 & 0 \\ 0.0001 & 0.0002 & 0.9992 & 0.0001 & 0.0002 & 0.0001 \end{bmatrix},$$

$$\mathbf{E}(1) = \begin{bmatrix} \mathbf{O}_{5\times6} \\ 0 & 0 & 0 & 2.3998e-5 & 0 & 0 \end{bmatrix},\ \mathbf{E}(2) = \begin{bmatrix} \mathbf{O}_{5\times6} \\ 0 & 0 & 0 & 2.3996e-5 & 0 & 0 \end{bmatrix},$$

$$\mathbf{E}(3) = \begin{bmatrix} \mathbf{O}_{5\times6} \\ 0 & 0 & 0 & 0 & 2.3998e-5 & 0 \end{bmatrix},\ \begin{aligned} &\mathbf{C}(1) = \mathbf{C}(2) = \mathbf{C}(3) = \mathbf{C}(4) = \mathbf{I}_{6\times6}, \\ &\mathbf{F}(1) = \mathbf{F}(2) = \mathbf{F}(3) = \mathbf{F}(4) = 10^{-3} \times \mathbf{I}_{6\times6}, \end{aligned}$$

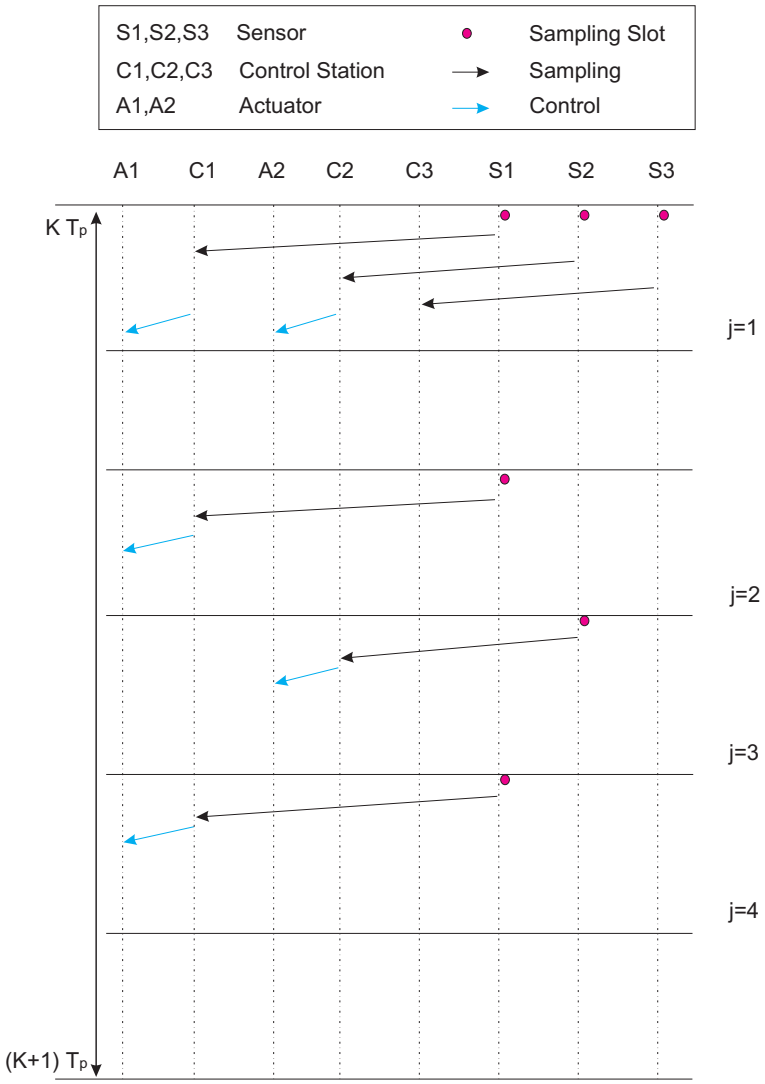

Figure 7.2: Scheduler for 4-periodic system

$$\mathbf{E}(4) = \begin{bmatrix} & & \mathbf{O}_{3\times 6} & & \\ & 0 & 0 & 0 & 2.3998e-5 \\ \mathbf{O}_{3\times 2} & 0 & 0 & 2.3996e-5 & 0 \\ & 2.3991e-5 & 0 & 0 & 0 \end{bmatrix}. \tag{7.6}$$

The scheduler of sensor-to-CS and CS-to-actuator in one T_p is shown specifically in Fig.7.2. The whole system is designed to be a 4-periodic system. In view of control mechanism, the biggest change from the one in [21] is that 4 times (instead of once) control commands are generated in one period T_p, and the control commands will be broadcast not until the end of each T_p. In this scheduler, a new control command will be calculated and scheduled immediately when the newly sampled data have been scheduled

and received. Therefore, there will be 4 times control in one T_p, which will improve the real-time control by a huge margin.

It is assumed that in each time instant, all the information needed to be delivered can be packed into one packet and the length of each packet doesn't exceed the maximal length of one frame, which is defined by protocol, hence the packet can be successfully delivered in one time slot. In our case, the GCD of sensors' sampling cycles $T_{c,min} = 0.004$s and the time slot is set to $1ms$, which means in every $T_{c,min}$, 4 times transmissions can be scheduled. For the sake of simple notation, $\varsigma_j,\ j = 1, 2, 3, 4$, denote the time instants, when the transmission tasks during the k-th T_p are generated. As displayed in Fig.7.2, there are 4 time instants in our scheduler, $\varsigma_1 = 0,\ \varsigma_2 = 2T_{c,min},\ \varsigma_3 = 3T_{c,min},\ \varsigma_4 = 4T_{c,min}$, respectively.

An ideal network condition has been considered in our experiment, and all the latest information will arrive their destination on time, so we have $\phi_1(j) = \mathbf{I}_{6\times6},\ \phi_2(j) = \mathbf{I}_{3\times3},\ j = 1, 2, 3, 4$. The scheduler, shown in Fig.7.2, are formulated into the state-space model (4.10) and the system matrices of scheduler are given as follows,

$$
\begin{aligned}
&\mathbf{A}_s(1) = \mathbf{A}_s(2) = \mathbf{A}_s(3) = \mathbf{O}_{2\times2}, \mathbf{A}_s(4) = \mathbf{O}_{5\times5},\\
&\mathbf{B}_{sr}(1) = \mathbf{B}_{sr}(2) = \mathbf{B}_{sr}(3) = \begin{bmatrix} 0 & 0 & 0 & 0 & 0 & 1 \\ 0 & 0 & 0 & 0 & 0 & 0 \end{bmatrix}, \mathbf{B}_{su}(1) = \mathbf{B}_{su}(2) = \mathbf{B}_{su}(3) = \begin{bmatrix} 0 \\ 1 \end{bmatrix},\\
&\mathbf{C}_{sr}(1) = \mathbf{C}_{sr}(2) = \mathbf{C}_{sr}(3) = \mathbf{O}_{6\times2}, \mathbf{C}_{sr}(4) = \mathbf{O}_{6\times5},\\
&\mathbf{D}_{sr}(1) = \mathbf{D}_{sr}(2) = \mathbf{D}_{sr}(3) = \mathbf{D}_{sr}(4) = \mathbf{I}_{6\times6},\\
&\mathbf{C}_{su}(1) = \mathbf{C}_{su}(2) = \mathbf{C}_{su}(3) = \mathbf{O}_{1\times2}, \mathbf{C}_{su}(4) = \mathbf{O}_{2\times5},\\
&\mathbf{D}_{su}(1) = \mathbf{D}_{su}(2) = \mathbf{D}_{su}(3) = \mathbf{1}, \mathbf{D}_{su}(4) = \mathbf{I}_{2\times2},\\
&\mathbf{B}_{sr}(4) = \begin{bmatrix} 0 & 0 & 0 & 1 & 0 & 0 \\ 0 & 0 & 0 & 0 & 1 & 0 \\ 0 & 0 & 0 & 0 & 0 & 1 \\ 0 & 0 & 0 & 0 & 0 & 0 \\ 0 & 0 & 0 & 0 & 0 & 0 \end{bmatrix}, \mathbf{B}_{su}(4) = \begin{bmatrix} 0 & 0 \\ 0 & 0 \\ 0 & 0 \\ 1 & 0 \\ 0 & 1 \end{bmatrix}.
\end{aligned}
\tag{7.7}
$$

7.3 Implementation of FTC scheme for AFs

It is considered in our experiment that tank 2 has an actuator fault $f_2^a(k, j)$ while tank 3 has a sensor fault $f_3^s(k, j)$, and

$$
f_2^a(k, j) = \begin{cases} 0.3 \cdot Q_{2,max} (= 36.56\ \mathrm{cm}^3/\mathrm{s}), & 10500 \le k \le 12500 \\ 0, & \text{others} \end{cases},
$$

$$f_3^s(k,j) = \begin{cases} 1 \text{ cm}, & 8500 \leq k \leq 10000 \\ 0, & \text{others} \end{cases}.$$

Since $T_p = 0.024$ s, in the continuous time domain the actuator fault occurs during $[252\text{ s}, 300\text{ s}]$ while the sensor fault appears during $[204\text{ s}, 240\text{ s}]$. Since not all time instants are with fault, so our experiment is in case II.

The fault $\mathbf{f}(k,j),\ j = 1,2,3,4$ is defined as follows

$$\mathbf{f}(k,1) = \mathbf{f}(k,2) = \begin{bmatrix} f_2^a(k-1,3) \\ f_2^a(k,1) \\ f_3^s(k,1) \end{bmatrix}, \mathbf{f}(k,3) = \mathbf{f}(k,4) = \begin{bmatrix} f_2^a(k,1) \\ f_3^s(k,1) \\ f_2^a(k,3) \end{bmatrix}.$$

The system matrices of the faults are set as

$$\mathbf{E}_f(1) = \mathbf{E}_f(3) = \mathbf{O}_{6\times 3},$$
$$\mathbf{E}_f(2) = \begin{bmatrix} \mathbf{O}_{5\times 3} \\ 0 \quad 0.0779 \quad 0 \end{bmatrix}, \mathbf{E}_f(4) = \begin{bmatrix} \mathbf{O}_{5\times 3} \\ 0 \quad 0 \quad 0.0779 \end{bmatrix}, \mathbf{F}_f(1) = \begin{bmatrix} \mathbf{O}_{5\times 3} \\ 0 \quad 0 \quad 1 \end{bmatrix},$$
$$\mathbf{F}_f(2) = \begin{bmatrix} \mathbf{O}_{4\times 3} \\ 0 \quad 0 \quad 1 \\ \mathbf{O}_{1\times 3} \end{bmatrix}, \mathbf{F}_f(3) = \begin{bmatrix} \mathbf{O}_{3\times 3} \\ 0 \quad 1 \quad 0 \\ \mathbf{O}_{2\times 3} \end{bmatrix}, \mathbf{F}_f(4) = \begin{bmatrix} \mathbf{O}_{2\times 3} \\ 0 \quad 1 \quad 0 \\ \mathbf{O}_{3\times 3} \end{bmatrix}.$$

Until now, a feasible solution for the state observer gain $\mathbf{L}(j)$ and fault estimator gain $\mathbf{G}(j)$ can be achieved by applying Theorem 5.2. The estimation performance of the sensor and actuator faults is demonstrated as in Fig.7.3 and Fig.7.4.

A control strategy is constructed only based on the estimated states. Then the output performance without fault compensation is shown in Fig.7.5. There is a big deviation from the operation point when the fault occurs, and the fault has been propagated to other tanks. By applying Theorem 5.4 to the aforementioned three-tank system model, we can achieve the feedback gain $\mathbf{K}_1(j)$ and $\mathbf{K}_2(j)$. Fig.7.6 displays the output performance with FTC strategy. By comparing Fig.7.5 and Fig.7.6, we have the following conclusion. With the proposed FTC strategy, there is only a small deviation at the beginning of the actuator fault, then the system shows a very good tolerance to the fault.

In the former part of [21], it was designed that the CSs only use their own residuals to calculate the state observer, which leads to:

(1) On the positive side, the communication volume is quite small which can ensure the real-time communication of critical informations and save energy;

(2) While on the negative side, the structure limitations of the observer gain $\mathbf{L}(j)$ will be very severe, which causes great difficulty to obtain a feasible solution.

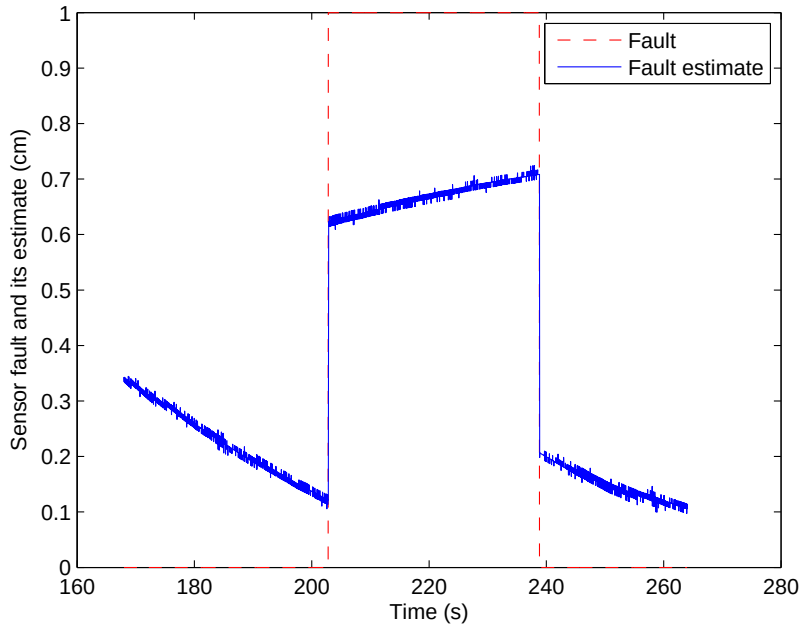

Figure 7.3: Sensor fault and its estimate

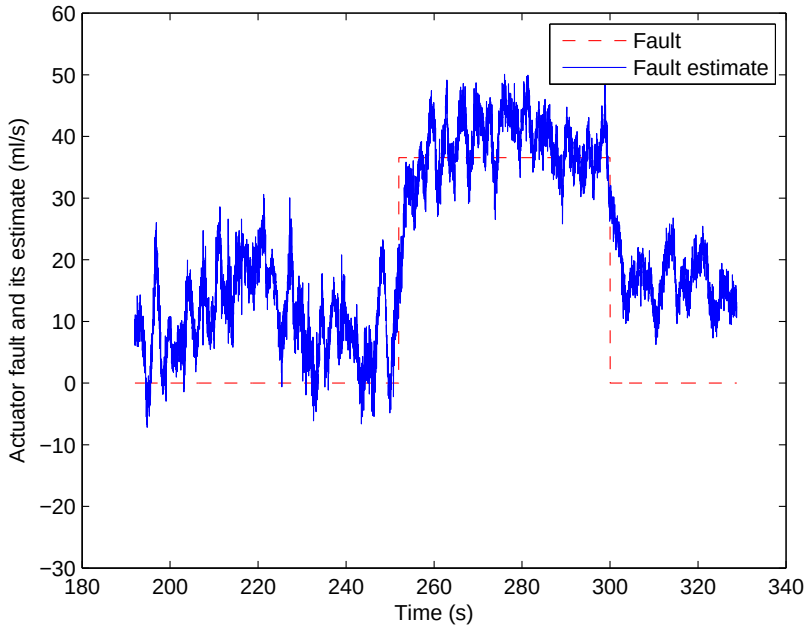

Figure 7.4: Actuator fault and its estimate

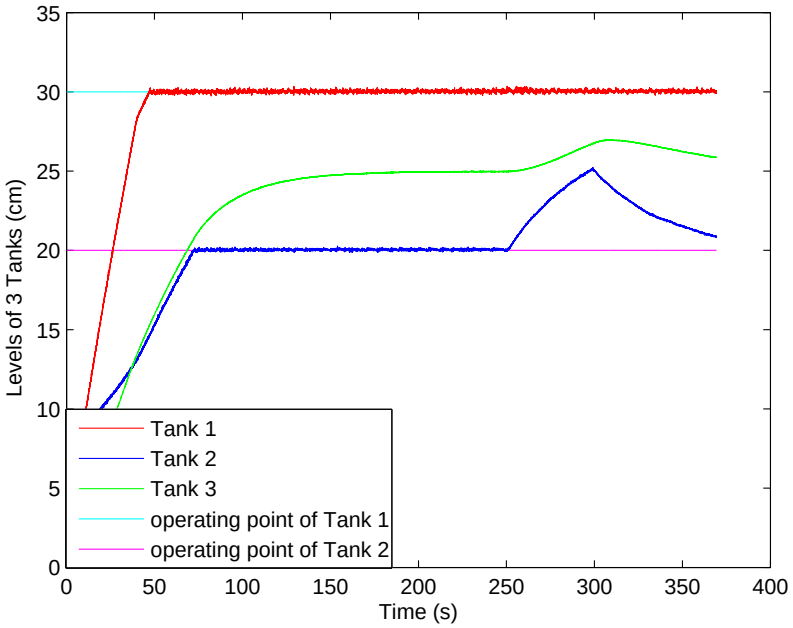

Figure 7.5: Output without FTC strategy

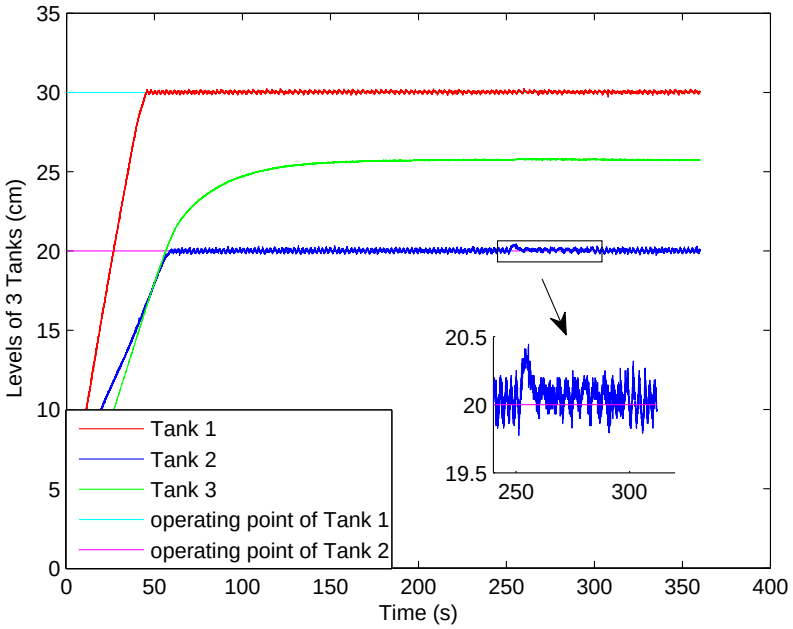

Figure 7.6: Output with FTC strategy

It has also suggested an advanced design issue in [21], by increasing data transmissions among the subsystems to improve the FTC performance of W-NCSs. That means to share residuals among CSs. However, this will cause:

(1) On the positive side, the structure limitation problem of the observer gain $\mathbf{L}(j)$ will be relaxed, which means more easier to get a feasible solution, and with more information shared among CSs, the estimation performance will be better, which also leads to a better FTC performance;

(2) While on the negative side, increasing communication volume the quality of the wireless network will be weakened which will somewhat let down the system control performance.

So it's very critical to decide which information, and how much of it, can be increased to guarantee the system FTC performance. It's still a trade-off problem between increasing communication volume and guaranteeing the system FTC performance. On our platform, it can be realized by programming, whether to share the residuals among the virtual CSs in the remote controller or not. A result comparison will be presented in the sequels.

7.3.1 FTC performance with unshared residuals

In the case with unshared residuals, the system matrices of fault estimator are set as $\beta_2(1) = 1$, $\beta_2(4) = 0.997$, $\beta_3(1) = 1$, the circular regions $\mathcal{D}_1(0,1)$, $\mathcal{D}_2(0,1)$, H_∞ performance levels $\gamma_{1,1} = \gamma_{1,2} = \gamma_{1,3} = \gamma_{1,4} = 10.254$ and $\gamma_{2,1} = \gamma_{2,2} = \gamma_{2,3} = \gamma_{2,4} = 6.345$ are given. The gain matrices are obtained as

$$\mathbf{L}_o(1) = \begin{bmatrix} \mathbf{O}_{8\times 6} \\ 0 & 0 & 0 & 0.9999 & 0 & 0 \end{bmatrix}$$

$$\mathbf{L}_o(2) = \begin{bmatrix} \mathbf{O}_{7\times 6} \\ 0 & 0 & 0 & 1.0021 & 0 & 0 \\ 0 & 0 & 0 & 0.0317 & 0 & 0 \end{bmatrix},$$

$$\mathbf{L}_o(3) = \begin{bmatrix} \mathbf{O}_{8\times 6} \\ 0 & 0 & 0 & 0 & 0.9999 & 0 \end{bmatrix},$$

$$\mathbf{L}_o(4) = \begin{bmatrix} \mathbf{O}_{4\times 6} \\ 0 & 0 & 0 & 0 & 0 & 0.9999 \\ 0 & 0 & 0 & 0 & 1.0021 & 0 \\ 0 & 0 & 0 & 0 & 0.0317 & 0 \\ 0 & 0 & 0.4992 & 0 & 0 & 0 \\ 0 & 0 & 0.5004 & 0 & 0 & 0 \end{bmatrix},$$

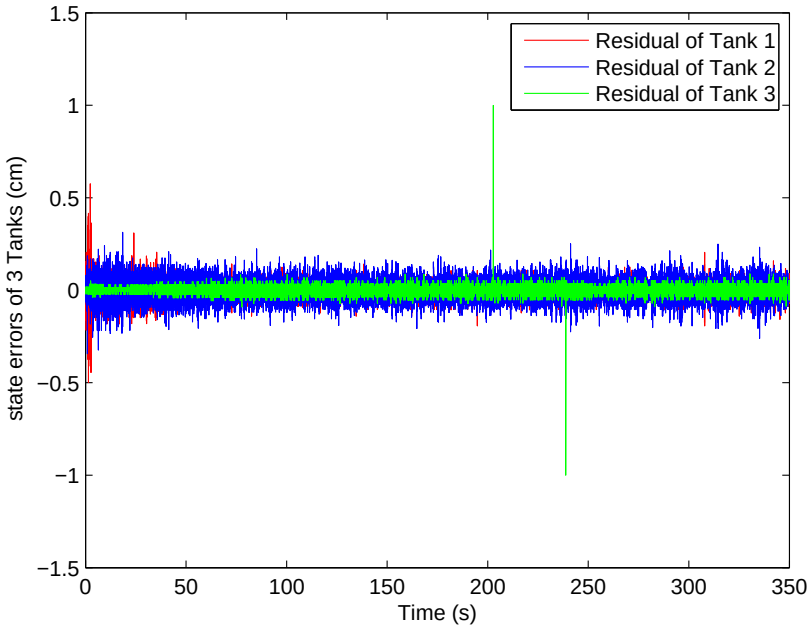

Figure 7.7: unshared residuals of three-tank system

$$\mathbf{K}_1(1) = \begin{bmatrix} 0 & 0 & 0 & -0.9809 & 0 & 0 \end{bmatrix}, \mathbf{K}_2(1) = \mathbf{O}_{1\times 3},$$
$$\mathbf{K}_1(2) = \begin{bmatrix} 0 & 0 & 0 & -0.6558 & 0 & 0 \end{bmatrix}, \mathbf{K}_2(2) = \begin{bmatrix} 0 & -0.1000 & 0 \end{bmatrix},$$
$$\mathbf{K}_1(3) = \begin{bmatrix} 0 & 0 & 0 & 0 & -0.9171 & 0 \end{bmatrix}, \mathbf{K}_2(3) = \mathbf{O}_{1\times 3},$$
$$\mathbf{K}_1(4) = \begin{bmatrix} 0 & 0 & 0 & 0 & 0 & -1.0420 \\ 0 & 0 & 0 & 0 & -0.6699 & 0 \end{bmatrix}, \mathbf{K}_2(4) = \begin{bmatrix} 0 & 0 & 0 \\ 0 & 0 & -0.1000 \end{bmatrix}.$$

The reference values of control signals are set as $R_{ef,1} = 2.751 \times 10^5$ cm^3/s, $R_{ef,2} = 1.309 \times 10^5$ cm^3/s. The change ranges of the two inputs are $0 \leq u_1 \leq 124.165$ cm^3/s, 40.627 cm^3/s$\leq u_2 \leq 121.882$ cm^3/s, where the lower of u_2 is set higher than 0 to reduce the disturbance caused by flow mutation of the pump 2. Fig.7.7 demonstrates the unshared residuals of 3 tanks. The output of three-tank system with unshared residuals is presented in Fig.7.8.

7.3.2 FTC performance with shared residuals

In the case with shared residuals, $\beta_2(1) = 1$, $\beta_2(4) = 0.9977$, $\beta_3(1) = 1$, the circular regions $\mathcal{D}_1(0,1)$, $\mathcal{D}_2(0,1)$, H_∞ performance levels $\gamma_{1,1} = \gamma_{1,2} = \gamma_{1,3} = \gamma_{1,4} = 10.254$ and

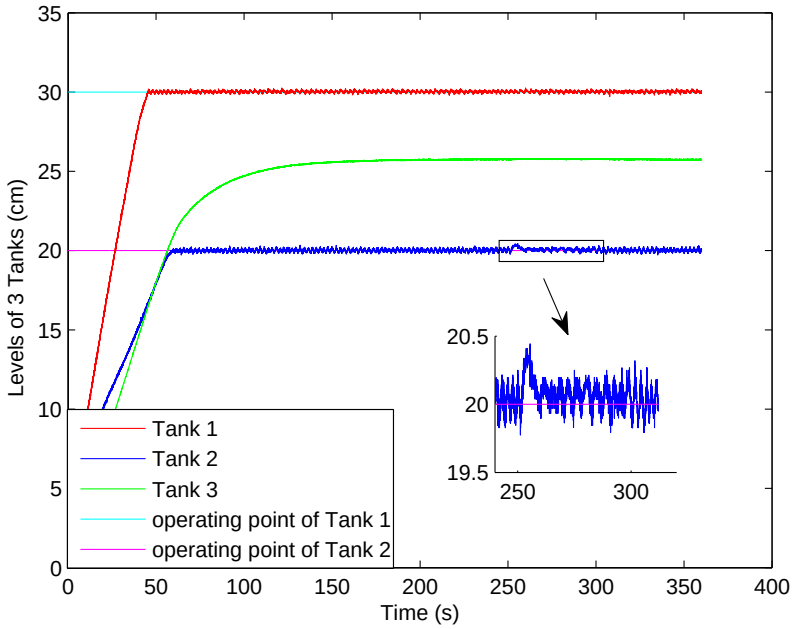

Figure 7.8: Outputs of three-tank system with unshared residuals

$\gamma_{2,1} = \gamma_{2,2} = \gamma_{2,3} = \gamma_{2,4} = 6.345$ are given. The gain matrices are obtained as

$$\mathbf{L}_o(1) = \begin{bmatrix} \mathbf{O}_{8\times 3} \\ 1.2017e-13 \quad 8.9143e-9 \quad -1.5661e-5 \\ \mathbf{O}_{8\times 3} \\ 0.9999 \quad -6.9195e-10 \quad 3.1967e-5 \end{bmatrix},$$

$$\mathbf{L}_o(2) = \begin{bmatrix} \mathbf{O}_{7\times 3} \\ -6.8625e-6 \quad 2.1588e-9 \quad 1.5930e-4 \\ -7.9518e-5 \quad 2.6335e-7 \quad 9.6874e-11 \\ \mathbf{O}_{7\times 3} \\ 1.0021 \quad 9.5672e-5 \quad 4.6789e-8 \\ 0.0317 \quad -6.0782e-8 \quad 6.0290e-7 \end{bmatrix},$$

$$\mathbf{L}_o(3) = \begin{bmatrix} \mathbf{O}_{8\times 3} \\ -2.7900e-16 \quad 1.2734e-8 \quad -1.0812e-6 \\ \mathbf{O}_{8\times 3} \\ 3.8550e-5 \quad 0.9999 \quad -1.2097e-9 \end{bmatrix},$$

$$\mathbf{K}_1(1) = \begin{bmatrix} 0 & 0 & 0 & -0.9809 & 0 & 0 \end{bmatrix}, \mathbf{K}_2(1) = \mathbf{O}_{1\times 3},$$

$$\mathbf{K}_1(2) = \begin{bmatrix} 0 & 0 & 0 & -0.6558 & 0 & 0 \end{bmatrix}, \mathbf{K}_2(2) = \begin{bmatrix} 0 & -0.1000 & 0 \end{bmatrix},$$

$$\mathbf{K}_1(3) = \begin{bmatrix} 0 & 0 & 0 & 0 & -0.9170 & 0 \end{bmatrix}, \mathbf{K}_2(3) = \mathbf{O}_{1\times 3},$$

$$\mathbf{K}_1(4) = \begin{bmatrix} 0 & 0 & 0 & 0 & 0 & -1.0420 \\ 0 & 0 & 0 & 0 & -0.6699 & 0 \end{bmatrix}, \mathbf{K}_2(4) = \begin{bmatrix} 0 & 0 & 0 \\ 0 & 0 & -0.1000 \end{bmatrix}.$$

$$\mathbf{L}_o(4) = \begin{bmatrix} & \mathbf{O}_{4\times 3} & \\ 6.7305e-11 & 1.6917e-10 & 3.8554e-5 \\ 1.6719e-10 & -6.8533e-6 & 9.6375e-5 \\ -1.3489e-11 & -7.9201e-5 & 6.6354e-9 \\ 7.8042e-5 & 1.9511e-4 & 0.4993 \\ -8.7692e-7 & -2.2042e-6 & 0.5004 \\ & \mathbf{O}_{4\times 3} & \\ -1.2977e-15 & 1.1106e-9 & 0.9999 \\ -6.1502e-11 & 1.0021 & -1.5359e-6 \\ -7.6858e-10 & 0.0318 & -1.9842e-5 \\ 7.7154e-5 & 2.0723e-4 & 7.7148e-5 \\ 1.7020e-11 & -1.4462e-5 & -9.7249e-9 \end{bmatrix},$$

The reference values of control signals are set as $R_{ef,1} = 2.75 \times 10^5$ cm^3/s, $R_{ef,2} = 1.313 \times 10^5$ cm^3/s. The change ranges of the two inputs are the same as in the case with unshared residuals. Fig.7.9 demonstrates the shared residuals. Fig.7.10 displays the outputs of three-tank system with shared residuals. The system has a very tiny deviation from its operation point, which means the system is very tolerant to the fault.

By comparing the output performance between two cases: with unshared and shared residuals, we can find that, the FTC performance of the case with shared residuals is better than that with unshared residuals. This is reasonable with a cost of communication load.

Although only the ideal network condition has been concerned during the experiment, for the case with delay or packet loss, some changes only need to be taken in the system matrices of the scheduler (4.10). The FTC performance of W-NCSs will be a little worse, the advantage of that with shared residuals does still exist. This part of work has been demonstrated in [134]. Due to the limitation of space, we are not going to present all other experimental results.

7.4 Modeling of three-tank system with MFs

In this section, the proposed adaptive estimation method and FTC strategy for actuator MFs will be tested on the WiNC platform. Based on Fig.7.1 and linear model (7.1), the continuous-time model of three-tank system with MFs after linearization can be modeled

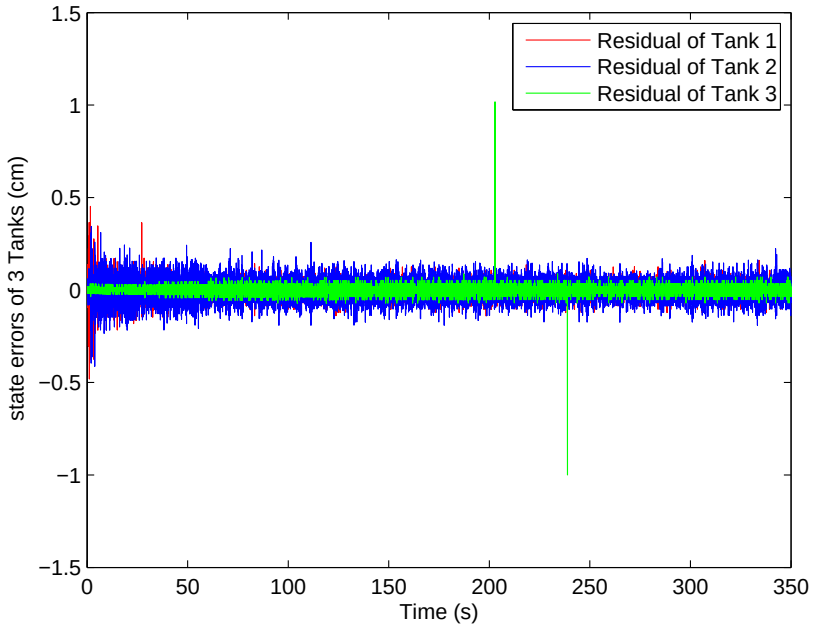

Figure 7.9: shared residuals of three-tank system

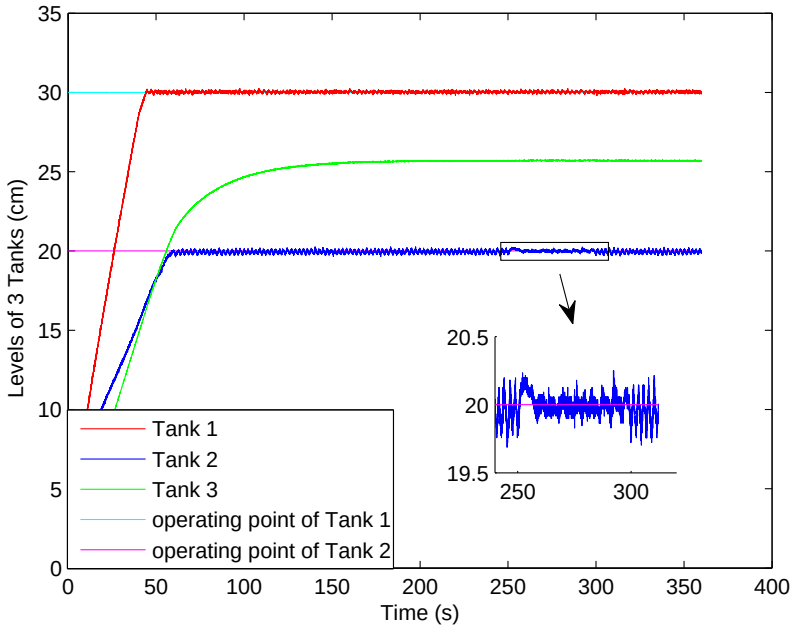

Figure 7.10: Outputs of three-tank system with shared residuals

as follows,

$$\begin{bmatrix} \dot{x}_1(t) \\ \dot{x}_2(t) \\ \dot{x}_3(t) \end{bmatrix} = \begin{bmatrix} -A_{13} & 0 & A_{13} \\ 0 & -A_2 - A_{32} & A_{32} \\ A_{13} & A_{32} & -A_{32} - A_{13} \end{bmatrix} \begin{bmatrix} x_1(t) \\ x_2(t) \\ x_3(t) \end{bmatrix} + \frac{1}{S} \begin{bmatrix} 1 & 0 \\ 0 & 1 \\ 0 & 0 \end{bmatrix} \begin{bmatrix} \theta_1(t) & \\ & \theta_2(t) \end{bmatrix} \begin{bmatrix} u_1(t) \\ u_2(t) \end{bmatrix}$$

$$\begin{bmatrix} y_1(t) \\ y_2(t) \\ y_3(t) \end{bmatrix} = \begin{bmatrix} 1 & 0 & 0 \\ 0 & 1 & 0 \\ 0 & 0 & 1 \end{bmatrix} \begin{bmatrix} x_1(t) \\ x_2(t) \\ x_3(t) \end{bmatrix}$$

where $\theta_i(t),\ i = 1, 2$, are the MF coefficients of the incoming flow mass $u_i(t)$.

Following the scheduler of sensor-to-CS and CS-to-actuator in one T_p in Fig. 7.2, the periodic system induced by multi-rate sampling is modeled in the k-th period T_p as follows,

$$\begin{aligned}
x_1(kT_p + T_{s1}) &= x_2(k, 2) \\
&= A_{d1}x_1(k, 1) + A_{d13}x_3(k, 1) + B_{d1}\theta_1(k, 1)u_1(k, 1), \\
x_2(kT_p + T_{s2}) &= x_2(k, 3) \\
&= A_{d2}x_2(k, 1) + A_{d23}x_3(k, 1) + B_{d2}\theta_2(k, 1)u_2(k, 1), \\
x_1(kT_p + 2T_{s1}) &= x_1(k, 4) \\
&= A_{d1}x_1(k, 2) + A_{d13}x_3(k, 1) + B_{d1}\theta_1(k, 2)u_1(k, 2), \\
x_1(kT_p + 3T_{s1}) &= x_1(k + 1, 1) \\
&= A_{d1}x_1(k, 4) + A_{d13}x_3(k, 1) + B_{d1}\theta_1(k, 4)u_1(k, 4), \\
x_2(kT_p + 2T_{s2}) &= x_2(k + 1, 1) \\
&= A_{d2}x_2(k, 3) + A_{d23}x_3(k, 1) + B_{d2}\theta_2(k, 3)u_2(k, 3), \\
x_3(kT_p + T_{s3}) &= x_3(k + 1, 1) \\
&= A_{d3}x_3(k, 1) + A_{d311}x_1(k, 1) + A_{d312}x_1(k, 2) + A_{d313}x_1(k, 4) \\
&\quad + A_{d321}x_2(k, 1) + A_{d322}x_2(k, 3),
\end{aligned}$$

where $x_i(k, j),\ i = 1, 2, 3,\ j = 1, 2, 3, 4$, are the water level of i-th tank at time instant $kT_p + \varsigma_j$, and the corresponding system matrices are defined as in (7.2).

According to the operation mechanism in Fig.7.1, the sampling cycles of the three tank levels are set the same as in the last subsection and the GCD of the sampling cycles $T_p = 24$ms. Following the modeling process of (7.3) and (7.4) in [116], the periodic system

model with MFs is formulated as follows,

$$\begin{aligned}\mathbf{x}(k,j+1) &= \mathbf{A}(j)\mathbf{x}(k,j) + \mathbf{B}(j)\mathbf{f}_\theta(k,j)\mathbf{u}_s(k,j) + \mathbf{E}(j)\mathbf{w}(k,j) \\ \mathbf{y}(k,j) &= \mathbf{C}(j)\mathbf{x}(k,j) + \mathbf{F}(j)\mathbf{v}(k,j),\ j = 1,2,3,4\end{aligned} \tag{7.8}$$

where $\mathbf{w}(k,j)$ and $\mathbf{v}(k,j)$ are noise vectors. $\mathbf{u}_s(k,j)$ is defined by

$$\mathbf{u}_s(k,j) = \begin{bmatrix} u'_{s,1}(k,j) & u'_{s,2}(k,j) \end{bmatrix}',\ j = 1,2,3,4$$

The MF coefficient matrix $\mathbf{f}_\theta(k,j)$ is constructed as follows

$$\mathbf{f}_\theta(k,j) = \begin{bmatrix} \theta_1(k,j) & \\ & \theta_2(k,j) \end{bmatrix},\ j = 1,2,3,4$$

where $\theta_i(k,j),\ i = 1,2;\ j = 1,2,3,4$, denotes the MF on the pump i at the time instant (k,j). It is assumed that the faults vary very slowly during one T_p. In another word, there is

$$\mathbf{f}_\theta(k,1) = \mathbf{f}_\theta(k,2) = \mathbf{f}_\theta(k,3) = \mathbf{f}_\theta(k,4)$$

The system matrices $\mathbf{A}(j)$, $\mathbf{B}(j)$, $\mathbf{C}(j)$, $\mathbf{E}(j)$ and $\mathbf{F}(j)$ are obtained the same as in (7.6).

We choose $j = 1$ as the initial time instant. Therefore, following the lifting procedure in (6.19)-(6.20), the system matrices of the lifted systems are expressed as

$$\mathbf{A}_1 = \mathbf{\Phi}(5,1),\ \psi_{1,1}(k) = \sum_{i=1}^{4} \mathbf{\Phi}(5,i+1)\mathbf{B}(i)\mathbf{u}_s(k,i)$$

$$\mathbf{E}_1 = \begin{bmatrix} \mathbf{\Phi}(5,2)\mathbf{E}(1) & \mathbf{\Phi}(5,3)\mathbf{E}(2) & \mathbf{\Phi}(5,4)\mathbf{E}(3) & \mathbf{E}(4) \end{bmatrix}$$

$$\mathbf{C}_1 = \begin{bmatrix} \mathbf{C}(1) \\ \mathbf{C}(2)\mathbf{\Phi}(2,1) \\ \mathbf{C}(3)\mathbf{\Phi}(3,1) \\ \mathbf{C}(4)\mathbf{\Phi}(4,1) \end{bmatrix},\ \psi_{2,1}(k) = \begin{bmatrix} \mathbf{O}_{6\times 2} \\ \mathbf{C}(2)\mathbf{B}(1)\mathbf{u}_s(k,1) \\ \mathbf{C}(3)\sum_{i=1}^{2} \mathbf{\Psi}(4,1+i)\mathbf{B}(i)\mathbf{u}_s(k,i) \\ \mathbf{C}(4)\sum_{i=1}^{3} \mathbf{\Psi}(4,1+i)\mathbf{B}(i)\mathbf{u}_s(k,i) \end{bmatrix}$$

$$\mathbf{F}_1 = \begin{bmatrix} \mathbf{F}(1) & \mathbf{O}_{6\times 6} & \mathbf{O}_{6\times 6} & \mathbf{O}_{6\times 6} \\ \mathbf{C}(2)\mathbf{E}(1) & \mathbf{F}(2) & \mathbf{O}_{6\times 6} & \mathbf{O}_{6\times 6} \\ \mathbf{C}(3)\mathbf{\Psi}(3,2)\mathbf{E}(1) & \mathbf{C}(3)\mathbf{E}(2) & \mathbf{F}(3) & \mathbf{O}_{6\times 6} \\ \mathbf{C}(4)\mathbf{\Psi}(4,2)\mathbf{E}(1) & \mathbf{C}(4)\mathbf{\Psi}(4,3)\mathbf{E}(2) & \mathbf{C}(4)\mathbf{E}(3) & \mathbf{F}(4) \end{bmatrix}$$

The matrices $\mathbf{B}_1$ and $\mathbf{D}_1$ defined in (6.41)-(6.42) are obtained by

$$\mathbf{B}_1 = \begin{bmatrix} \mathbf{\Phi}(5,2)\mathbf{B}(1) & \mathbf{\Phi}(5,3)\mathbf{B}(2) & \mathbf{\Phi}(5,4)\mathbf{B}(3) & \mathbf{B}(4) \end{bmatrix},$$

$$\mathbf{D}_1 = \begin{bmatrix} \mathbf{O}_{6\times6} & \mathbf{O}_{6\times6} & \mathbf{O}_{6\times6} & \mathbf{O}_{6\times6} \\ \mathbf{C}(2)\mathbf{B}(1) & \mathbf{O}_{6\times6} & \mathbf{O}_{6\times6} & \mathbf{O}_{6\times6} \\ \mathbf{C}(3)\mathbf{\Psi}(3,2)\mathbf{B}(1) & \mathbf{C}(3)\mathbf{B}(2) & \mathbf{O}_{6\times6} & \mathbf{O}_{6\times6} \\ \mathbf{C}(4)\mathbf{\Psi}(4,2)\mathbf{B}(1) & \mathbf{C}(4)\mathbf{\Psi}(4,3)\mathbf{B}(2) & \mathbf{C}(4)\mathbf{B}(3) & \mathbf{O}_{6\times6} \end{bmatrix}.$$

During this experiment, the scheduler is considered under an ideal network condition and all the latest information will arrive on time, so $\phi(1) = \phi(2) = \phi(3) = \phi(4) = \mathbf{I}_{6\times6}$. The scheduler, which has been shown in Fig.7.2, can be expressed as the state-space model (4.10) and the system matrices of the scheduler are given as in (7.7).

7.5 Implementation of FTC scheme for MFs

According to the physical parameters of the three-tank system presented in Table 7.1, the system matrices of the lifted system after discretization are stated as follows

$$\mathbf{A}_1 = \begin{bmatrix} & 0.9999 & 0 & 1.0264e-4 \\ & 0 & 0.9996 & 2.0063e-4 \\ \mathbf{O}_{6\times3} & 0.9998 & 0 & 2.0527e-4 \\ & 0.9997 & 0 & 3.0789e-4 \\ & 0 & 0.9993 & 4.0118e-4 \\ & 3.0780e-4 & 4.0111e-4 & 0.9993 \end{bmatrix},$$

$$\mathbf{B}_1 = \begin{bmatrix} 0.5195 & 0 & 0 & 0 & 0 & 0 & 0 & 0 \\ 0 & 0 & 0 & 0.7791 & 0 & 0 & 0 & 0 \\ 0.5194 & 0 & 0 & 0 & 0.5195 & 0 & 0 & 0 \\ 0.5193 & 0 & 0 & 0 & 0.5194 & 0 & 0.5195 & 0 \\ 0 & 0 & 0 & 0.7788 & 0 & 0 & 0 & 0.7791 \\ 1.0658e-4 & 0 & 0 & 1.5625e-4 & 5.3289e-5 & 0 & 0 & 0 \end{bmatrix},$$

$$\mathbf{C}_1 = \begin{bmatrix} \mathbf{I}_{6\times6} & \\ \mathbf{O}_{18\times1} & \mathbf{C}_{1,1} \end{bmatrix}, \mathbf{C}_{1,1} = \begin{bmatrix} \mathbf{I}_{5\times5} & \\ \mathbf{O}_{13\times1} & \mathbf{C}_{1,2} \end{bmatrix},$$

$$\mathbf{D}_{1,1} = \begin{bmatrix} 0.5195 \\ \mathbf{O}_{4\times1} \\ 0.5195 \\ \mathbf{O}_{4\times1} \\ 0.5195 \\ 0 \\ 0.5194 \end{bmatrix}, \mathbf{D}_{1,2} = \begin{bmatrix} \mathbf{O}_{6\times2} & \\ 0.7791 & 0 \\ \mathbf{O}_{4\times2} & \\ 0.7791 & 0 \\ 0 & 0.5195 \end{bmatrix},$$

$$\mathbf{D}_1 = \begin{bmatrix} \mathbf{O}_{11\times 8} & & & \\ \mathbf{D}_{1,1} & \mathbf{O}_{13\times 2} & \mathbf{D}_{1,2} & \mathbf{O}_{13\times 3} \end{bmatrix},$$

$$\mathbf{C}_{1,2} = \begin{bmatrix} 0 & 0.9999 & 0 & 1.0264e-4 \\ 1 & 0 & 0 & 0 \\ 0 & 1 & 0 & 0 \\ 0 & 0 & 1 & 0 \\ 0 & 0 & 0 & 1 \\ 0 & 0.9999 & 0 & 1.0264e-4 \\ 0 & 0 & 0.9996 & 2.0063e-4 \\ 0 & 1 & 0 & 0 \\ 0 & 0 & 1 & 0 \\ 0 & 0 & 0 & 1 \\ 0 & 0.9999 & 0 & 1.0264e-4 \\ 0 & 0 & 0.9996 & 2.0063e-4 \\ 0 & 0.9998 & 0 & 2.0527e-4 \end{bmatrix},$$

$$\mathbf{E}_1 = \begin{bmatrix} \mathbf{O}_{6\times 3} & \mathbf{E}_{1,1} & \mathbf{O}_{6\times 5} & \mathbf{E}_{1,2} & \mathbf{O}_{6\times 6} & \mathbf{E}_{1,3} & \mathbf{O}_{6\times 3} & \mathbf{E}_{1,4} \end{bmatrix},$$

$$\mathbf{E}_{1,1} = \begin{bmatrix} 0.0080 \\ 0 \\ 0.0080 \\ 0.0080 \\ 0 \\ 1.6414e-6 \end{bmatrix}, \mathbf{E}_{1,2} = \begin{bmatrix} 0 \\ 0.00120 \\ 0 \\ 0 \\ 0.0120 \\ 2.4063e-6 \end{bmatrix}, \mathbf{E}_{1,3} = \begin{bmatrix} 0 \\ 0 \\ 0.0080 \\ 0.0080 \\ 0 \\ 8.2065e-7 \end{bmatrix},$$

$$\mathbf{E}_{1,4} = \begin{bmatrix} \mathbf{O}_{3\times 4} & & & \\ 0 & 0 & 0 & 0.0080 \\ 0 & 0 & 0.0120 & 0 \\ 0.0240 & 0 & 0 & 0 \end{bmatrix},$$

$$\mathbf{F}_1 = \begin{bmatrix} \mathbf{I}_{11\times 11} * 1.000e-3 & & & & \mathbf{O}_{11\times 13} \\ \mathbf{O}_{13\times 3} & \mathbf{F}_{1,1} & \mathbf{O}_{13\times 5} & \mathbf{F}_{1,2} & \mathbf{O}_{13\times 1} & \mathbf{F}_{1,3} \end{bmatrix},$$

$$\mathbf{F}_{1,3} = \begin{bmatrix} \mathbf{I}_{6\times 6} * 1.000e-3 & \mathbf{O}_{6\times 7} \\ \mathbf{F}_{1,4} & \mathbf{I}_{7\times 7} * 1.000e-3 \end{bmatrix}, \mathbf{F}_{1,4} = \begin{bmatrix} \mathbf{O}_{6\times 6} \\ \mathbf{O}_{1\times 5} \quad 0.0080 \end{bmatrix},$$

$$\mathbf{F}_{1,1} = \begin{bmatrix} 0.0080 \\ \mathbf{O}_{4\times 1} \\ 0.0080 \\ \mathbf{O}_{4\times 1} \\ 0.0080 \\ 0 \\ 0.0080 \end{bmatrix}, \mathbf{F}_{1,2} = \begin{bmatrix} \mathbf{O}_{6\times 1} \\ 0.0120 \\ \mathbf{O}_{4\times 1} \\ 0.0120 \\ 0 \end{bmatrix}, .$$

During our experiment, pump 1 doesn't appear an MF while pump 2 does, and they are expressed as follows

$$\theta_1(k,j)=1,\ \theta_2(k,j)=\begin{cases}0.7, & 18750\le k\le 20833\\ 1, & \text{others}\end{cases}.$$

Since $T_p = 0.024$ s, the MF in the continuous time domain occurs on pump 2 during $[450\text{ s}, 500\text{ s})$.

By increasing the communication volume, the residuals are shared among CSs. Therefore, the problem of structure limitations on the observer gain $\mathbf{L}_1$ is avoided. With the help of the MATLAB command 'place', the observer gain $\mathbf{L}_1$ can be achieved as follows

$$\mathbf{L}_1=\begin{bmatrix}\mathbf{L}_{1,1} & \mathbf{L}_{1,2} & \mathbf{L}_{1,3} & \mathbf{L}_{1,4} & \mathbf{L}_{1,5}\end{bmatrix},$$

$$\mathbf{L}_{1,1}=\begin{bmatrix}-0.0200 & 0 & 0 & 0.1250 & -6.4360e-10 & 9.6249e-6\\ 0 & 0.0100 & 0 & -2.1455e-9 & 0.1666 & 3.3446e-5\\ 0 & 0 & -0.0066 & 0.1250 & -2.3594e-9 & 3.5284e-5\\ 0 & 0 & 0 & 0.1275 & -4.0537e-9 & 6.0622e-5\\ 0 & 0 & 0 & -5.3836e-9 & 0.1633 & 8.3924e-5\\ 0 & 0 & 0 & 2.2135 & 4.9830e-9 & 0.2548\end{bmatrix},$$

$$\mathbf{L}_{1,2}=\begin{bmatrix}0 & 0 & 0.1250 & -6.4360e-10 & 9.6249e-6 & 0.1250\\ 0.0100 & 0 & -2.1455e-9 & 0.1666 & 3.3446e-5 & 1.2877e-9\\ 0 & -0.0066 & 0.1250 & -2.3594e-9 & 3.5284e-5 & 0.1250\\ 0 & 0 & 0.1275 & -4.0537e-9 & 6.0622e-5 & 0.1275\\ 0 & 0 & -5.3836e-9 & 0.1633 & 8.3924e-5 & 3.2310e-9\\ 0 & 0 & 2.2135 & 4.9830e-9 & 0.2548 & 4.8286e-5\end{bmatrix},$$

$$\mathbf{L}_{1,3}=\begin{bmatrix}0 & 0.1250 & -6.4360e-10 & 9.6249e-6 & 0.1250\\ 0 & -2.1455e-9 & 0.1666 & 3.3446e-5 & 1.2877e-9\\ -0.0066 & 0.1250 & -2.3594e-9 & 3.5284e-5 & 0.1250\\ 0 & 0.1275 & -4.0537e-9 & 6.0622e-5 & 0.1275\\ 0 & -5.3836e-9 & 0.1633 & 8.3924e-5 & 3.2310e-9\\ 0 & 2.2135 & 4.9830e-9 & 0.2548 & 4.8286e-5\end{bmatrix},$$

$$\mathbf{L}_{1,4}=\begin{bmatrix}1.2877e-9 & 0.1250 & -6.4360e-10 & 9.6249e-6 & 0.1250\\ 0.1666 & -2.1455e-9 & 0.1666 & 3.3446e-5 & 1.2877e-9\\ 4.7205e-9 & 0.1250 & -2.3594e-9 & 3.5284e-5 & 0.1250\\ 8.1102e-9 & 0.1275 & -4.0537e-9 & 6.0622e-5 & 0.1275\\ 0.1632 & -5.3836e-9 & 0.1633 & 8.3924e-5 & 3.2310e-9\\ 1.0093e-4 & 2.2135 & 4.9830e-9 & 0.2548 & 4.8286e-5\end{bmatrix},$$

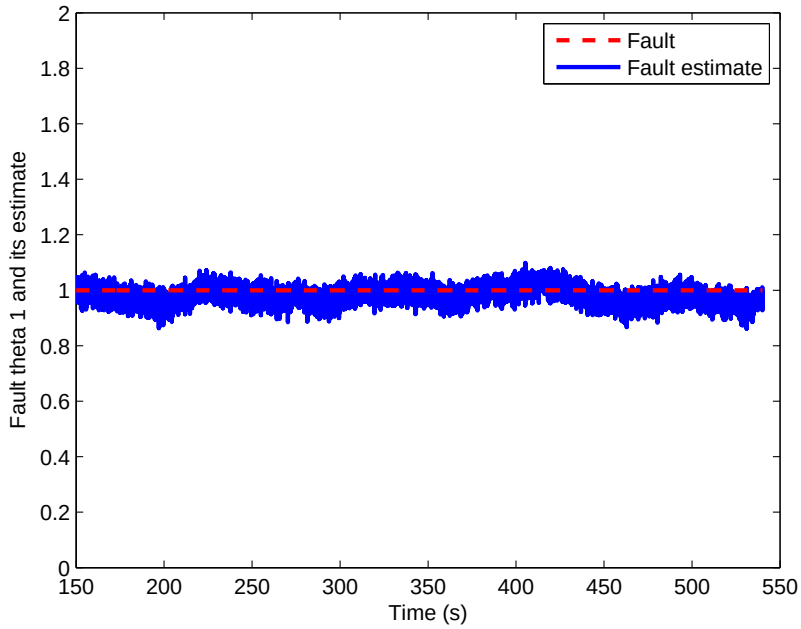

Figure 7.11: Fault θ_1 and its estimate

$$\mathbf{L}_{1,5} = \begin{bmatrix} 1.2877e-9 & 0.1250 \\ 0.1666 & 4.7205e-9 \\ 4.7205e-9 & 0.1250 \\ 8.1102e-9 & 0.1274 \\ 0.1632 & 1.1845e-8 \\ 1.0093e-4 & 7.4434e-5 \end{bmatrix}.$$

In the process, pump 2 appears an MF and the flow rate is reduced. A comparison of MFs and their estimates on pump 1 and pump 2 are presented in Fig.7.11 and Fig.7.12. The change trend of the MF on pump 2 has been embodied on Fig.7.12. Due to the wave fluctuation on the surface of the water, the imprecise measurement of the water level is unavoidable. The change range of the residuals has reflected on the line width of the fault estimates. Fig.7.13 demonstrates the output residuals of 3 tanks.

The same as the experiment of FTC strategy for AFs, a control strategy is constructed only based on the estimated states. Then the output performance without FTC strategy is shown in Fig.7.14. There is a big deviation from the operation point when the fault occurs, and the fault has been propagated to other tanks. By applying Theorem 6.3 on the aforementioned three-tank system model, a solution for the controller gain $\mathbf{K}_1$ can be achieved. During the way to obtain a feasible solution, LMI tool box has exhibited its great operational capability and convenience. Fig.7.15 displays the output performance

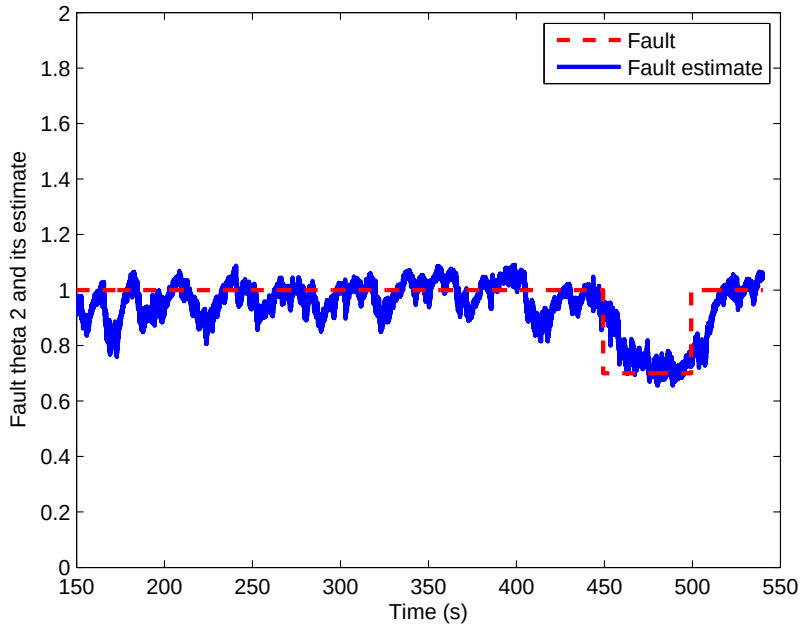

Figure 7.12: Fault θ_2 and its estimate

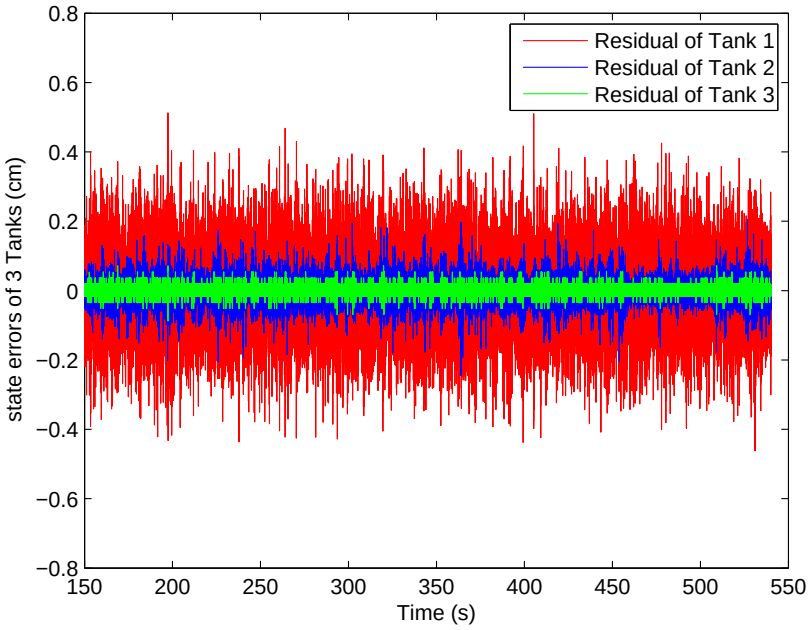

Figure 7.13: Residuals of water levels

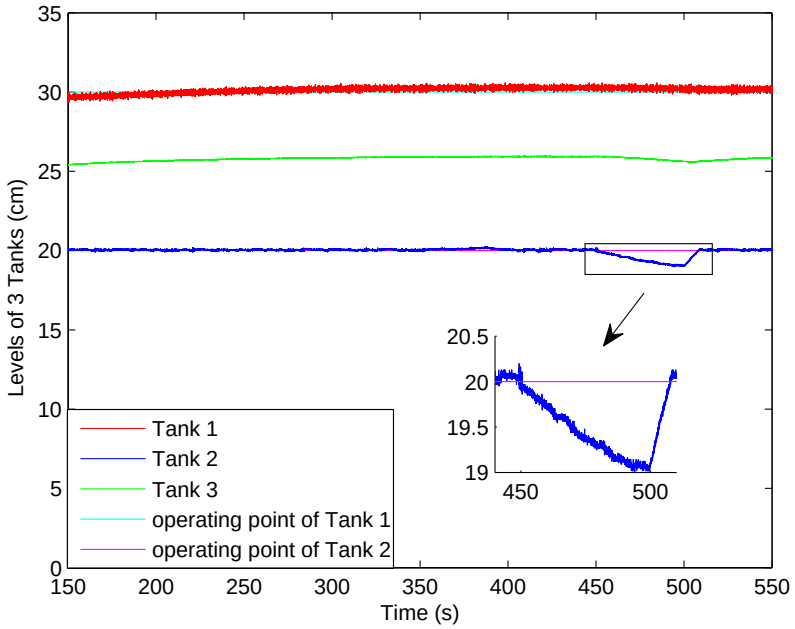

Figure 7.14: Output without FTC strategy

with FTC strategy. By comparing Fig.7.14 and Fig.7.15, we can see that, the system shows a very good tolerance to the fault with the proposed FTC strategy.

Following the equation (6.44), the controller gain $\mathbf{K}_1$ is divided into $\mathbf{K}(j),\ j = 1, 2, 3, 4$, for LCs, where the local commands are calculated according to the received state estimates. As we have discussed in section 6.4, it depends on the bandwidth of the wireless network to decide that, how much information can be scheduled to transmit. It could be only the state estimate of the current subprocess or these of all the subprocesses that will be transmitted to LCs. Similarly as in the experiment of FTC scheme for AFs, there also exists a trade-off problem between increasing the communication volume and guaranteeing the system FTC performance. A comparison of the results respect to the cases with unshared and shared state estimates will be presented in the following subsections.

7.5.1 FTC performance with unshared state estimates

In the case with unshared state estimates, within a circular region $\mathcal{D}(0, 1)$, H_∞ performance levels $\gamma = 1$ is given. The controller gain matrices are obtained as

$$\mathbf{K}(1) = \begin{bmatrix} -0.0152 & 0 & -0.0134 & -0.1820 & 0 & 0 \\ 0 & -0.0060 & 0 & 0 & -0.3454 & 0 \end{bmatrix},$$

$$\mathbf{K}(2) = \begin{bmatrix} 6.1154e-8 & 0 & 2.7152e-7 & -2.8048e-6 & 0 & 0 \end{bmatrix},$$

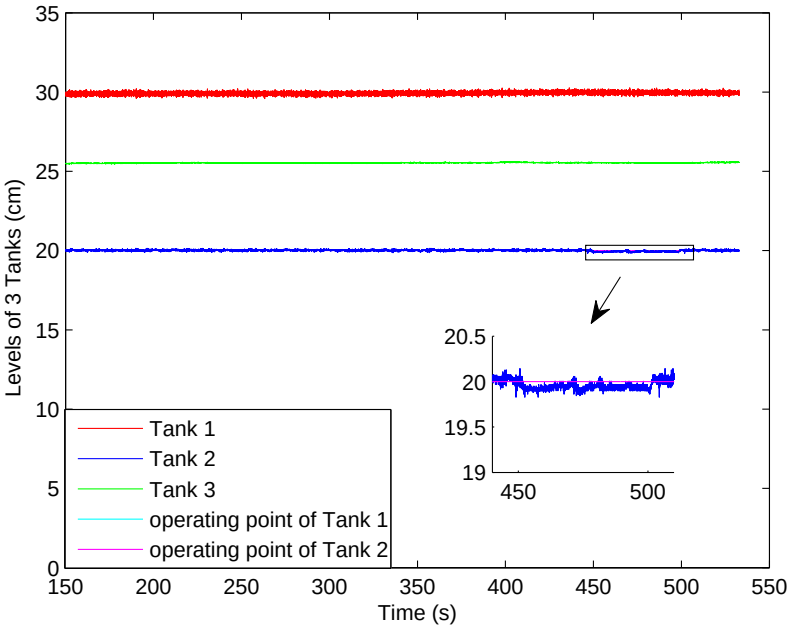

Figure 7.15: Output with FTC strategy

$$\mathbf{K}(3) = \begin{bmatrix} 0 & -6.8018e-6 & 0 & 0 & 5.3396e-4 & 0 \end{bmatrix},$$
$$\mathbf{K}(4) = \begin{bmatrix} 3.4306e-5 & 0 & 3.4623e-5 & -0.0023 & 0 & 0 \end{bmatrix}.$$

The reference values of control signals, that keep the system working at the operating points, are set as $R_{ef,1} = 2.7 \times 10^4 \text{cm}^3/\text{s}, R_{ef,2} = 4.2 \times 10^4 \text{cm}^3/\text{s}$. The outputs of three-tank system is presented in Fig.7.16. From the impact of the proposed FTC strategy in Fig.7.16, we can see, the output of tank 2 has only a small deviation from the operating point in the fault case.

7.5.2 FTC performance with shared state estimates

In the case with shared residuals, we prescribe the circular region $\mathcal{D}(0,1)$ and H_∞ performance levels $\gamma = 1$. The controller gain matrices are achieved as

$$\mathbf{K}(1) = \begin{bmatrix} -0.0152 & -2.5338e-9 & -0.0134 \\ -2.1850e-9 & -0.0060 & -2.3196e-9 \\ -0.1820 & -3.9743e-10 & -9.1218e-5 \\ 1.7720e-8 & -0.3454 & -1.7625e-4 \end{bmatrix},$$

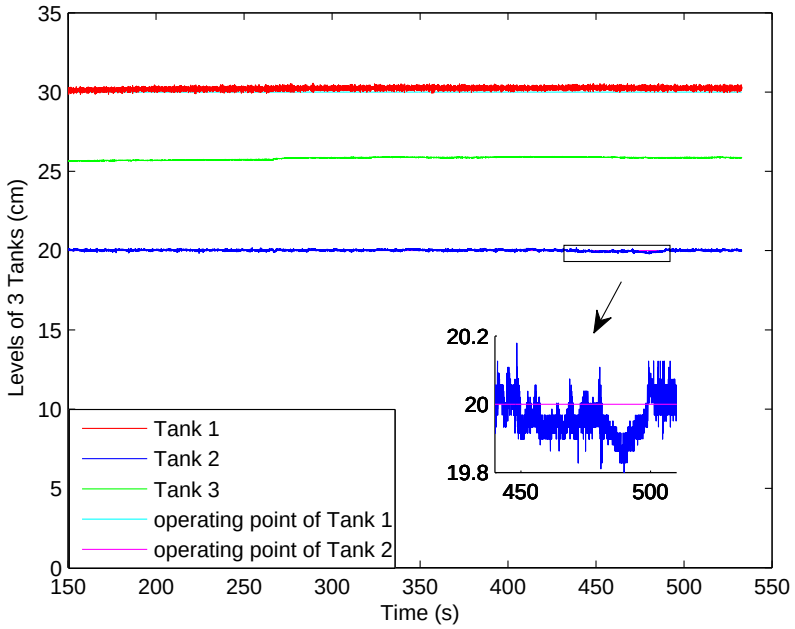

Figure 7.16: Outputs of three-tank system with unshared state estimates

$$\mathbf{K}(2) = \begin{bmatrix} 6.1482e-8 & -4.5399e-10 & 2.7192e-7 \\ -2.7967e-6 & 4.1455e-9 & -7.6403e-5 \end{bmatrix},$$
$$\mathbf{K}(3) = \begin{bmatrix} 1.7160e-10 & -6.8017e-6 & 1.4693e-10 \\ 2.7544e-9 & 5.3396e-4 & -3.9502e-6 \end{bmatrix},$$
$$\mathbf{K}(4) = \begin{bmatrix} 3.4306e-5 & 1.1265e-10 & 3.4623e-5 \\ -0.0023 & 9.9874e-9 & -8.6129e-6 \end{bmatrix}.$$

It is found that $\mathbf{K}(j),\ j = 1, 2, 3, 4$, have small changes from the case with unshared state estimates. To ensure the system working at the operating points, The reference values of control signals are set the same as before, $R_{ef,1} = 2.7 \times 10^4$ cm^3/s, $R_{ef,2} = 4.2 \times 10^4$ cm^3/s. The outputs of three-tank system are displayed in Fig.7.17. The deviation of the outputs in Fig.7.17 is smaller than that in Fig.7.16, which means the case with shared state estimates in Fig.7.17 have a little bit better performance. The most important reason for this situation is that (1) only very small changes exist in the controller gain $\mathbf{K}(j)$ of both cases; (2) The three-tank system works actually as a slow process, the tiny change in the controller couldn't reflect obviously during the process in a short time. So far, our experiment has not only verified the proposed FTC strategy, but also confirmed a better

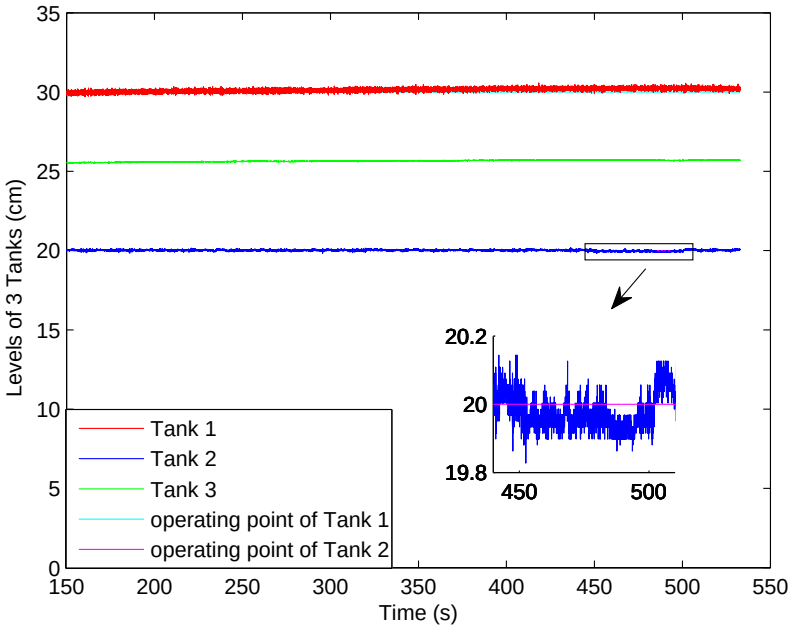

Figure 7.17: Outputs of three-tank system with shared state estimates

control performance with shared state estimates.

In the above experiment, only the ideal network condition has been concerned. When it comes to the unideal network conditions, some changes are only required in the system matrices of the scheduler (4.10). Although the system control performance in this situation will be a little worse, the advantage of that with shared information still exists. Space lacks for a detailed description of it.

7.6 Summary

In this chapter, the three-tank system on the WiNC experimentation platform has been modeled as a 4-periodic system integrated with a 4-periodic scheduler. Based on this integrated system, the sensor/actuator AFs and actuator MFs have been considered during the process, respectively. Aiming at the types of faults, the corresponding FTC strategies are implemented to accommodate the effects caused by faults. Considering the communication volume, a comparison of the system FTC performances with unshared and shared information (such as residuals and state estimates) has been presented. The experiment results indicate that, the proposed FTC strategies are quite tolerant to the relevant faults. In addition, the system with shared information (at the cost of communication load) achieves a better FTC performance than that with unshared information.

8 Conclusion and future directions

This chapter summarizes the results obtained in this thesis. Some directions for further developments of the proposed schemes are also suggested.

8.1 Conclusion

The major objective of this thesis is the investigation of FTC strategies for the decentralized W-NCSs, which are developed for the industrial real-time automation applications. For the real-time requirement in industrial systems, the FTC performances of W-NCSs not only depend on the developed control algorithms but also on the network protocols at the medium access control (MAC) layer. These protocols, in form of schedulers, determine the transmission orders of messages and play significant roles in the control performances of W-NCSs. Under these circumstances, it is challenging but promising to investigate FTC schemes for W-NCSs with an integrated scheduler.

In the first part of this thesis, the procedures of integrating a scheduler into W-NCSs are introduced. Due to the formal limitation of the information scheduler, as well as its physical meaning, the information scheduler couldn't be directly integrated into the W-NCSs. We have introduced a mathematical scheduler, which contains the crucial messages (such as transmission order, time delay, packet loss, etc) of the information scheduler. The procedures of transferring an information scheduler into its mathematical scheduler have been presented. The mathematical scheduler is taken as a dynamic system, and has been further reformulated into the form of state-space representation. By considering the multi-rate sampling and control in each cycle, as well as the communication mechanism, W-NCSs with an integrated mathematical scheduler has been modeled as integrated discrete LTP systems. Meanwhile, the scheduler has also been modeled as discrete LTP systems, where the system matrices depict the imperfect transmission behaviors, such as deterministic delay, packet loss and so on.

The second part of this thesis focuses on the developments of FTC schemes for the integrated W-NCSs. Based on the integrated discrete LTP systems, FE and FTC schemes for W-NCSs with sensor/actuator AFs have been developed. According to the time instants in a period T_p, two cases are taken into account in our work: faults are considered during

the process: (1) at all T_p time instants and (2) at partial time instants. With respect to these two cases, the corresponding state observer, fault estimator and the feedback controller are constructed. Moreover, we have dealt with the investigation of FTC strategy for W-NCSs with actuator MFs. A lifting technology and the adaptive estimation method are applied to the discrete LTP systems and an adaptive observer is constructed. A nominal controller is designed for the system with fault-free case. Finally, based on this nominal controller and the adaptive observer, an FTC strategy is developed to compensate the effects caused by faults and ensure the LTP systems continue operating properly. Due to the distribution of W-NCSs and the limitation of communication bandwidth, the structure limitation problem in the gains of estimators and controllers is unavoidable. Therefore, improved theorems are presented to obtain the feasible solutions for these gains.

Finally, all the developed FE approaches and FTC strategies for W-NCSs with AFs and MFs have been demonstrated on the WiNC platform, respectively. The FE and FTC methods have been designed according to two situations: with unshared and shared information (i.e., residual signals or state estimates). The results show that the system with the developed methods will be tolerant to the corresponding faults. We have also compared the system FTC performances, after applying the proposed FTC strategies with shared and unshared information, respectively. The results indicate that the system achieves better FTC performances with shared information, of course, it is at the cost of communication load.

8.2 Future directions

The preceding section summarized the results obtained in this thesis. the proposed procedures, methods and their applications to improve the FTC performances of W-NCSs in the occurrence of faults were briefly described. Besides the admired features of the proposed approaches, there is a room for further improvements. In the following, some possible research directions for further extension of the proposed FTC schemes are outlined.

In this thesis, a given static scheduler has been concerned and formulated into discrete LTP systems. Sometimes, there might be some abrupt and urgent signals generated during the process. The transmissions of these signals will be aperiodic. A dynamic scheduler has to be designed to accommodate these emergency situations. Hence, a possible future direction to extend the proposed approaches is to model the W-NCSs with the dynamic scheduler. Besides, the information scheduler for the updates of the state estimates among other CSs in a broadcast mode above the Management layer are much more complex and haven't been taken into account. Another future direction is to extend this broadcast

scheduler into the integrated W-NCSs.

Furthermore, considering the model complexity of real applications, the W-NCSs can be modeled with model uncertainties or nonlinear systems. The design of FE and FTC schemes for a more complex W-NCSs is expected. In this thesis, only the sensor/actuator AFs and actuator MFs have been considered. The researches of FTC strategies for W-NCSs with sensor MFs and even component faults are still lacked and could be one of the future directions.

Bibliography

[1] K. Ji and D. Wei, "Resilient Control for Wireless Networked Control Systems," *International Journal of Control Automation, and Systems*, vol. 9, pp. 285–293, 2011.

[2] Y. Xia, W. Xie, X. Bian, and S. Chai, "Application of the Networked Predictive Control in Servo Systems," *Circuits Syst Signal Process*, vol. 32, pp. 1537–1549, 2013.

[3] Y. Shi, J. Huang, and B. Yu, "Robust Tracking Control of Networked Control Systems: Application to a Networked DC Motor," *IEEE Transaction on Industrial Electronics*, vol. 60, pp. 5864–5874, 2013.

[4] D. Daza, M. Diaz, C.Rubia, M. C. Delgado, and P. Cortes, "Network Management Algorithms for Wireless Field Bus Control of Vertial Transportation Systemss," *Intelligent Automation and Soft Computing*, vol. 16, pp. 123–131, 2010.

[5] G. Franze and F. Tedesco, "Constrained load/frequency control problems in networked multi-area power systems," *Journal of the Franklin Institute*, vol. 348, pp. 832–852, 2011.

[6] V. Veselý and T. Quang, "Robust Power System Stabilizer via Networked Control System," *Journal of Electrical Engineering*, vol. 62, pp. 286–291, 2011.

[7] N. Bibinagar and W. jong Kim, "Switched Ethernet-Based Real-Time Networked Control System with Multiple-Client-Server Architecture," *IEEE/ASME transactions on Mechatronics*, vol. 18, pp. 104–112, 2013.

[8] R. Gupta and M.-Y. Chow, "Networked Control System: Overview and Research Trends," *IEEE Transactions on Industrial Electronics*, vol. 57, pp. 2527–2535, 2010.

[9] L. Zhang, H. Gao, and O. Kaynak, "Network-Induced Constraints in Networked Control Systems-A Survey," *IEEE Transaction on Industrial Informatics*, vol. 9, pp. 403–416, 2013.

[10] N. J. Ploplys, P. A. Kawka, and A. G. Alleyne, "Closed-loop control over wireless network," *IEEE Control Systems Magazine*, vol. 24, pp. 58–71, 2004.

[11] B. Galloway and G. P. Hancke, "Introduction to Industrial Control Networks," *IEEE Communications Surveys & Tutorials*, vol. 15, pp. 860–880, 2013.

[12] D. Yashiro and T. Yakoh, "Feedback Controller With Low-Pass-Filter-Based Delay Regulation for Networked Control Systems," *IEEE Transactions on Industrial Electronics*, vol. 61, pp. 3744–3752, 2014.

[13] Z. Hong, J. Gao, and N. Wang, "Output-Feedback Controller Design of a Wireless Networked Control System with Packet Loss and Time Delay," *Mathematical Problems in Engineering*, http://dx.doi.org/10.1155/2014/206475, 2014.

[14] X. Tang and B. Ding, "Model predictive control of linear systems over networks with data quantizations and packet losses," *Automatica*, vol. 49, pp. 1333–1339, 2013.

[15] D. Du, M. Fei, and T. Jia, "Modelling and stability analysis of MIMO networked control systems with multi-channel random packet losses," *Transactions of the Institute of Measurement and Control*, DOI: 10.1177/0142331211406605, 2013.

[16] K. Chabir, D. D. Sauter, I. Al-Salami, and C. Aubrun, "On Fault Detection and Isolation (FDI) Design for Networked Control Systems with Bounded Delay Constraints," *8th IFAC Symposium on Fault Detection, Supervision and Safety of Technical Processes*, vol. 8, pp. 1107–1112, Mexico City, Mexico, 2012.

[17] "TDMA," *http://en.wikipedia.org/wiki/Time-division-multiple-access*.

[18] Y. Zhang, S. Zheng, and S. Xiong, "A Scheduling Algorithm for TDMA-based MAC Protocol in Wireless Sensor Networks," *First International Workshop on Education Technology and Computer Science*, Wuhan, China, March 2009.

[19] T. Ho and K. Chen, "Performance analysis of IEEE 802.11 CSMA/CA medium access control protocol," *7th IEEE International Symposium on Personal, Indoor and Mobile Radio Communications*, 1996.

[20] "CSMA/CA," *http://searchnetworking.techtarget.com/definition/CSMA-CA*.

[21] S. X. Ding, P. Zhang, S. Yin, and E. Ding, "An Integrated Design Framework of Fault-Tolerant Wireless Networked Control Systems for Industrial Automatic Control Applications," *IEEE Transaction on Industrial Informatics*, vol. 9, no. 1, pp. 462–471, Fer. 2013.

[22] L. Zhang and D. Hristu-Varsakelis, "Communication and control co-design for networked control systems," *Automatica*, vol. 42, no. 6, pp. 953–958, 2006.

[23] M. Gaid, A. Cela, and Y. Hamam, "Optimal integrated control and scheduling of networked control systems with communication constraints: application to a car suspension system," *IEEE Trans. Control Systems Technology*, vol. 14, no. 4, pp. 776–787, July 2006.

[24] Y. Zhao, G. Liu, and D. Rees, "Integrated predictive control and scheduling co-design for networked control systems," *IET Control Theory Applications*, vol. 2, pp. 7–15, 2008.

[25] D. B. Dačić and D. Nešić, "Quadratic Stabilization of Linear Networked Control Systems via Simultaneous Protocol and Controller Design," *Automatica*, vol. 43, pp. 1145–1155, 2007.

[26] S. X. Ding, "A Survey of Fault-Tolerant Networked Control System Design," *8th IFAC Symposium on Fault Detection, Supervision and Safety of Technical Processes*, vol. 8, pp. 874–885, Mexico City, Mexico, August 2012.

[27] B. Jiang, M. Staroswiecki, and V. Cocquempot, "Fault Accommodation for Nonlinear Dynamic Systems," *IEEE Transaction on Automatic Control*, vol. 51, pp. 1578–1583, 2006.

[28] H. Noura, D. Theilliol, J.-C. Ponsart, and A. Chamseddine, *Fault-tolerant Control Systems Design and Practical Applications.* Springer, 2009.

[29] K. Zhang, B. Jiang, and P. Shi, *Observer-Based Fault Estimation and Accomodation for Dynamic Systems.* Springer, 2013.

[30] J. P. Georges, D. Theilliol, V. Cocquempot, J. C. Ponsart, and C. Aubrun, "Fault Tolerance in Networked Control Systems under Intermittent Observations," *International Journal of Applied Mathematics and Computer Science*, vol. 21, pp. 639–648, Dec. 2011.

[31] Y. Zhang and J. Jiang, "Bibliographical review on reconfigurable faulttolerant control systems," *Annual Review in Control*, vol. 32, pp. 229–252, 2008.

[32] B. Boussaid, C. Aubrun, M. Abdelkrim, and M. Gayed, "Performance evaluation based fault tolerant control with actuator saturation avoidance," *International Journal of Applied Mathematics and Computer Science*, vol. 21, pp. 457–466, 2011.

[33] E. Tian, C. Peng, and Z. Gu, "Fault Tolerant Control for Discrete Networked Control Systems with Random Faults," *Int. J. of Control, Automation and Systems*, vol. 10, pp. 444–448, 2012.

[34] J. Zhang, "Fault-tolerant Control for Networked Control System with bounded Packet Loss," *8th International Conference on Computer Science and Education (ICCSE)*, pp. 1407–1410, Sri Lanka Inst Informat Technol, Colombo, Sri Lanka, Apr. 2013.

[35] Q. Zhang, D. Gong, and Y. Guo, "Fault-Tolerant Control of a Class of Nonlinear Networked Control Systems with Time-Varied Delays," *27th Chinese Control Conference*, vol. 3, Kunming, China, Jul. 2008.

[36] D. Xie, G. Chen, and D. Zhang, "Guaranteed Cost Fault-tolerant Control for Uncertain Networked Control System with Packet Dropouts," *Proceeding of the IEEE International Conference on Automation and Logistics*, pp. 35–40, Zhengzhou, China, Aug. 2012.

[37] Y. Wang, B. Jiang, and Z. Mao, "Fault-tolerant Control Design for a kind of Nonlinear Networked Control System with Communication Constraints," *21st Chinese Control and Decision Conference*, vol. 1-6, Guilin, China, Jun. 2009.

[38] X. Li, X. Huang, and X. Wu, "A Cooperative Design Approach of Fault-Tolerant Controller and Observer for Nonlinear Networked Control Systems Based on T-S Model," *Conference on Electronic Commerce, Web Application and Communication*, pp. 123–131, Wuhan, China, Mar. 2012.

[39] P.Millán, L.Orihuela, C.Vivas, F.R.Rubio, D.V.Dimarogonas, and K.H.Johansson, "Sensor-network-based robust distributed control and estimation," *Control Engineering Practice*, vol. 21, pp. 1238–1249, 2013.

[40] P. Panagi and M. Polycarpou, "Decentralized Fault Tolerant Control of a Class of Interconnected Nonlinear Systems," *IEEE Transactions on Automatic Control*, vol. 56, pp. 178–184, 2011.

[41] P. Panagi and M. M. Polycarpou, "A Coordinated Communication Scheme for Distributed Fault Tolerant Control," *IEEE Transactions on Industrial Informatics*, vol. 9, pp. 386–393, 2013.

[42] S. Ghantasala and N. H. El-Farra, "Robust diagnosis and fault-tolerant control of distributed processes over communication networks," *International Journal of Adaptive Control Signal Process*, vol. 23, pp. 699–721, 2009.

[43] A. Challouf, A. Tellili, N. Abdelkrim, and C. Aubrun, "Distributed robust adaptive fault tolerant control for N-interconnected subsystems," *Conférence Méditerranéenne sur l'Ingénierie Sûre des Systèmes Complexes*, Agadir, Maroc, 2011.

[44] K. Menighed, J.-J. Yamé, C. Aubrun, and B. Boussaid, "Fault Tolerant Cooperative Control: A Distributed Model Predictive Control Approach," *19th Mediterranean Conference on Control and Automation*, pp. 1094–1099, Corfu, Greece, June 2011.

[45] T. Herman and S. Tixeuil, "A Distributed TDMA Slot Assignment Algorithm for Wireless Sensor Networks," *AlgoSensors*, vol. 3121, 2004.

[46] IEEE Std 802.11, "IEEE Computer Society LAN/MAN Standards Commitee, Part 11: Wireless LAN Medium Access Control (MAC) and Physical Layer (PHY) Specifications," 1999.

[47] P. Santi, "Topology control in wireless ad hoc and sensor networks," *ACM Computing Surveys*, vol. 37, pp. 164–194, 2005.

[48] F. Zhao and L. Guibas, *Wireless Sensor Networks: An Information Processing Approach.* Morgan Kaufmann, 2004.

[49] V. L. Ferrando, "Topology and Time Synchronization algorithms in wireless sensor networks," Facultat ďInformàtica de Barcelona,Universitat Polit'ecnica de Catalunya, Tech. Rep., Juny 2011.

[50] F. Sivrikaya and B. Yener, "Time Synchronization in Sensor Networks: A Survey," *Network, IEEE*, vol. 18, pp. 45–50, 2004.

[51] I.-K. Rhee, J. Lee, J. Kim, E. Serpedin, and Y.-C. Wu, "Clock Synchronization in Wireless Sensor Networks: An Overview," *Sensors*, vol. 9, pp. 56–85, 2009.

[52] S. M. Lasassmeh and J. M. Conrad, "Time synchronization in wireless sensor networks: A survey," *IEEE Proceedings of the SoutheastCon*, pp. 242–245, March 2010.

[53] B. Sundararaman, U. Buy, and A. D. Kshemkalyani, "Clock Synchronization for Wireless Sensor Networks: A Survey," *Ad Hoc Networks*, vol. 3, pp. 281–323, 2005.

[54] K. Römer, P. Blum, and L. Meier, *Chapter 7. Time Synchronization and Calibration in Wireless Sensor Networks.* ETH Zrich, Schweiz, 2005.

[55] J. Elson, L. Girod, and D. Estrin, "Fine-Grained Network Time Synchronization Using Reference Broadcasts," *ACM SIGOPS Operating Systems Review*, vol. 36, pp. 147–163, 2002.

[56] W. Xu, G. Yang, and J. Zhou, "Simulation Study on Time Synchronization Based on RBS in Wireless Sensor Networks," *Applied Mechanics and Materials*, vol. 321-324, p. 630, 2013.

[57] D. Djenouri, "Estimators for RBS-Based Time Synchronization in Heterogeneous Wireless Networks," *IEEE GLOBECOM Workshops*, pp. 298–302, 2011.

[58] S. Ganeriwal, R. Kumar, and M. B. Srivastava, "Timing-sync Protocol for Sensor Networks," *Proceedings of the 1st international conference on Embedded networked sensor systems*, pp. 138–149, ACM New York, NY, USA 2003.

[59] D. Capriglione, V. Paciello, L. Ferrigno, and A. Pietrosanto, "A step forward the on-line minimization of the synchronization events in TPSN," *Instrumentation and Measurement Technology Conference*, pp. 2780–2784, Graz, Austria, May 2012.

[60] Y. Gong, H. Ogai, and W. Li, "A Partial TPSN Time Offset Synchronization Scheme in Wireless Sensor Network applied for Bridge Health Diagnosis System," *International Conference on Computer Science and Network Technology (ICCSNT)*, pp. 254–258, Harbin, China, Dec. 2011.

[61] H. Dai and R. Han, "TSync: A lightweight bidirectional time synchronization service for wireless sensor networks," *ACM SIGMOBILE Mobile Computing and Communications Review*, vol. 8, pp. 125–139, 2004.

[62] Y. Dai, L. Yan, and Z. Chen, "A Study on Time Synchronization Algorithm Based on Energy Effective Strategy," *2nd International Conference on Mechatronics and Intelligent Materials*, vol. 490-495, pp. 1976–1980, March 2012.

[63] X. Tian, Y. Miao, T. Hu, B. Fan, J. Pan, and W. Xu, "Maximum Likelihood Estimation Based on Time Synchronization Algorithm for Wireless Sensor Networks," *2nd ISECS International Colloquium on Computing, Communication, Control and Management*, pp. 416–420, 2009.

[64] S. Ping, "Delay measurement time synchronization for wireless sensor networks," *Intel Research*, 2003.

[65] Y. Zhu and Y. Lv, "A Time Synchronization Protocol in WSN Applied in RAMR," *4th International Conference on Wireless Communications, Networking and Mobile Computing*, vol. 1, pp. 3954–3957, 2008.

[66] M. Maróti, B. Kusy, G. Simon, and Ákos Lédeczi, "The flooding time synchronization protocol," *Proceedings of the 2nd international conference on Embedded networked sensor systems*, pp. 39–49, ACM New York, NY, USA 2004.

[67] K. S. Yildirim and A. Kantarci, "Time Synchronization Based on Slow-Flooding in Wireless Sensor Networks," *IEEE Transaction on Parallel and Distributed Systems*, vol. 25, pp. 244–253, 2014.

[68] D. Huang, W. Teng, and K. Yang, "Secured flooding time synchronization protocol with moderator," *International Journal of Communication Systems*, vol. 26, pp. 1092–1115, 2013.

[69] A. Pantelidou and A. Ephremides, *Scheduling in Wireless Networks.* Now Publishers, 2011.

[70] J. A. Stankovic, T. F.Abdelzaer, C. Lu, L. Sha, and J. C. Hou, "Real-time communication and coordination in embedded sensor networks," *Proceedings of the IEEE*, vol. 91, pp. 1002–1022, 2003.

[71] I. Rhee and J. Lee, "Distributed scalable TDMA Scheduling Algorithm," Ph.D. dissertation, Department of Computer Science, North Carolina State University, 2004.

[72] J. Ramis, L. Carrasco, G. Femenias, and F. Riera-Palou, "Sheduling algorithms for 4G wireless networks," *The International Federation for Information Processing (IFIP)*, vol. 245, pp. 264–276, 2007.

[73] Y. Wu, X. Li, Y. Liu, and W. Lou, "Energy-Efficient Wake-Up Scheduling for Data Collection and Aggregation," *IEEE Transaction on Parallel and Distributed System*, vol. 21, pp. 275–287, 2010.

[74] T. Çevik, A. H. Zaim, and D. Yiltaş, "Localized power-aware routing with an energy-efficient pipelined wakeup schedule for wireless sensor networks," *Turkish Journal of Electrical Engineering & Computer Sciences*, vol. 20, pp. 964–978, 2012.

[75] L. Shi and A. O. Fapojuwo, "TDMA Scheduling with Optimized Energy Efficiency and Minimum Delay in Clustered Wireless Sensor Networks," *IEEE Transaction on Mobile Computing*, vol. 9, pp. 927–940, 2010.

[76] P. Djukic and S. Valaee, "Link Scheduling for Minimum Delay in Spatial Re-use TDMA," *26th IEEE International Conference on Computer Communications (INFOCOM)*, pp. 28–36, 2007.

[77] B. Yu, J. Li, and Y. Li, "Distributed Data Aggregation Scheduling in Wireless Sensor Networks," *IEEE INFOCOM*, pp. 2159–2161, 2009.

[78] V. Rajendran, K. Obraczka, and J. J. Garcia-Luna-Aceves, "Energy-Efficient, Collision-Free Medium Access Control for Wireless Sensor Networks," *Proceedings of the 1st international conference on Embedded networked sensor systems*, pp. 181–192, ACM New York, NY, USA 2003.

[79] H. Gong, M. Liu, Y. Mao, L. Chen, and L. Xie, "Traffic Adaptive MAC Protocol for Wireless Sensor Network," *Networking and Mobile Computing,*, vol. 3619, pp. 1134–1143, 2005.

[80] G. Lu, B. Krishnamachari, and C. S. Raghavendra, "An Adaptive Energy-Efficient and Low-Latency MAC for Data Gathering in Wireless Sensor Networks," *Proceedings of 18th International Parallel and Distributed Processing Symposium*, pp. 26–30, April 2004.

[81] S. C. Ergen and P. Varaiya, "TDMA scheduling algorithms for wireless sensor networks," *Wireless Networks*, vol. 16, pp. 985–997, 2010.

[82] H. Kang, Y. Zhao, and F. Mei, "A Graph Coloring Based TDMA Scheduling Algorithm for Wireless Sensor Networks," *Wireless Personal Communications*, vol. 72, pp. 1005–1022, 2013.

[83] I. Jemili, D. Ghrab, A. Belghith, B. Derbel, and A. Dhraief, "Collision Aware Coloring Algorithm for wireless sensor networks," *9th International Wireless Communications and Mobile Computing Conference (IWCMC)*, pp. 1546–1553, Sardinia, Italia, July 2013.

[84] S. Kumar and S. Chauhan, "A Survey on Scheduling Algorithms for Wireless Sensor Networks," *International Journal of Computer Applications*, vol. 20, pp. 7–13, 2011.

[85] Y. Xu, B. Jiang, Z. Gao, and K. Zhang, "Fault tolerant control for near space vehicle: a survey and some new results," *Journal of Systems Engineering and Electronics*, vol. 22, pp. 88–94, 2011.

[86] J. Lunze and J. Richter, "Reconfigurable Fault-tolerant Control: A Tutorial Introduction," *European Journal of Control*, vol. 5, pp. 359–386, 2008.

[87] S. Yin, H. Luo, and S. X. Ding, "Real-Time Implementation of Fault-Tolerant Control Systems With Performance Optimization," *IEEE Transaction on Industrial Electronics*, vol. 61, pp. 2402–2411, 2014.

[88] D. Campos-Delgado, D. Espinoza-Trejo, and E. Palacios, "Fault-tolerant control in variable speed drives: a survey," *IET Electric Power Applications*, vol. 2, pp. 121–134, 2008.

[89] A. Mirzaee and K. Salahshoor, "Fault Tolerant Control of an Industrial Gas Turbine Based on a Hybrid Fuzzy Adaptive Unscented Kalman Filter," *Journal of Engineering for Gas Turbines and Power*, vol. 135, 2013.

[90] K. Zhou and J. C. Doyle, *Essentials Of Robust Control*. Prentice Hall, 1997.

[91] M. Blanke, M. Kinnaert, J. Lunze, and M. Staroswiecki, *Diagnosis and Fault-Tolerant Control*. Springer, 2nd ed. 2006.

[92] S. X. Ding, *Model-Based Fault Diagnosis Techniques - Design Schemes, Algorithms, and Tools*. Springer-Verlag, 2nd ed. 2013.

[93] O. Hrizil, B. Boussaid, M. N. Abdelkrim, and C. Aubrun, "Fast adaptive fault estimation algorithm : application to unicycle robot," *Conference on Control and Fault-Tolerant Systems*, vol. 15, pp. 714–719, . Nice, France, Oct. 2013.

[94] M. Rodrigues, D. Theilliol, S. Aberkane, and D. Sauter, "Fault Tolerant Control Design for Polytopic LPV Systems," *International Journal of Applied Mathematics and Computer Science*, vol. 17, pp. 27–37, 2007.

[95] M. Pourgholi and V. Majd, "Robust Adaptive Observer Design for Lipschitz Class of Nonlinear Systems," *World Academy of Science, Engineering and Technology*, vol. 63, pp. 29–33, 2012.

[96] Q. Zhang, "Adaptive Observer for Multiple-Input-Multiple-Output (MIMO) Linear Time-Varying Systems," *IEEE Transaction on Automatic Control*, vol. 47, pp. 525–529, 2002.

[97] A. Xu and Q. Zhang, "Nonlinear system fault diagnosis based on adaptive estimation," *Automatica*, vol. 40, pp. 1181–1193, 2004.

[98] A. Guyader and Q. Zhang, "Adaptive observer for discrete time linear time varying systems," *13th IFAC/IFORS Symposium on System Identification (SYSID)*, vol. 1, pp. 1743–1748, 2003.

[99] S. Jagannathan and F. L. Lewis, "Discrete-Time Neural Net Controller for a Class of Nonlinear Dynamical Systems," *IEEE Transaction on Automatic Control*, vol. 41, pp. 1693–1699, 1996.

[100] B. T. Thumati and S. Jagannathan, "A Model-Based Fault-Detection and Prediction Scheme for Nonlinear Multivariable Discrete-Time Systems With Asymptotic Stability Guarantees," *IEEE Transaction on Neural Networks*, vol. 21, pp. 404–423, 2010.

[101] H. Ferdowsi and S. Jagannathan, "A unified model-based fault diagnosis scheme for non-linear discrete-time systems with additive and multiplicative faults," *Transaction of the Institute of Measurement and Control*, vol. 35, pp. 742–752, 2013.

[102] B. T. Thumati, G. R. Halligan, and S. Jagannathan, "A Novel Fault Diagnostics and Prediction Scheme Using a Nonlinear Observer With Artificial Immune System as an Online Approximator," *IEEE Transaction on Control Systems Technology*, vol. 21, pp. 569–578, 2013.

[103] F. Caccavale, L. Villani, and F. Pierri, "Adaptive Observer for Fault Diagnosis in Nonlinear Discrete-Time Systems," *Journal of Dynamic Systems, Measurement, and Control*, vol. 130, 2008.

[104] H. Fang, H. Ye, and M. Zhong, "Fault diagnosis of networked control systems," *Annual Reviews in Control*, vol. 31, pp. 55–68, 2007.

[105] B. Jiang and F. N. Chowdhury, "Fault Estimation and Accommodation for Linear MIMO Discrete-Time Systems," *IEEE Transaction on Control Systems Technology*, vol. 13, pp. 493–499, 2005.

[106] R. M. Ferrari, T. Parisini, and M. M. Polycarpou, "A Fault Detection and Isolation Scheme for Nonlinear Uncertain Discrete-Time Sytems," *46th IEEE Conference on Decision and Control*, vol. New Orleans, LA, USA, pp. 1009–1014, 2007.

[107] R. Ferrari, T. Parisini, and M. Polycarpou, "A Robust Fault Detection and Isolation Scheme for a Class of UncertainInput-output Discrete-time Nonlinear Systems," *American Control Conference*, vol. Seattle, Washington, USA, pp. 2804–2809, 2008.

[108] D. Du, B. Jiang, and P. Shi, "Active fault-tolerant control for switched systems with time delay," *International Journal of Adaptive Control and Signal Processing*, vol. 25, pp. 466–480, 2011.

[109] W. Han, J. Park, and B. Lee, "Analysis of Thyristor Controlled series Compensator Dynamics Using the State Variable Approach of a Periodic System Model," *IEEE Transactions on Power Delivery*, vol. 12, pp. 1744–1750, Oct. 1997.

[110] H. Zhang, Y. Zhang, and X. Ma, "Dimensionless Approach to Multi-Parametric Stability Analysis of Nonlinear Time-Periodic Systems: Theory and Its Applications to Switching Converters," *Journal of Intelligent & Robotic Systems*, vol. 60, pp. 491–504, 2013.

[111] P. Zhang, S. X. Ding, and P. Liu, " A Lifting Based Approach to Observer Based Fault Detection of Linear Periodic Systems," *IEEE Transaction on Automatic Control*, vol. 57, pp. 457–462, 2012.

[112] S. Bittanti and P. Colaneri, *Periodic Systems, Filtering and Control.* Springer, 2009.

[113] M. Branicky, S. Phillips, and W. Zhang, "Scheduling and Feedback Co-Design for Networked Control Systems," *Proc. of the 41st IEEE Conference on Decision and Control*, vol. 2, pp. 1211–1217, Las Vegas, Nevada USA, Dec. 2002.

[114] T. Yang, "Networked control system: a brief survey," *Proc. of IEEE Conference on Control Theory Applications*, vol. 153, pp. 403–412, 2006.

[115] Z. Huo, Z. Zhixue, and F. Huajing, "Research on fault-tolerant control of networked control systems based on information scheduling," *Journal of Systems Engineering and Electronics*, vol. 19, no. 5, pp. 1024 –1028, Oct. 2008.

[116] Y. Wang, S. X. Ding, D. Xu, and B. Shen, "An H_∞ Fault Estimation Scheme of Wireless Networked Control Systems for Industrial Real-Time Applications," *Transactions on Control Systems Technology*, vol. PP:99, DOI:10.1109/TCST.2014.2305393, 2014.

[117] A. Paoli, "Fault detection and fault tolerant control for distributed systems: A general framework," Ph.D. dissertation, University of Bologna, 2004.

[118] C. I. Chihaia, "Active Fault-Tolerance in Wireless Networked Control Systems," Ph.D. dissertation, University of Duisburg-Essen, 2010.

[119] S. Bittanti and F. A. Cuzzola, "An LMI Approach to Periodic Discrete-Time Unbiased Filtering," *Systems and Control Letters*, vol. 42, pp. 21–35, 2001.

[120] K. Zhang, B. Jiang, V. Cocquempot, and H. Zhang, "A framework of robust fault estimation observer design for continuous-time/discrete-time systems," *Optimal Control Applications and Methods*, 2012.

[121] H. Yang, B. Jiang, and V. Cocquempot, "A fault tolerant control framework for periodic switched non-linear systems," *International Journal of Control*, vol. 82, pp. 117–129, 2009.

[122] H. Freeman, *Discrete-time systems: an introduction to the theory.* John Wiley and Sons, 1965.

[123] A. Xu and Q. Zhang, "Residual Generation for Fault Diagnosis in Linear Time-Varying Systems," *IEEE Transaction on Automatic Control*, vol. 49, pp. 767–772, 2004.

[124] C. A. B. Hann and T. Ahmed-Ali, "Continuous adaptive observer for state affine sampled-data systems," *International Journal of Robust and Nonlinear Control*, vol. 24, pp. 669–681, 2014.

[125] Y. Han, S. Oh, B. Choi, D. Kwak, H. Kim, and Y. Kim, "Fault detection and identification of aircraft control surface using adaptive observer and input bias estimator," *IET Control Theory and Applications*, vol. 6, pp. 1367–1387, 2012.

[126] Q. Zhang, "An adaptive observer for sensor fault estimation in linear time varying systems," *IFAC World Congress, Prague, Czech*, 2005.

[127] X. Li and G. Yang, "Fault diagnosis for non-linear single output systems based on adaptive high-gain observer," *IET Control Theory and Applications*, vol. 7, pp. 1969–1977, 2013.

[128] H. Ma and G. Yang, "Residual generation for fault detection and isolation in a class of uncertain nonlinear systems," *International Journal of Control*, vol. 86, pp. 263–275, 2013.

[129] M. Farza, M. M'Saad, T. Maatoug, and M. Kamoun, "Adaptive observers for nonlinearly parameterized class of nonlinear systems," *Automatica*, vol. 45, pp. 2292–2299, 2009.

[130] Q. Zhang and G. Besançon, "An adaptive observer for sensor fault estimation in a class of uniformly observable non-linear systems," *International Journal of Modelling, Identification and Control*, vol. 4, pp. 37–43, 2008.

[131] X. Li, Q. Zhang, and H. Su, "An adaptive observer for joint estimation of states and parameters in both state and output equations," *International Journal of Adaptive Control Signal Process*, vol. 25, pp. 831–842, 2011.

[132] C. I. Chihaia, O. Bredtmann, E. Goldschmidt, W. Li, S. X. Ding, and A. Czylwik, Barcelona, Juli 2009.

[133] "Torricelli's law," *http://en.wikipedia.org/wiki/Torricelli's_law*.

[134] Y. Wang, "Fault Estimation Design for Wireless Networked Control Systems for Industrial Real-Time Applications," Ph.D. dissertation, University of Duisburg-Essen, 2014.